Proceedings of The International Symposium on Global Change in East Asia - Vegetation Monitoring -

December 10-11,1998

Center for Environmental Remote Sensing,
Chiba University, Japan

Edited by Yoshiaki Honda and Koji Kajiwara

Published by
Center for Environmental Remote Sensing (CEReS), Chiba University
1-33 Yayoi-cho, Inage-ku, 263-8522 Japan
Fax: +81-43-290-3857

The International Symposium on Global Change in East Asia - Vegetation Monitoring -

December 10-11, 1998
Chiba University

CEReS

Center for Environmental Remote Sensing
Chiba University, Japan

Preface

The plain is occupying about 1/3 of all the land. The plant of the plain is sensitive in environment fluctuation even from a/the forest plant. Also, most of the food for mankind is obtained from an/the herbaceous plant. The plain monitoring is extremely important when it grasps earth environment. Sixteen presentations with regard to the plain monitoring were done in this symposium. We understood that the projects of numerous global scale and area scale are raissing the result. We felt the need that an individual project cooperates and coordinate mutually. However, there is the technical problem such as a data crisis and software crisis in order that the mutual cooperation between a/the project is materialized. Also, we were able to understand even that whether is a big problem to take the adjustment between a/the project with what kind of method.

Yoshiaki Honda

CEReS, Chiba Univ.

The International Symposium on Global Change in East Asia - vegetation Monitoring -

December 10-11, 1998, Chiba University

CONTENTS

Session : Activity of CEReS

Session : Huge data set generation

APAN Earth Monitoring and Disaster Warning Working Group

Haruhiro Fujita
Ministry of Agriculture, Forestry and Fisheries Research Network (MAFFIN)
Shikoku National Agricultural Research Institute, 1-3-1, Senyu, Zentsuji,
Kagawa, Japan 765-8508
e-mail:fujitah@skk.affrc.go.jp

Christopher Elvidge
National Oceanic and Atmospheric Administration (NOAA)
National Geophysical Data Center (NOAA-NGDC)
325 Broadway, Boulder, Colorado, USA 80303
e-mail:cde@ngdc.noaa.gov

1. Introduction

The Asian Pacific Advanced Network (APAN) is a non-profit international consortium established on 3 June 1997. APAN is intended to be a high-performance network for research and development on advanced applications and services. APAN provides an advanced networking environment for research community, and promotes international collaboration. APAN has already established a substantial set of network connections for use by the scientific community (Figure 1).

The Asia Pacific region contains 60% of the planet's population. The region is correspondingly rich in its marine and terrestrial biotic resources, many of which are increasingly impacted by anthropogenic activities.

The APAN Earth Monitoring and Disaster Warning Working Group was established in July 1998. The mission of this working group (WG) is to implement remote sensing applications within APAN which promote sustainable economic development, preservation of the region's biotic resources, and early identification of events or conditions which may lead to disasters.

2. Environmental Issues of the Asian Pacific Region

There are a number of pressing environmental issues in the region, including deforestation, coral reef degradation, and pollution of air and water resources. In addition, there are major questions regarding the sustainability of fishery resources, which have supplied the region's people with protein for millenia, but are now being heavily exploited with an array of technologies.

The region is subjected to a wide range of natural disasters. The region is a part of the circum-pacific "ring of fire", with hundreds of potentially active volcanoes and a significant history of earthquakes. Monsoons bring torrential rains and flooding. When monsoons falter, due to events such as El Nino, drought and devastating fires can occur.

3. Observation, Processing, and Distribution

Satellite remote sensing technologies have proven capabilities for environmental monitoring and disaster warning. However, the full value and benefit of current sensor systems is seldom realized due to limited
distribution of the data and derived products, which are constrained, in part, by large data volumes. Recent advances in high performance networking technologies opens up new opportunities for wider access and utilization of remotely sensed data.

The WG will utilize APAN to distribute remote sensing data and derived information products to new sets of data users which will be developed through the APAN nodes. The WG will seek to democratize the decision making impact of the distributed data through local media outlets, universities, government laboratories, and non-governmental organizations (NGOs).

The WG will monitor the feedback from data users and attempt to respond through changes and adjustment in the products and delivery patterns to better serve the objectives of the end users.

The WG has established a set of implementation objectives detailed below, tapping into capabilities available at WG member institutions. In the longer term, the WG will seek out collaborations with a broader range of remote sensing data and product providers to serve as a regional hub for
distribution of earth observations into the Asian Pacific region.

4. Implementation

The WG plans to focus initially on the remote sensing of three phenomena which have wide impact on the region: 1) wildfires (biomass burning), 2) the intensity of fishing effort, and 3) torrential rains.

Fire is used to clear land, as a tool of agriculture and forestry. Other burning may be of religious or cultural origin. However, during drought years it is difficult to control. Fire is closely associated with
deforestation, land cover change, land degradation, and losses in species diversity. Smoke from fires can become a regional health and navigation issue. Anthropogenic fires are the second largest source of greenhouse gas emissions, only exceeded by fossil fuel combustion as a source.

Because of their distinct spectral emissions, fires can be directly observed in data from certain meteorological satellite sensors such as the Defense Meteorological Satellite Program - Operational Linescan System (DMSP-OLS) and NOAA Advanced Very High Resolution Radiometer (NOAA-AVHRR). Smoke can be spectrally distiguished from clouds in data from Japan's Geostationary Meteorological Satellite (GMS) and NOAA-AVHRR. GMS data was used successfully to monitor smoke sources and smoke movement during the 1997 fires of Indonesia. Figure 2 shows a DMSP-OLS fire

We propose to develop a multisource program to monitor fires and smoke in Southeast Asia. Initially this will be based on the near real-time distribution of DMSP-OLS fire products (processed by NOAA-NGDC) and digitally enhanced GMS data for monitoring of smoke sources, extent and movement. APAN nodes for data delivery and distribution will be the Asian

Institute of Technology (AIT), Bangkok, Thailand, the Institute of Technology, Bandung (ITB), Sumatra, Indonesia, and Australian institutes.

Fisheries provide a major source of protein for people in Asia Pacific countries. The cumulative impacts of overfishing using advanced technologies could lead to a major loss in food security for the region.
Monitoring of fishing effort, in terms of the number of fishing vessels which are active, when combined with total catch, can be used to assess the population of the fished species.

As a proof of concept we propose to implement a monitoring program for the regions squid fishing activities. Squid fishing vessels use large banks of high intensity lights to attract squid to the ocean surface for netting. The squid fishing boats can be detected using night time data from the
DMSP-OLS. We propose to generate and distribute nightly georeferenced visible and thermal band OLS products (at NOAA-NGDC) of squid fishing areas in the Sea of Japan (Figure 3). If successful, this effort will later be expanded to the Philippines and Gulf of Thailand.

Torrential rains can be observed directly with data from the DMSP Special Sensor Microwave Imager (SSMI) and with data from the NASA-NASDA Tropical Rainfall Mapping Mission (TRMM). We propose to distribute SSMI and TRMM data and data products in near real-time using APAN. By rapidly distributing these products the WG intends to enhance the available information on powerful storm systems prior to landfall.

The initial WG data delivery or mirroring services in the APAN nodes will be accomplished through the Ministry of Agriculture, Forestry and Fisheries Research Network (MAFFIN) of Japan.

5. Conclusion

In reviewing the available satellite remote sensing programs we conclude that substantial capabilities for earth observation and disaster warning are being under utilized. The vast majority of satellite remote sensing data enters digital archives having limited accessibility rather than being widely distributed for open use by the scientific community. This is the legacy of decades in which the electronic transport of image data was cumbersome and limited to small data volumes. With today's advanced bandwidth networks, such as APAN, it is possible to distribute significant volumes of satellite image data on a daily basis. The APAN Earth Monitoring and Disaster Warning Working Group has initiated a set of international scientific collaborations to tap in to satellite remote sensing data streams, performing processing to make usable products, and then distribute the data products. This will greatly enhance the benefit that society receives from the massive investments made to develop, launch, and operate satellite remote sensing programs.

6. References

APAN (1997).
http://apan.net

Elvidge, C.D (1998). APAN Earth Monitoring and Disaster Warning WG, http://apan.net/groups/earth-monitoring.html

Fujita, H., Prakoso, J.H. and Aziz, L.H. (1998). Development of wild fire monitoring by APAN, Proceedings of IWC98, 51

Fujita, H., Ueda, T., Prakoso, J.H. and Otsuka, M. (1998) Development of fast dissemination of remote sensed and GIS data of fires by APAN. Proceedings of the 27th International Conference on Remote Sensing of Environment.

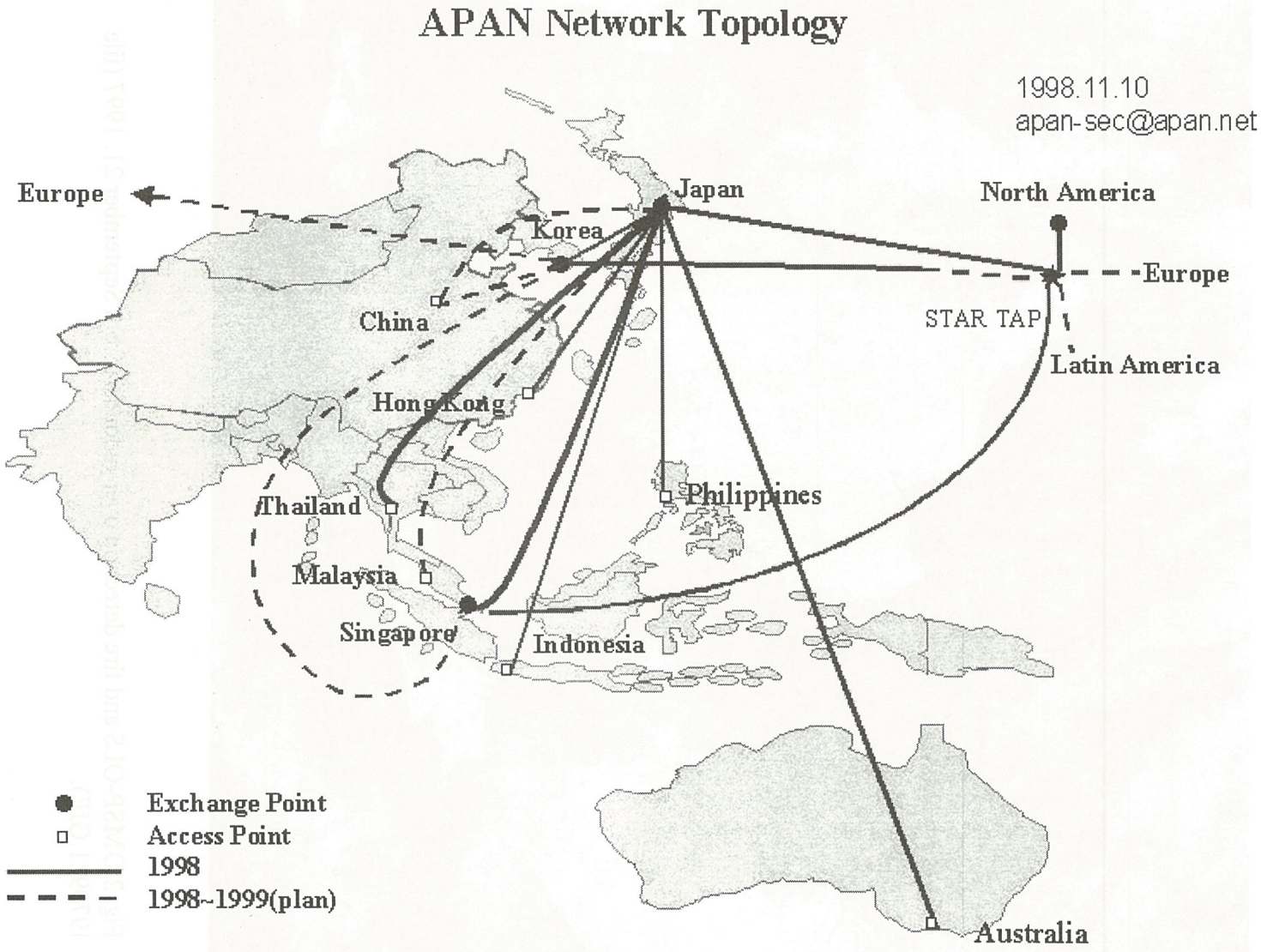

Fig. 1 Network connections of APAN (file APAN.JPG).

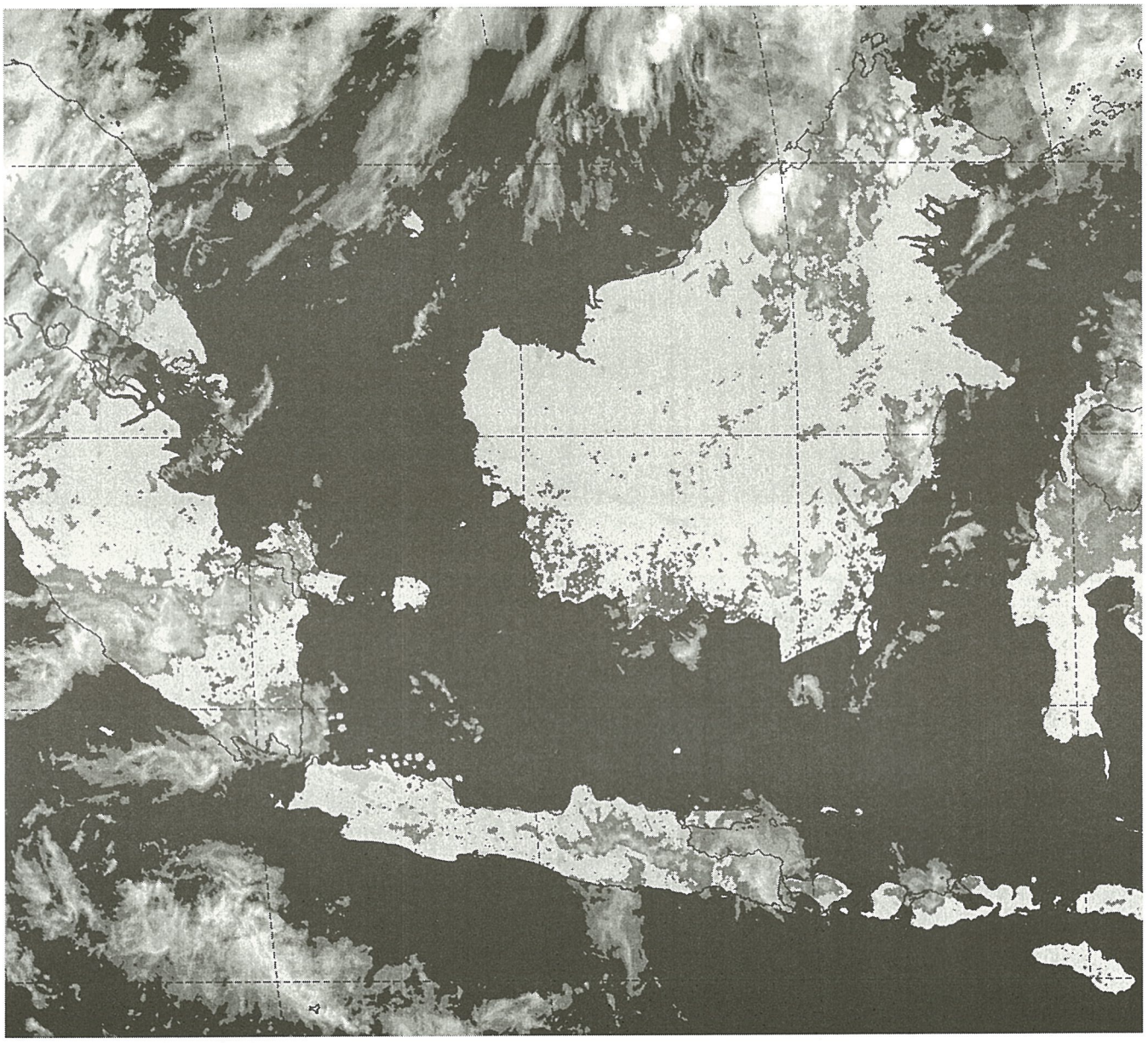

Fig. 2 DMSP-OLS and fire detection over Indonesia from September 21, 1997 (file I970921.GIF).

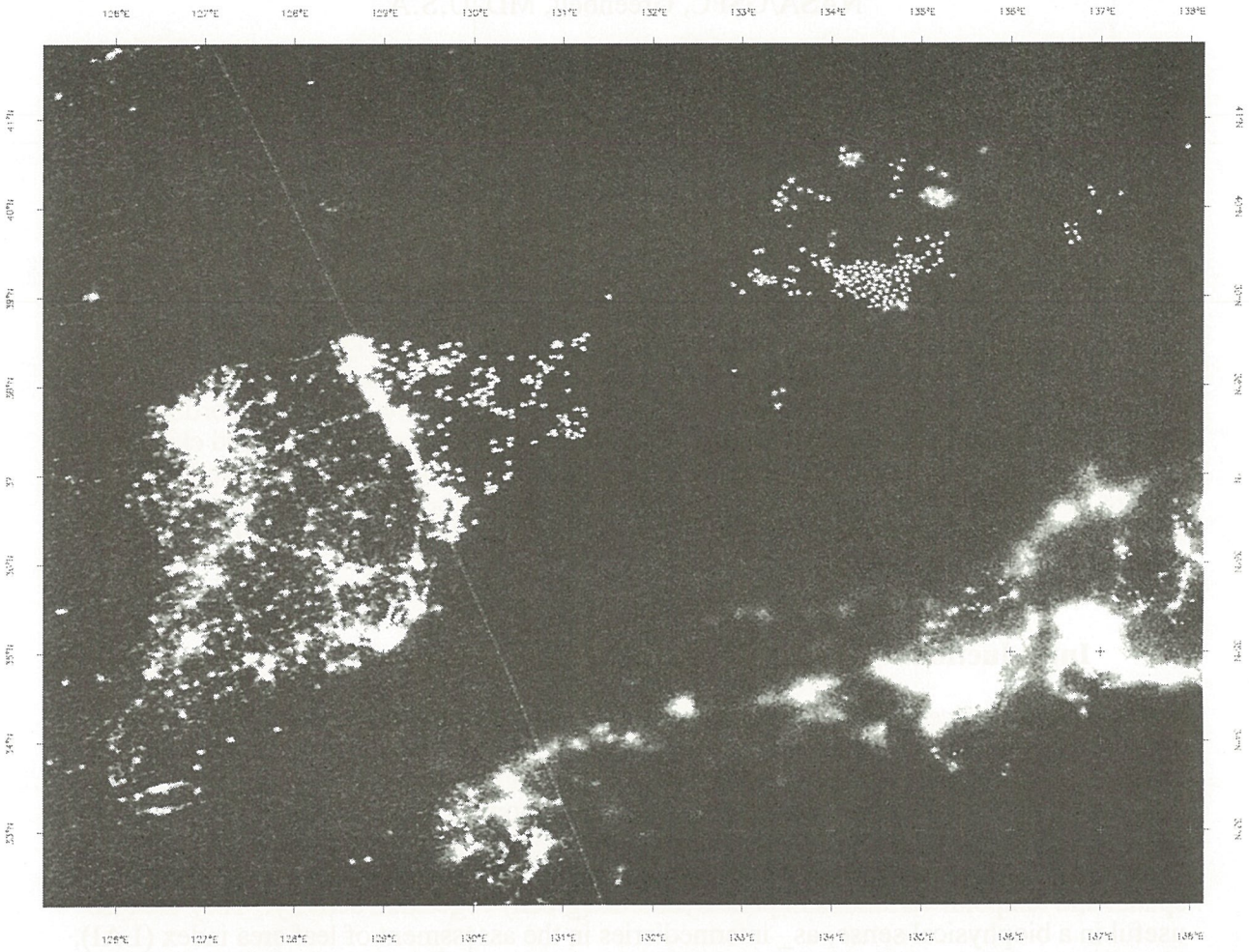

Fig. 3. Georeferenced DMSP-OLS image of lights from squid fishing boats in the Sea of Japan from September 19, 1998 (file J98919A.GIF).

The use of vegetation indices for coarse resolution monitoring of terrestrial vegetation with SeaWiFS sensor

A.R. Huete[1], K. Didan[1], W.J.D. van Leeuwen[1], and E. Vermote[2]
[1]University of Arizona, Tucson, AZ U.S.A.
[2]NASA/GSFC, Greenbelt, MD, U.S.A.

ABSTRACT

In this study, the Sea-viewing Wide Field-of-View sensor (SeaWiFS) is used to prototype and analyze coarse resolution monitoring of the Earth's surface with vegetation indices. Histograms and transects of the normalized difference vegetation index (NDVI) and enhanced vegetation index (EVI) are analyzed over four continental regions as well as the entire global land surface. Unique distributions of NDVI and EVI values were displayed in the histograms. The EVI had a more normal distribution of values over the global set of biomes while the NDVI was skewed toward higher values approaching saturation over forested regions. The NDVI mimicked the skewed distributions found in the red band while the EVI resembled the normal distributions found in the NIR band. The EVI was also found to greatly minimize smoke contamination over extensive portions of the tropics. Smoke was found to degrade histogram peaks in the NDVI and red channel but had minimal effects in the NIR and EVI histograms. The results how that multiple indices are necessary for effective monitoring of the diverse set of global biomes with the EVI being particularly useful in high biomass, forested regions, while the NDVI being useful in semiarid regions.

1. Introduction:

Vegetation indices (VI's) have emerged as an important tool in the monitoring, mapping, and resource management of the Earth's terrestrial vegetation (Townshend, 1994; Myneni et al., 1997). Vegetation indices are radiometric measures of the amount, structure, and condition of vegetation. These serve as useful_ monitoring indicators of seasonal and inter-annual variations in vegetation and resultant_ climatic and anthropogenic influences on the environment.__ As a radiometric quantity, vegetation indices are a precise measure of spatial and temporal variations in photosynthetic (green) vegetation activity. They are also useful in a biophysical sense, as_ intermediaries in the assessment of leaf area index (LAI), percent green cover, green biomass, and fraction of absorbed photosynthetically active radiation (fAPAR).

_Coarse resolution sensors such as the Advanced Very High Resolution Radiometer (AVHRR), VEGETATION, the Sea-viewing Wide Field-of-View sensor (SeaWiFS), and the soon to be launched Moderate Resolution Imaging Spectroradiometer (MODIS), and the Global Imager (GLI) onboard the Earth Observing System (EOS) AM1 and ADEOS-2 platforms, respectively, are particularly useful _due to the high frequency coverage (daily to 2x/week) obtainable. _These sensors are designed to generate standard 'vegetation' products and stable time series data sets for accurate discrimination of inter-annual and intra-annual variations in vegetation. Cloud-free vegetation index maps_ are designed to best depict the spatial and temporal variations in vegetation at the finest spatial and temporal resolutions possible. There are tradeoff's however, between temporal resolution and cloud- and noise-free pixels. Atmospheric contamination from aerosols and subpixel clouds along with variable sun-surface-sensor geometries and their associated bidirectional effects are some of the sources of noise prevalent in the vegetation products. _

Optimization of VI's for global vegetation monitoring and mapping

Spatial and temporal variability in VI's arise from several vegetation- related properties, including LAI, fAPAR, canopy structure/ architecture, species composition, land cover type, leaf optics, canopy crown cover, understory vegetation, and green biomass. A change in any one property or set of properties will result in a given change in a VI value. However, aside from vegetation changes, the VI may also vary due to other factors including;

- factors external to the canopy such as atmospheric gaseous absorption and aerosol variations, subpixel clouds and cloud shadows, topographic variations, and viewing and illumination geometries;

sensor and orbit characteristics which include instrument calibration, navigation and geometric registration errors, band to band registration error and filter degradation; and

- factors inherent to the canopy, including canopy background variations (soil, roughness, gravels/rocks, snow, water, organic matter) and the presence of non-photosynthetic vegetation materials (litter, senesced vegetation, dead plant matter, bark).

The normalized difference vegetation index (NDVI), as a normalized ratio of the NIR and red bands,

$$NDVI = (\rho nir - \rho red) / (\rho nir + \rho red) \quad (1)$$

is successful in that it is sufficiently stable to permit meaningful comparisons of seasonal and inter-annual changes in vegetation growth and activity. The strength of the NDVI is in its ratioing concept, which reduces the multiplicative noise (illumination differences, cloud shadows, atmospheric attenuation) present in multiple bands. Current research is aimed at operational 'external' noise removal through atmospheric correction and standardization of sun-surface-sensor geometries with BRDF models (van Leeuwen et al., 1998; Vermote et al., 1997). State-of-the-art instruments with improved radiometric and registration accuracies are also being developed. These have facilitated improved stability and comparisons among pixels.

As the 'external' and sensor characteristic sources of noise and error in satellite data are reduced, the need for 'ratioing-based' indices decreases allowing for the introduction of alternative and enhanced vegetation indices for operational monitoring of the Earth's vegetation (Huete et al., 1997). Ratios are not always optimal for vegetation studies due to non-linearities, scaling, and asymptotic (saturated) signals. Alternative, non-ratioing, indices are generally more linear with less saturation problems, but require reflectances as inputs. Thus, external and sensor noise removals are accomplished in the derivation of surface reflectances, prior to VI computation.

Vegetation indices can be "optimized" in several ways; (1) to minimize inherent noise such as canopy background; (2) for the retrieval of specific biophysical parameters such as fAPAR; or (3) for biome-specific applications. It has become clear that more than one index is needed for the retrieval of biophysical parameters and for monitoring of all land cover types and that no single index is capable of discerning all quantities of interest. Furthermore, since biophysical quantities tend to be non-linear with each other (e.g. fAPAR and LAI), no single index can be linear with all vegetation parameters.

The enhanced vegetation index (EVI) was developed to optimize the vegetation signal while minimizing aerosol and canopy background sources of noise (Huete et al., 1997). The equation takes the form,

$$EVI = 2.5 * (\rho nir - \rho red) / (L + \rho nir + C_1 \rho red - C_2 \rho blue) \quad (2)$$

Where L is the canopy background correction that addresses differential NIR and red radiant transfer through a canopy and C_1 and C_2 are the coefficients of the aerosol term, which uses the blue band to correct for aerosols in the red band (Kaufman and Tanre′, 1992). The coefficients being tested here are: L=1, C_1 = 6, and C_2 = 7.5.

In this study we prototype and analyze a set of VI's with global SeaWiFS imagery. Histograms of different continents are analyzed along with transects through diverse sets of biomes. The goal is to investigate the feasibility of an alternative or enhanced VI for global operational use.

2. Methods and Study Sites

Global SeaWiFS imagery were used to prototype and analyze VI's for MODIS and GLI. SeaWiFS is tilted 20° along track and produces global fields of radiance in 8 visible and near-infrared channels similar to those of the 36 channel MODIS and the 36 channel GLI sensors (Table 1). There are two resolutions of data; Local Area Coverage (LAC) at ~1 km resolution and 4 km, Global Area Coverage (GAC). A 16-day series of SeaWiFS GAC data for the period, September 15 to October 1, 1997, was collected over the entire globe and composited to cloud-free, single channel reflectance images. The images were first degraded to 8km and corrected for Rayleigh scattering, ozone absorption, and water absorption as in the AVHRR Pathfinder procedure (James and Kalluri, 1994). A partial cloud mask was used to remove cloud contaminated pixels with reflectance thresholds, $\rho > 0.25$. However, because of appreciable residual cloud contamination, the maximum value composite for NDVI (MVC-NDVI) and EVI (MVC-EVI) were utilized to reduce the 16 days into cloud-free VI and single channel reflectances of SeaWiFS (Holben, 1986). Other, BRDF-related, compositing methods were tried and analyzed (van Leeuwen et al., 1998), but these were found too sensitive to residual clouds remaining in the data. Histograms and transects were extracted over four 'continental' regions, North America, South America, Africa, and Asia, representing a wide range of land cover types (Fig. 1). The histograms of the individual bands and two vegetation indices are presented along with some transect plots crossing major transitional areas within each continent.

Table 1: MODIS, GLI, and SeaWiFS spectral bandwidths applicable to land studies in the visible and near-infrared.

#	SeaWiFS	#	GLI	#	MODIS
1	402-422				
2	433-453	4	438-448		
		5	455-465		
3	480-500	20	(425-495)	3	459-479
4	500-520	21	(520-570)		
5	545-565	9	560-570	4	545-565
		22	(630-690)	1	(620-670)

6	660-680	13	673-683		
		15	705-715		
7	(745-785)	17	759-767		
		23	(770-880)		
8	(845-885)	19	860-870	2	(841-876)

* parentheses denote bandwidths wider than 20 nm.

3. Results

Figure 2 is the resulting NDVI and EVI composited global images using the maximum NDVI and maximum EVI criteria, respectively. The two images are well correlated with a few differences. The boreal regions in Canada and Russia are much brighter (higher values) in the NDVI image relative to that in the EVI image. The Amazon, Central American, and Indian forested regions appear brighter in the EVI image. In addition the EVI image seems to have some artifact values in Antarctica, while the NDVI appears to have smoke-related variations in the tropical forested areas.

3.1 North America

The blue, red, and NIR band reflectance and VI histograms, representing the most cloud-free and minimal 'aerosol' pixel selections, are depicted for North America in Fig. 3. The blue and red bands do not have normal distributions and are skewed toward very low reflectance values with peaks of 0.03 in the blue and 0.04 in the red. These values are associated with the more densely vegetated, forested regions, particularly the eastern broadleaf forests, southern needleleaf Pine forests in the U.S.A and boreal forested areas in Canada. The skewed distribution also indicates saturation of these bands over most of the forested regions. The higher reflectance values are associated with the more arid and semiarid parts but there are very few pixels with red reflectances greater than 0.20. The shoulder peak observed in the red histogram at ~0.13 is not present in the blue histogram, indicating that this surface-related feature cannot be readily seen in the higher optical-depth blue image. The histogram of the NIR band showed a much more normal distribution of values, centered at 0.24. Despite the high amount of active forest vegetation in September, the NIR showed no apparent signs of saturation.

It is worth noting that there were slight differences in the spectral histograms between the MVC-NDVI and MVC-EVI selections of pixels. The NDVI based compositing scheme resulted in lower red and NIR reflectances with histogram peaks at 0.04 and 0.21, respectively; whereas the EVI-based compositing scheme produced histogram peaks at 0.05 and 0.24 in the red and NIR, respectively. There were no differences in the blue peak between the two schemes. Thus, the MVC-NDVI tends to select the lowest red reflectance while the MVC-EVI, the highest NIR reflectances.

The histograms of the two computed vegetation indices showed very contrasting results with the NDVI skewed toward its highest values, thus saturating in the densely vegetated areas (Fig. 3). The NDVI essentially responded to the similarly 'saturated' red band. The EVI, on the other hand appeared to respond more closely to the NIR band as both did not saturate, but produced fairly normal distributions of values. The EVI histogram had a sharp peak at ~0.32, a slight shoulder at ~0.42, and an overall range of ~0 to 0.7 (Fig. 4b). The NDVI histogram had a peak at 0.62, an 'ice peak' at –0.02 and a

range of ~0 to 0.85 (Fig. 3). The peaks in both the NDVI and EVI histograms contain, among other land cover types, the boreal forests. The shoulder on the right hand side of the EVI peak marked the transition from needleleaf forest to broadleaf forests. The left-hand side of the EVI peak is mostly arid and semi-arid land cover types with most of the grassland areas in the central U.S.A. present within the EVI peak. The left-hand side of the NDVI peak delineates a transition from arid, semi-arid, and grassland areas. Thus, in comparison with the EVI, the NDVI is compressed into a narrow range of values over the forests and stretch out over a larger range over the less vegetated grassland to desert, land cover types.

A line transect through the continent (north to the south) provide further insight into the nature of the two indices (Fig. 4). In transect 'a', both VI's start low in the tundra zone and continue to increase through the boreal forests and eastern broadleaf and finally southern Pine forests. The NDVI asymptotically reaches a maximum value of ~0.8 halfway through the transect (northeast U.S.A, broadleaf forests), while the EVI continues to increase until the final third portion of the transect where it starts to decrease again (Fig. 4). Thus for nearly half the transect, the NDVI is at its maximum value (~0.8), while the EVI showed no signs of saturating, increasing from 0.1 (tundra) to 0.65 (broadleaf forest) and then decreasing to ~0.5 (needleleaf Pine forest). The NDVI varied from 0.2 in the tundra to 0.8 in the forests and then decreased to ~0.65. The sudden drop in EVI values in the southern Pine forests is associated with a land cover change from broadleaf trees to needleleaf trees. In a radiometric sense, the EVI is sensitive to this major canopy structural change, independent or partly independent of any biophysical vegetation differences (biomass, LAI, %crown cover, etc...). The NDVI was not so responsive to this change in land cover type (Fig. 4), which may be due to the asymptotic or 'saturation' effect. It is worth noting the 'noise' or variability present in both VI's along most of the transects which may be due to a combination of sensor-sun angles, subpixel clouds, and real surface heterogeneities (Cihlar et al., 1994).

3.2 South America

The spectral histograms for the South American continent (Fig. 5) exhibited a few differences from those of North America (Fig. 3). The red histogram had a broken peak caused by extensive biomass burning and smoke, which can be seen in Fig. 1. The NIR histogram is still normally distributed but slightly skewed toward the right hand side relative to that encountered in North America. The peak also occurred at a higher value (0.28). The blue peak had no broken structure associated with smoke, however, the peak occurred at blue reflectances (0.06) twice that of North America (0.03).

The NDVI and EVI histograms for South America also showed distinct differences (Fig. 5). Both indices had a sharp edge at higher values indicative of some saturation over high biomass conditions. Both indices also showed 3 peaks, which were very sharp and pronounced in the EVI plot. The peaks depict the major bio-regions in South America; (1) the peak of highest VI values represent the most dominant biome, the Amazon forest; (2) the middle peak of intermediate VI values represent the second most dominant biome, the cerrado region; and (3) the low VI peak is associated with the coastal deserts and arid steppes of Patagonia. The distribution of pixels differs significantly for the two VI's with most of the pixels appearing in the third (sharp) peak in the case of the EVI, and most pixels occurring in the second (broad) peak in the case of the NDVI (Fig. 5). It appears that the second, broad NDVI peak is a result of smoke and the shifting of NDVI values through large portions of the Amazon to lower values.

Transect 'c' cuts through the Amazon rainforest from the Atlantic coast to the dense interior near Iquitos and continues through the Andes and drier Peru region (Fig. 4).

During the relatively 'dry' September time frame there is also a lot of biomass burning occurring before the onset of the rainy season. The NDVI transect shows the extreme sensitivity of the NDVI to smoke aerosol particles with values dropping, on average, 30% (Fig. 4). The EVI on the other hand is relatively unaffected by the smoke with average decreases of less than 10% (Fig. 4). Both plots also depict a high degree of scatter among adjacent pixels, which can be attributed to several factors including; inherent heterogeneity of the surface, dense smoke effects, and the angular conditions of the compositing procedure. The drier values over the Andes and Peru had a greater NDVI dynamic range of values (0.05 to 0.24). The EVI values over this zone ranged from 0.05 (base) to 0.14.

3.3 Africa

The spectral histograms of the African continent presented two strong features related to the large presence of hyperarid deserts and tropical forest region (Fig. 6). Even the blue histogram had two peaks, associated with dense vegetation (0.06) and with desert (0.16). The red histogram similarly had a desert peak at 0.40 and a broken, red peak at 0.07-0.08 due to smoke over the tropical forests. Red reflectances extended out to 0.5 in contrast to North and South America, where values were mostly within 0.25. The NIR histogram had a slightly broken peak at 0.28 (as in South America), possibly due to very dense smoke. There was also a bright shoulder (0.40-0.45) associated with the desert. The Saharan desert also contains significant areas of darker geologic substrates and thus contributes to both of the dual histogram peaks in Fig. 6.

The VI histogram plots both show sharp and narrow desert peaks at approximately 0.05 (Fig. 6). This serves as a useful and stable baseline from which sensor stability and calibration can be monitored. There is a second, broader peak associated with the tropical forest zone. This peak is not as obvious in the NDVI due to NDVI sensitivity to smoke influences. The smoke effect is readily seen in the north to south transect plot through the continent (Fig. 7). In the central forested zone, the NDVI decreased significantly (30%) in the smoke-contaminated areas. Both VI's showed stable baseline behavior through the desert.

3.4 Asia

The VI histograms for the eastern part of the Asian continent are shown in Fig. 8. Both VI's exhibited 4 histogram peaks or features, which were distributed quite differently in each VI. There are two, lower value peaks associated with ice (-0.02) and desert (0.05). The ice is from the most northern tundra zone while the desert peak is from the Gobi region. The other two, vegetated peaks are clearly seen in the EVI (0.24, 0.40), but are also noted in the NDVI (0.40, 0.65). Overall, the NDVI histogram more clearly depicted the two lower peaks, while the EVI histogram more clearly depicted the two, higher value peaks (Fig. 8). A north to south VI transect through Asia produced contrasting results with the two indices (Fig. 8). There were clear transitions present in the EVI from the northern biomes (tundra) through the central grasslands and southern tropical and subtropical forest areas. These were no so well defined in the NDVI, particularly in the second half of the transect where there is little noticeable trends in the NDVI. Overall, the NDVI transect appeared noisier.

3.5 Global

In Figure 9 we see the global distribution of values as depicted by VI histograms. The NDVI and EVI both showed the strong, concentrated peaks at values of 0.05, representative of the large, hyperarid landmasses, such as the Sahara, Kalahari, Gobi, and Atacama. A separate 'ice peak' also occurred at slightly negative values, -0.05 in the case of the NDVI and –0.02 for the EVI. The EVI 'ice peak' was not so developed due to a

problem with the blue band over ice, causing missing values for large portions of Antarctica and Greenland. The rest of the histogram structures were fairly normally distributed but different in shape between the two VI's. In comparison to the EVI, the NDVI histogram showed a higher percentage of pixels at the higher values. The NDVI enhances the values from semi-arid and sub-humid biome pixels, while compressing the signals from the Earth's forested regions. Thus, the NDVI, with a more dynamic range of values over the semiarid and sub-humid regions, may be more sensitive to change detection is such biomes while the EVI may be more useful in densely vegetated regions where it has an extended range of values.

4. Discussion and Conclusions

The continental-scale histograms of individual band reflectances and vegetation indices were found to be useful in the analysis of vegetation indices as monitoring tools. Both the NDVI and the EVI equations and compositing procedures were found to be operational and applicable at global and continental scales. The two vegetation indices exhibited varying sensitivities to different regions, which would affect their use for change detection and monitoring studies as well as the derivation of certain biophysical quantities. For change detection, land cover/ land use change analysis, and monitoring studies, the EVI would appear to be more reliable in densely vegetated areas since it does not readily saturate as in the case of the NDVI. Furthermore, the aerosol resistance capability of the EVI was depicted in both the transects and histograms. The EVI histograms were much sharper, delineating discrete land cover types. The NDVI histogram features became blurred with the presence of smoke from extensive and regional biomass burning. The transects through the Amazon as well as the Congo basin in Africa demonstrated how much the NDVI was compromised by smoke with an average 30% decrease in NDVI values, relative to the 5-10% drop in EVI values.

In drier, semiarid regions, the NDVI appears to be more sensitive with enhanced signals. The NDVI responded more readily to variations in vegetation in arid and semiarid regions. The NDVI histograms showed more features on the arid side (lower values) relative to the EVI. However, these enhanced signals must be weighted by potential 'enhancements' in canopy background noise. Although the baseline behavior of both indices in hyperarid sites was good, one could not assess the canopy background problem over vegetated areas with the data sets used in this study. Canopy background problems primarily occur through intimate mixing (first-order) of both vegetation and background components.

For certain biophysical quantities, such as %cover and fAPAR, the observed NDVI distribution of pixels may be the desired situation while for other parameters such as LAI and biomass, the EVI may be more useful. Further analysis is needed to better understand VI sensitivities within and across biomes. This includes the need to incorporate validation test site data as markers in both the transects and histograms of this type of study as well as to incorporate more quantitative biophysical data.

Acknowledgments

The authors thank Nazmi Z. El Saleous in providing the atmosphere corrected SeaWiFS images. This work is supported by NASA/MODIS Contract No. NAS5-31364 and NASDA/ GLI Contract G-0018.

5. References

Cihlar, J., Manak, D., and Voisin, N., 1994, AVHRR bidirectional reflectance effects and compositing, Remote Sens. Environ., 48:77-88.

Holben, B.N., 1986, Characterization of maximum value composites from temporal AVHRR data, Int. J. Remote Sensing, 7:1417-1434.

Huete, A.R.,.Liu,, H.Q., Batchily ,K., van Leeuwen. W.J.D., 1997, A comparison of vegetation indices over a global set of TM images for EOS-MODIS, Remote Sens. Environ., 59:440-451.

James, M.E, and Kalluri, S.N., 1994, The Pathfinder AVHRR land data set: an improved coarse resolution data set for terrestrial monitoring, Int. J. Remote Sensing, 15:3347-3363.

Kaufman Y.J., and Tanre, D., 1992, Atmospherically resistant vegetation index (ARVI) for EOS-MODIS, IEEE Trans. Geosci. Remote Sensing, 30:261-270.

Myneni, R.B., Keeling, C.D., Tucker, C.J., Asrar ,G,, and Nemani, R.R.,1997, Increased plant growth in the northern high latitudes from 1981 to 1991, Nature, 386:698-702.

Townshend, J.R.G., 1994, Global data sets for land applications for the advanced very high resolution radiometer: An introduction, Int. J. Remote Sens., 11:51-54.

van Leeuwen, W.J.D., Huete, A.R., Laing, T.W., 1998, Global vegetation index compositing approach for MODIS-EOS, Remote Sens. Environ., submitted.

Vermote, E.F., Saleous, N. El, Justice, C.O., Kaufman, Y.J., Privette, J.L., Remer, L. , Roger, J.C., Tanre, D., 1997, Atmospheric correction of visible to middle-infrared EOS-MODIS data over land surfaces: Background, operational algorithm and validation, J. Geophys. Res., 102:17131-17142.

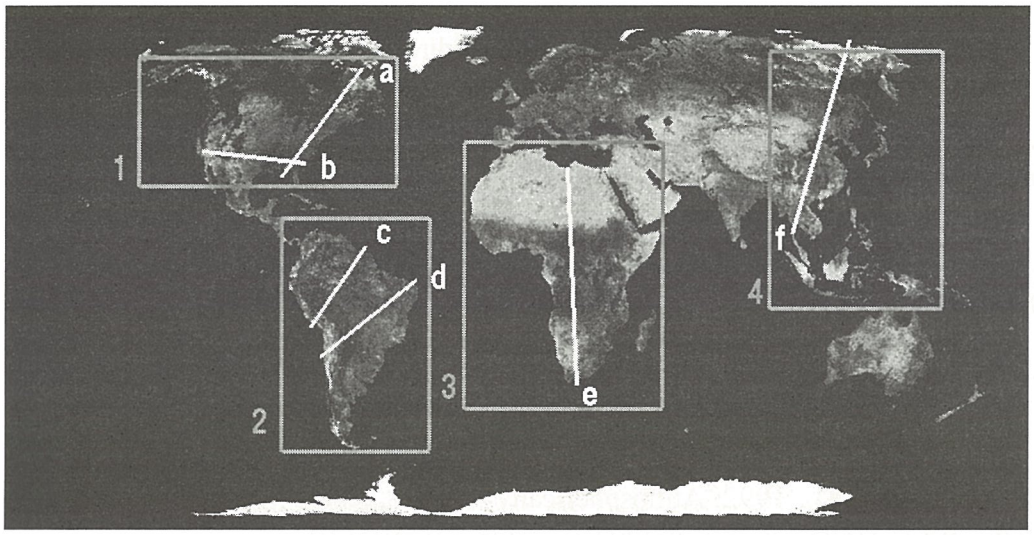

Figure 1. Three-band SeaWiFS color image (NIR, red, and green channels) of the 16-day MVC-based composite (September 15 – October 1, 1997).

Figure 2. Maximum NDVI (top) and EVI (bottom) composites of SeaWiFS data.

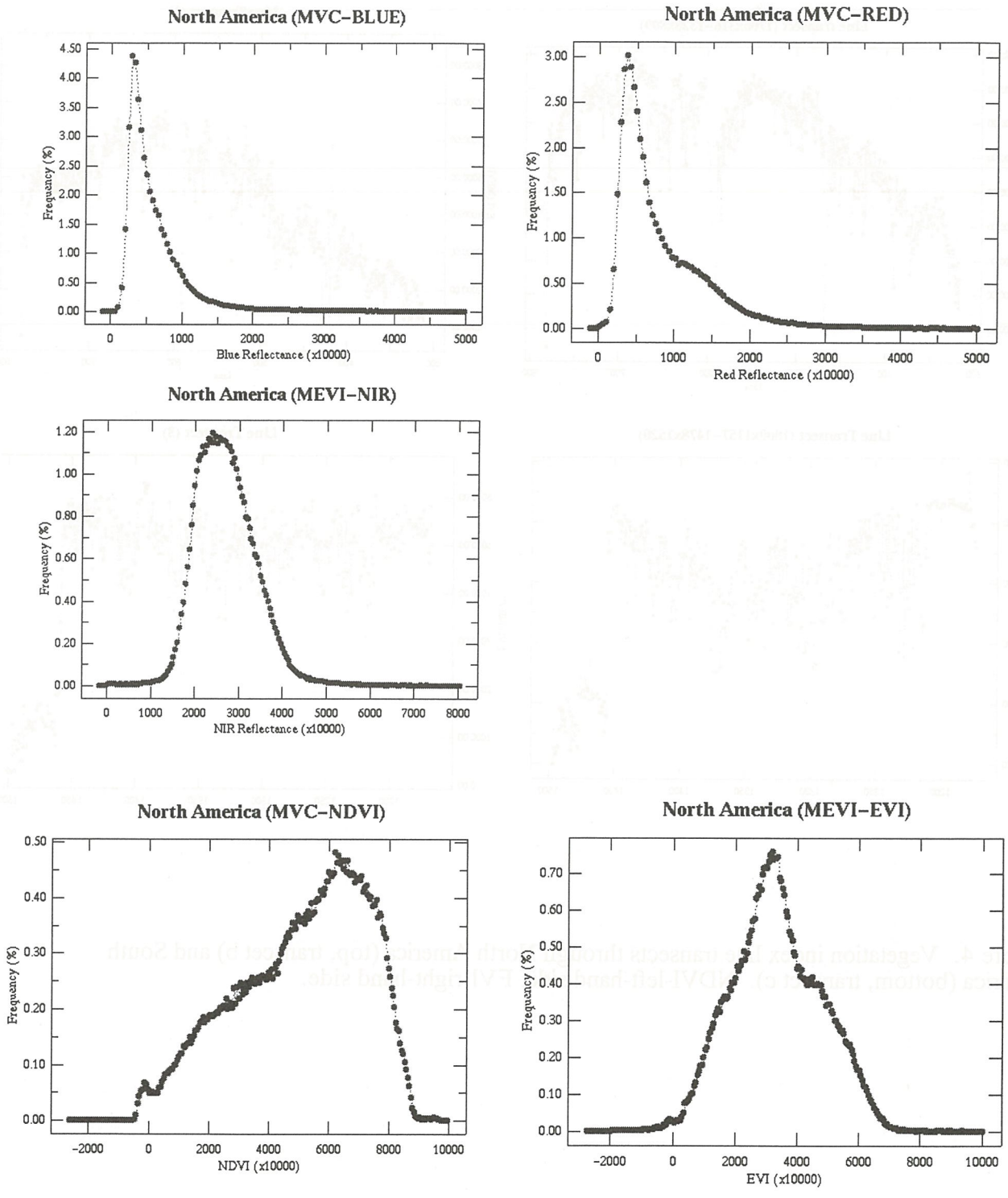

Figure 3. Spectral and vegetation index histograms of North America land surface.

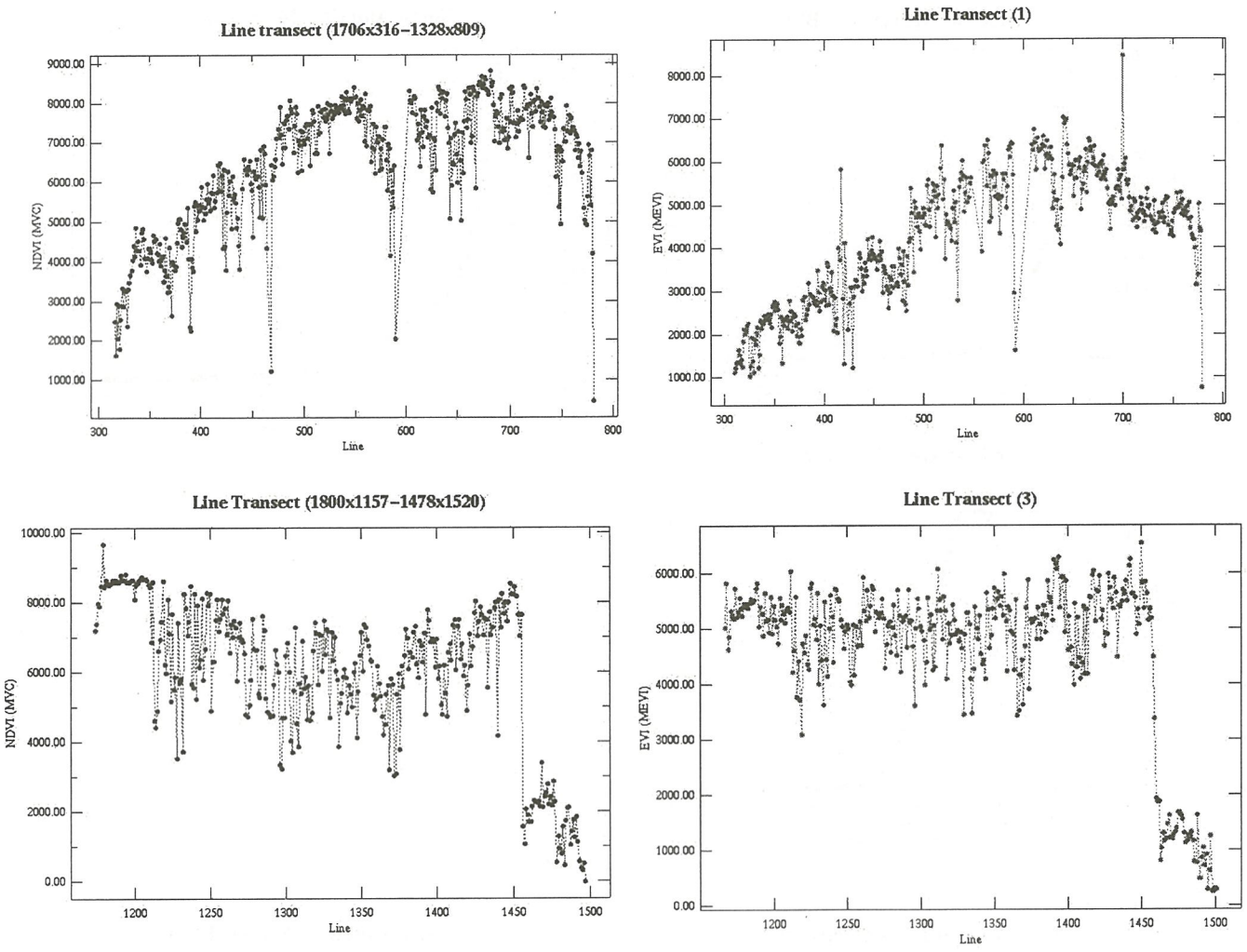

Figure 4. Vegetation index line transects through North America (top, transcet b) and South America (bottom, transect c). NDVI-left-hand side; EVI-right-hand side.

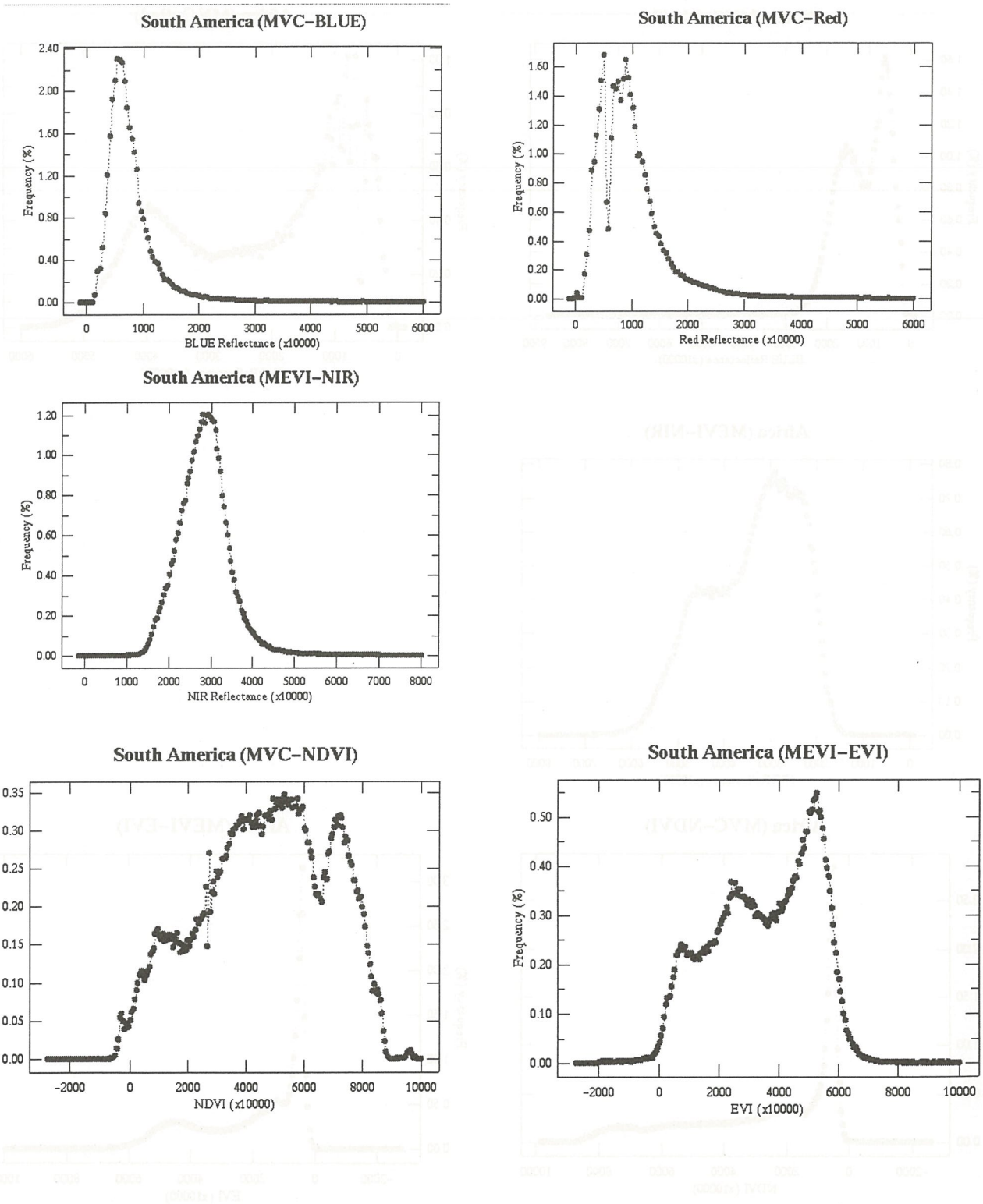

Figure 5. Spectral and vegetation index histograms of South America land surface.

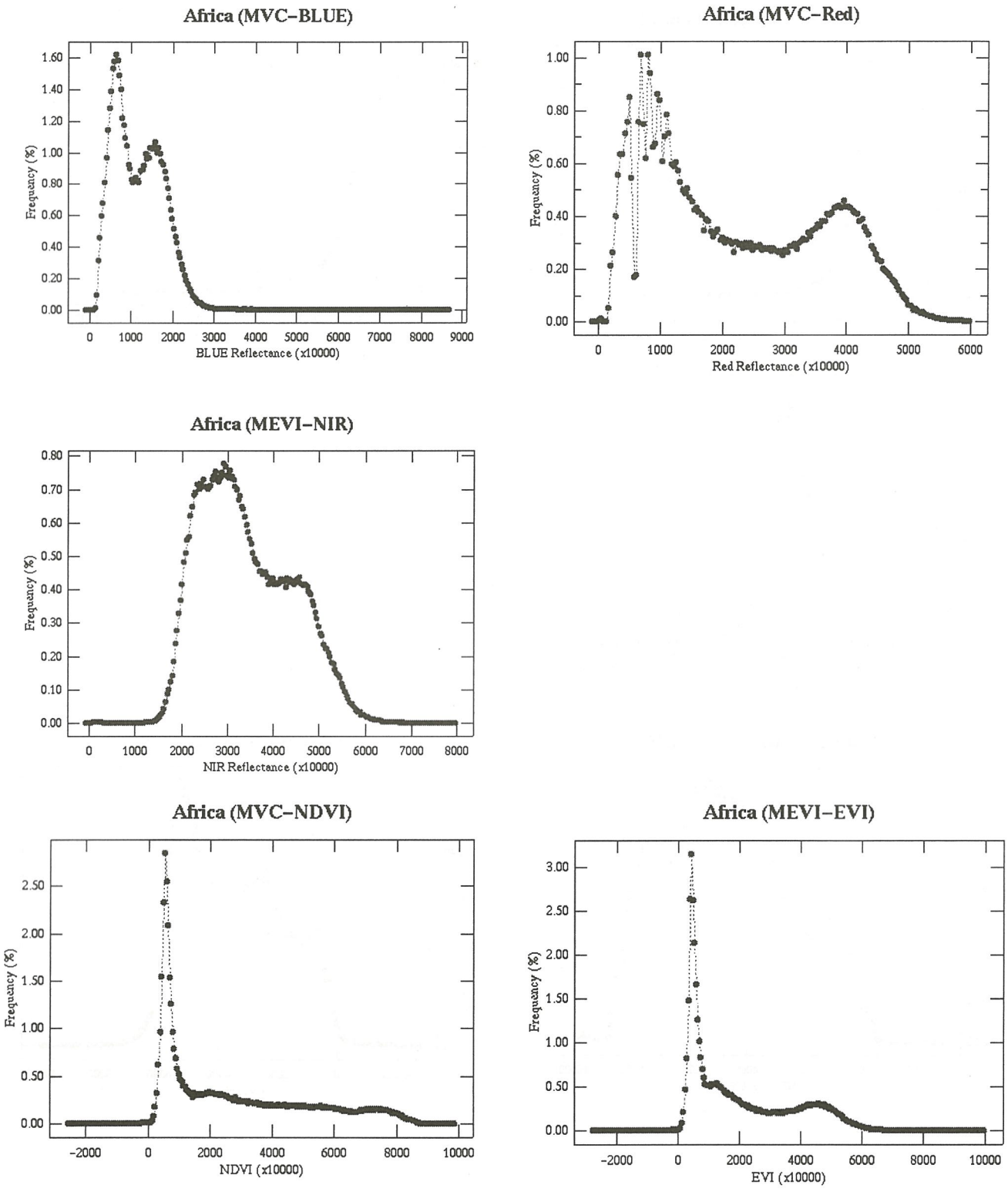

Figure 6. Spectral and vegetation index histograms of Africa land surface.

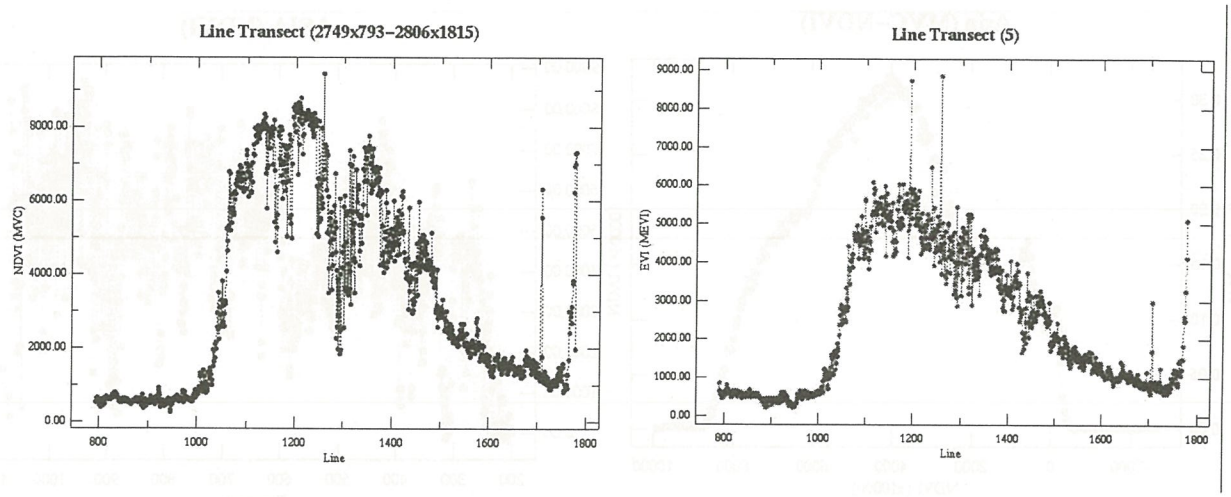

Figure 7. Vegetation index line transect through Africa from north to south (NDVI-top; EVI-bottom).

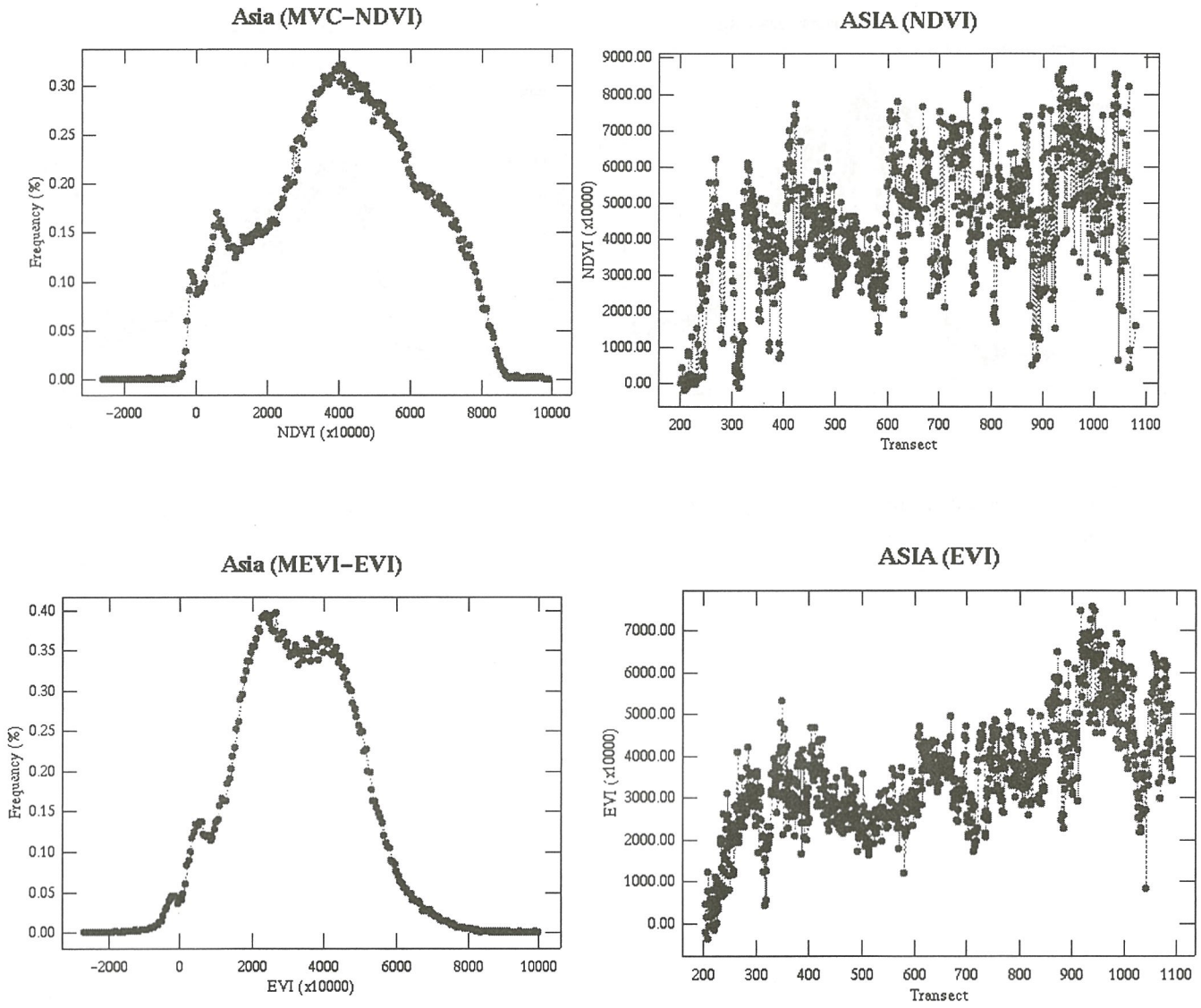

Figure 8. Vegetation index histograms and line transects (north to south) through Asia land surface.

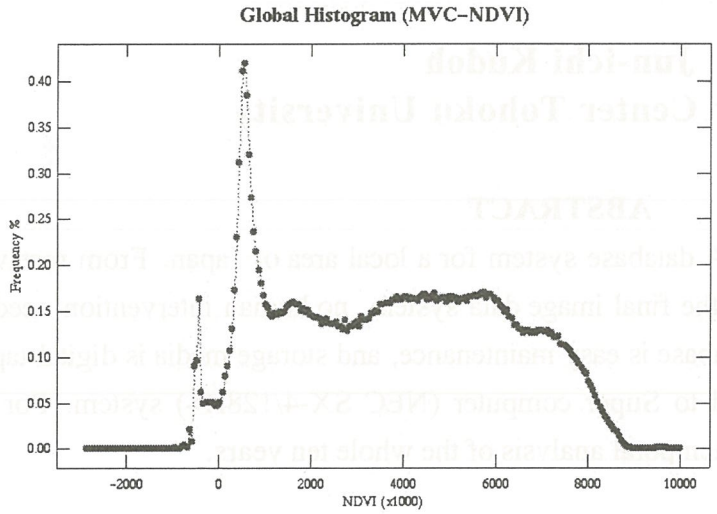

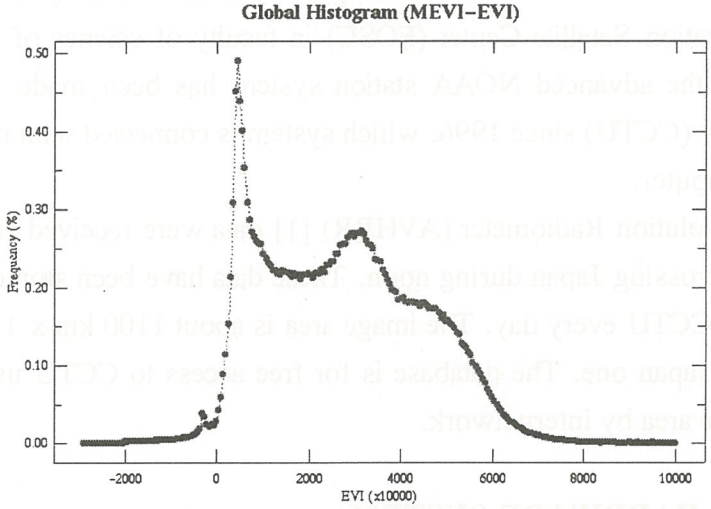

Figure 9. Vegetation index histograms for global land surface.

NOAA AVHRR Data Archives System and User's Service in Computer Center Tohoku University

Jun-ichi Kudoh
Computer Center Tohoku University

ABSTRACT

This paper describes a NOAA database system for a local area of Japan. From receiving the NOAA satellite data to making the final image data system, no human intervention needed. The management system of the database is easy maintenance, and storage media is digital tapes. And also this system is connected to Super computer (NEC SX-4/128H4) system. For the special case study, it is possible to temporal analysis of the whole ten years.

INTRODUCTION

Reception and analysis of the National Oceanic and Atmospheric Administration (NOAA) satellite data made by Earth Observation Satellite Center (EOSC) in faculty of science of Tohoku University from 1988. And the advanced NOAA station system has been made by Computer Center Tohoku University (CCTU) since 1996, which system is connected with high speed ATM network and Super computer.

The Advanced Very High Resolution Radiometer (AVHRR) [1] data were received from the daylight NOAA satellite, while crossing Japan during noon. These data have been stored in Japan Image Database (JAIDAS) at CCTU every day. The image area is about 1100 km x 1100 km with East Japan area and West Japan one. The database is for free access to CCTU users and also reduced version of the same area by internetwork.

HARDWARE SYSTEM

The CCTU serves for researchers and graduate students of the universities distributed in Japan. Figure 1 shows the outline of NOAA station and mainly NOAA AVHRR data processing system. The Super computer is NEC SX-4/128H4, which has total 256 Gflops, 32 Gbyte main memory and connect with Power Onyx and Onyx2 by HIPPI (800 Mbps) network. And also mainly computers are connected by the GIGA switch including the data server computer system which has total 1 TB storage disk.

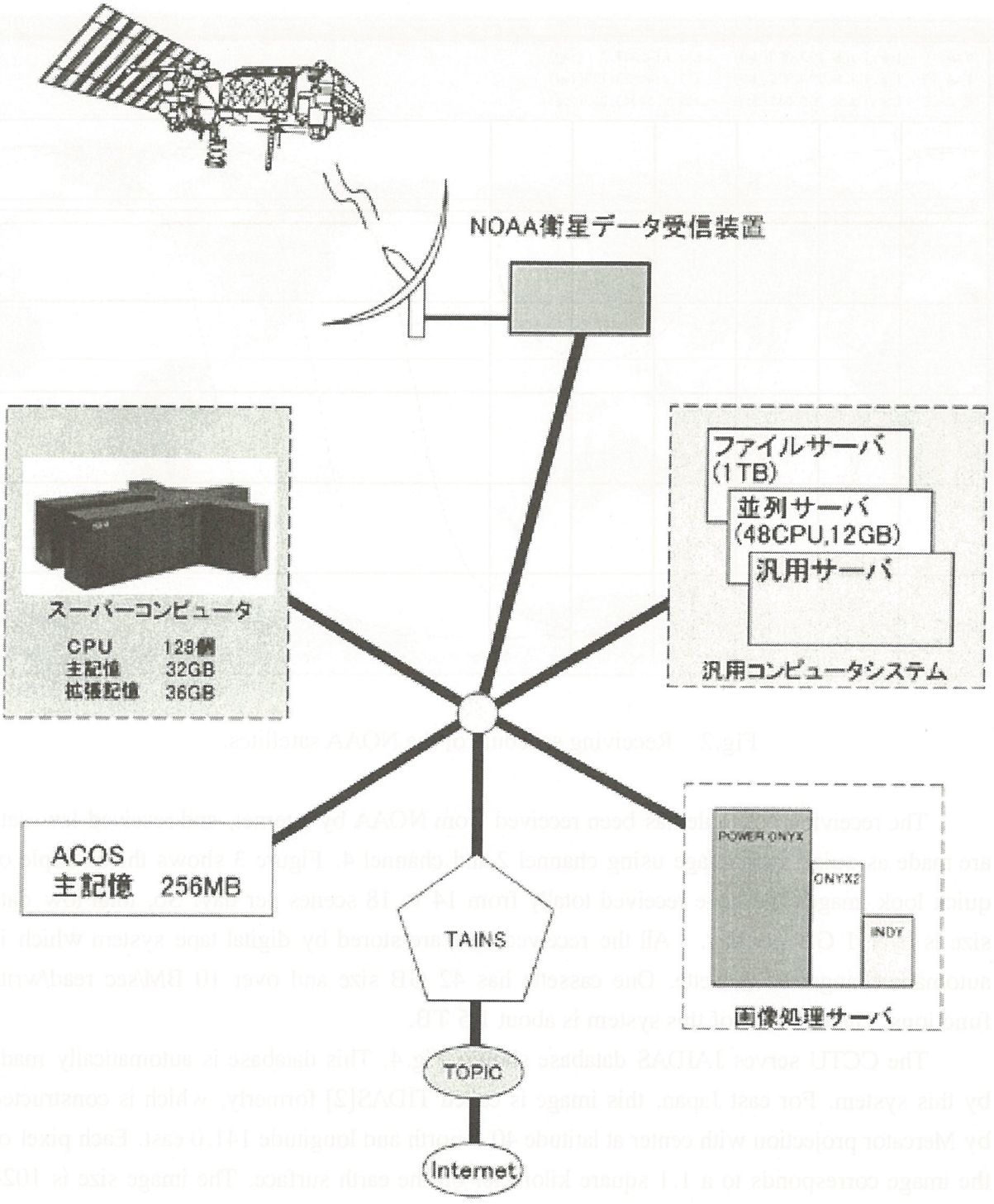

Fig.1 Outline of the Super computer system.

The coverage of NOAA station received in CCTU is shown Fig.2. This area is Far East

Region, especially, Kamchatka Yakutsk and lake Bikal etc Russia territory are interested.

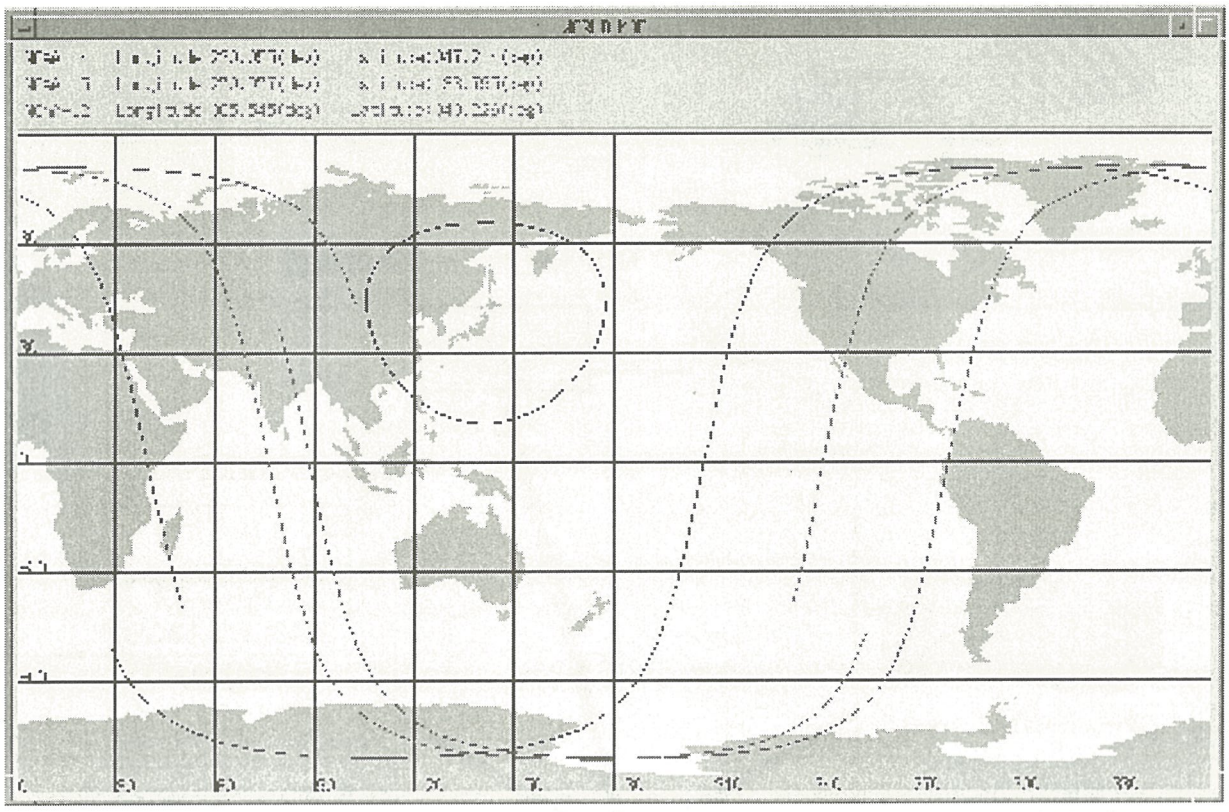

Fig.2 Receiving schedule of the NOAA satellites.

The receiving schedule has been received from NOAA by internet, and received law data are made as quick look image using channel 2 and channel 4. Figure 3 shows the example of quick look image. We have received totally from 14 to 18 scenes per day. So, total low data size is over 1 GB per day. All the received data are stored by digital tape system which is automatic change the cassette. One cassette has 42 GB size and over 10 BM/sec read/write functions. The total size of this system is about 1.5 TB.

The CCTU serves JAIDAS database shown Fig.4. This database is automatically made by this system. For east Japan, this image is called TIDAS[2] formerly, which is constructed by Mercator projection with center at latitude 40.0 north and longitude 141.0 east. Each pixel of the image corresponds to a 1.1 square kilometer on the earth surface. The image size is 1024 pixel x 1024 line.

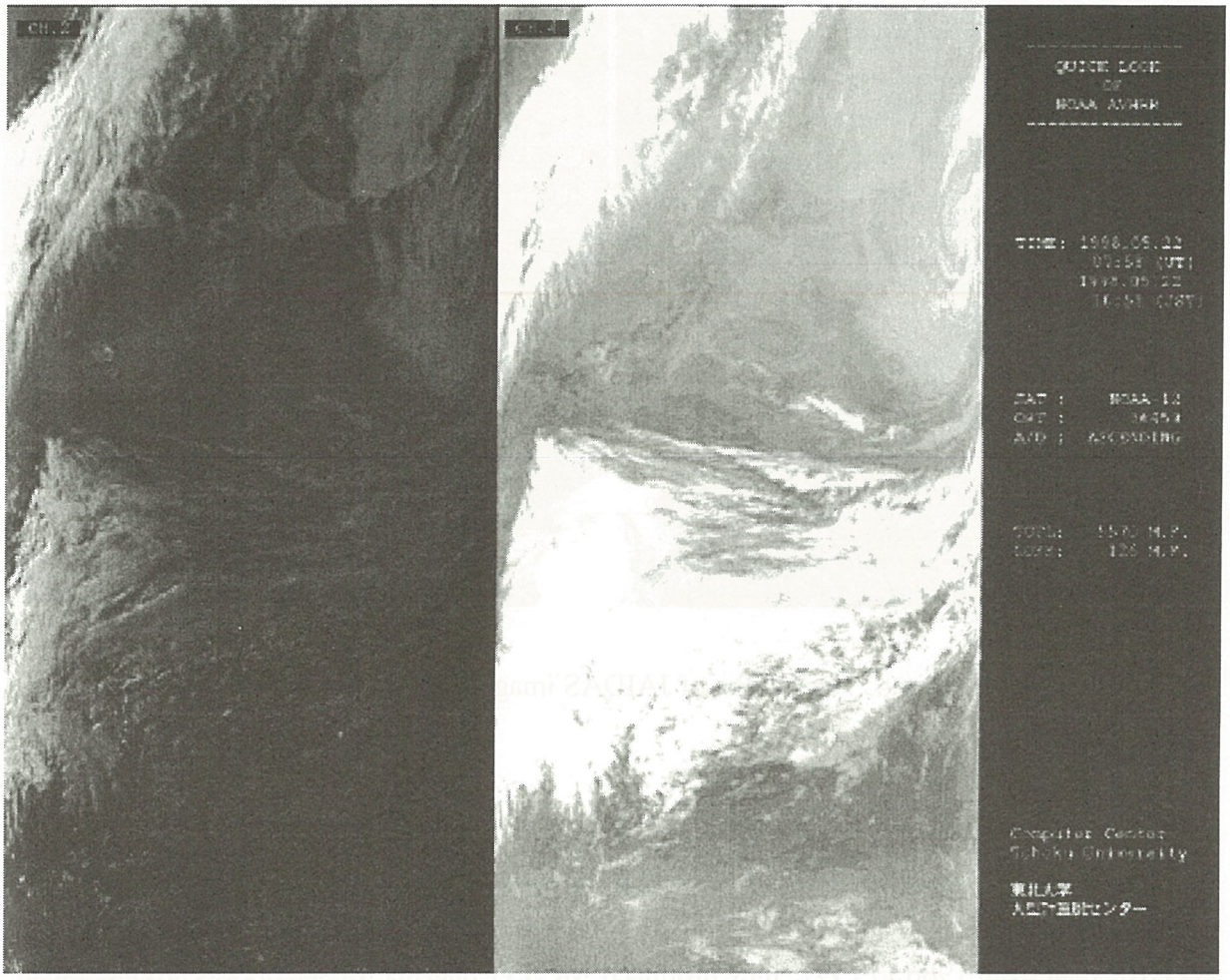

Fig.3 An example of Quick Look image.

So the subject area is about 1100 square kilometer around the center of Sendai city. For west Japan, the image structure is same with center at (31.1 N, 133.3 E). The search and browse the image are operated by internet browse such a Netscape.

JAIDAS was used for total over 80,000 images by internet in 1997.

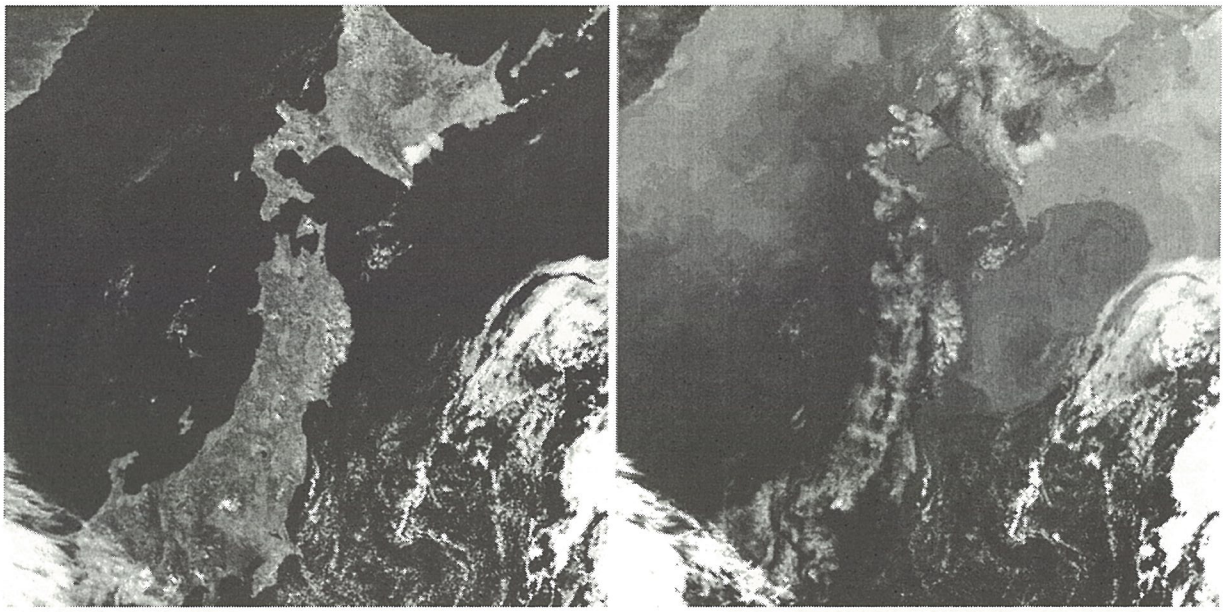

Fig.4 One scene of JAIDAS image for East Japan.

EXAMPLE STUDY USING SUPER COMPUTER OF AVHRR PROCESSING

A-HIGHERS was studied by H. Kawamura[3]. In this study, by using the archived AVHRR data from 1988 to 1997, they produced MCSST data set for the oceans around Japan. The processing are is 0.01 degree. Each AVHRR scene is processed and mapped on the processing area with the equal grided pixels of SST value. Each image consists of 4001 x 4001 pixels with the could and ancillary information. The volume of processed image is about 60 MB. Several test showed that the processing time in SX-3/44R, which is previous Super computer (25.6 Gflops and 4 GB memory), is about 15 minutes. Now SX-4 takes about 1/5 time of the same size data processing.

Forest fire problem for the Siberia is studied by J. Kudoh[4]. In this study, 99 scenes NOAA AVHRR images used of the Khabarovsk-Sakhalin region from April to October in 1998. Figure 5 shows the results of total burned area with red points and calculated about 2400 square kilometer. This study needed the very large size of memory of the Super computer.

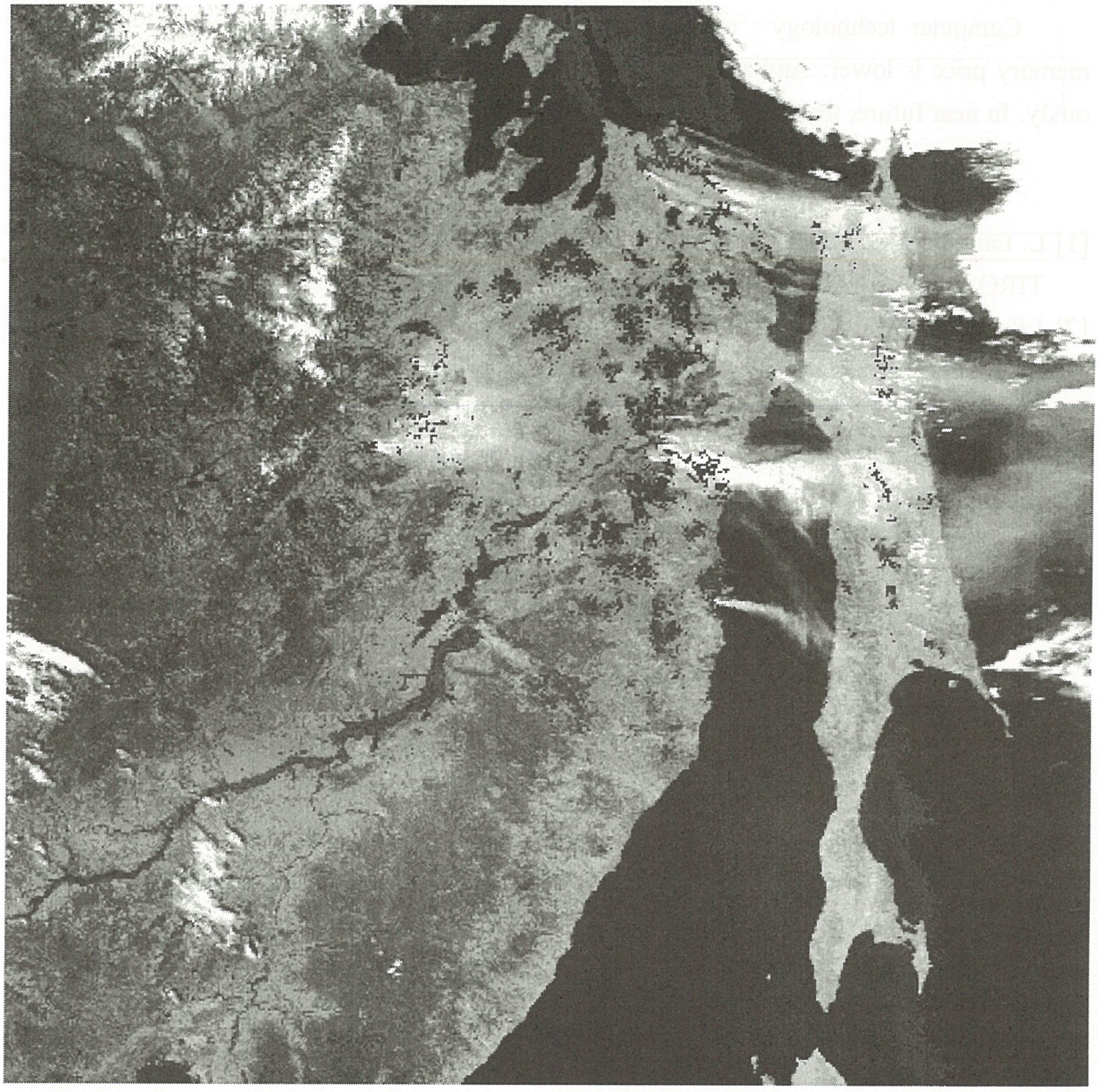

Fig.5 Forest fire study for Far East reggion of Russia (Khabarovsk-Sakhalin) in 1998.

CONCLUSIONS

The Super computing of NOAA AVHRR images is worth as follows;

(1) Temporal analysis for a long time periods, whcih need a high speed calculation and large size of data storage.

(2)Multidimensional analysis for a temporal image processing, which needs a very

large size of main memory.

Computer technology makes progress rapidly, so the CPU power is higher and memory price is lower. And also progress of large disk size and lower price are simultaneously. In near future, these super computing process will be done by personally.

REFERENCES

[1] L. Lauriston, G. J. nelson, F.W. Porto, Data Extraction and Calibration of TIROS-N / NOAA Radiometers, NOAA Technical Memorandum NESS1077 (1979).

[2] J.Kudoh , H.Kawamura , S.Matsuzawa, S.Obata, Y.Nemoto , A Building of New Tohoku Image Database(TIDAS), IEEE International Geoscience and Re mote Sensing Symposium, IV, (1993), 2099-2101.

[3] H.Kawamura, F.Sakaida, J.Kudo, Super computing of 10-years HRPT data set for analyses of AVHRR-derived SSTs, IEEE International Geoscience and Re mote Sensing Symposium, (1997), 1499-1501.

[4] J. Kudoh, Forest Fire Analysis with NOAA AVHRR images of the Far East Region of Russia in 1998, (submitted).

Monitoring and Mapping Land-Cover Change in East Asia

Cheng Shupeng, Professor, Academician of Chinese Academy of Sciences
Cheng Yufeng, Dr.
The State Key Laboratory of Resource and Environment Information System (LREIS)
Institute of Geography, Chinese Academy of Sciences
Beijing, 100101, China
E-mail: chensp@lreis.ac.cn, yufeng.chen@bj.col.com.cn

Abstract:

Some activities related to the land-cover change studies have been going since the early 1980's. Nowadays, the Chinese scientists have been conceiving of the international cooperative research project on land-cover change in East Asia by remote sensing and geo-information system as following: compiling a vegetation/land-cover maps of East Asia at a scale of 1:5M with the historical, current and future periods; estimating the terrestrial and marine biomass and net primary production; and projecting the tendency/variety of vegetation-land-cover change.

Keywords: Land-cover change, maps, remote sensing, geo-information system, East Asia

Global change, especially, land-cover change is the very urgent and important environmental and social issues facing to humanity nowadays. Over the past 3 years, Chinese scientific community has made a lot of progress on land-cover change for the global environmental change studies. It may be as support for the monitoring and mapping land-cover change in East Asia.

Research Progress related to the land-cover change

Some activities organized under the IGBP Committee of China, and the supported by the Institution of Chinese Academy of Sciences have been going since the early 80's, including as following: the studies on impacts of global climate change; macro-scale remote sensed investigation of national land resources and environment; monitoring and evaluation of land-cover change; The eco-physiological studies; the research on the North East China Transect (NECT); the PEP-II profile setting (Arctic-Antarctic-Equator).

Some important results may be introduced as following:

1. Geo-spatial database

A scientific geo-spatial database, named "LREIS data" loaded in a sheet of CD-ROM, has been developed in the State Key Laboratory of Resource and Environment Information System (LREIS), Institute of Geography, CAS. In the "LREIS data", 17 kinds of geo-spatial database at a scale of 1:4M with the formats such as ARC/INFO Coverage, E00, DLG, etc., were included in CD-ROM as following: political boundary with province and country, terrain isolines, soil, vegetation, drainage system, lakes, desert, swamp/marsh and so on.
A world commercial CD-ROM production, named by "ARC-China" including information of political boundary for province, municipality and country, and terrain isolines, drainage network and residential sites, etc. at a scale of 1:1M, has published trough the cooperation between the State Bureau of Surveying and Mapping of China and Environmental System Research Institute

of USA in 1998. In addition, the maps and databases at the scale of 1:1M such as land-use, land resource, grassland, etc. have been published in China.

A new edition of National Atlas of Physiography including more than 200 sheets of thematic maps has been drawing and printing by geographical information system (GIS), whose first edition was published 30 years ago. Moreover, the National Atlas of agriculture, population and economics were published by China Map Press and Oxford Press, which are the most detail and most integrated materials to study the land-cover and landuse so far. Moreover, In addition, more than two dozen of provincial and regional atlases have been published in the past 20 years. These atlases provide detailed historical and current information for studying the global change of China in the physical and human dimensions.

2. Macro-scale Remote Sensed Investigation of National Land Resources and Environment

From 1990 to 1995, the Project "Macro-scale Remote Sensed Investigation of National Land Resources and Environment" has been carried out, which used newly received TM imagery as main information sources and some space images produced by Chinese satellite as supplementary information sources, and produced the land-cover maps covering whole China (1:250 000 scale for the eastern part an d 1:500 000 scale for western part). Another project named "Resources and Environment Database of China" is under way in Chinese Academy of Sciences (CAS) from 1994, which aims to systematically collect and digitize the maps related to land use/land cover previously made in CAS. Since 1996, thematic layers of land cover have been planned to update once every two years and macro-scale change monitoring on land resources will be realized (Liu, 1996).

3. Monitoring and evaluation of land-cover change

Regionalization of land cover change in China using remote sensing data (1983-1992): Based on the NDVI from NOAA AVHRR with 1° and 8km resolution and ten-year time series, two indexes such as Land Cover Index and Sensibility Index of land cover change were put forward, and the maps of land cover index and the maps of sensitivity index of land cover change were made. Then the following conclusions can be drawn from the analysis of these above maps (Ging et al. 1996): (i) the sensitivity is small in the inland of northwest and Xizang plateau, and large in eastern region (so called the southeast and southwest monsoon region). These are a declining trend from southeast to northwest and an obvious strap regularity for the sensitivity; (ii) the land cover in China is deeply affected by monsoon climate and land use patterns at first, then by geomorphologic statement. Therefore, the three different regions such as southeast monsoon region, northwest and Qinghai-Xizang Plateau region, and southwest monsoon region are indicated firstly, which formed the first-class regions of China. It is shown that East-West differentiation of land cover in China is the most important and the South-North difference which means that the vulnerable ecological region (with low land cover index) might not be a sensible region for land cover change.

Seasonal patterns of spatial differentiation of land cover in China: The global 1° by 1° data from NOAA AVHRR visible and near-infrared channels are used to calculate the NDVI to cover China area from July of 1981 to August of 1994, it is revealed through principal component and factor analyses methods that there exist four types of seasonal patterns of spatial differentiation of land cover in China, i.e., November to next March type, June to September type, May or October type and April type (Chen, 1998).

4. Environmental factors monitoring

Land use and land cover change: 1:1M landuse maps and land resources maps over the whole country were published in 1990 and 1992, respectively. Then a more detail mapping work at a scale of 1:250 000 has been launching since 1992 in order to build a digital data bank. Now, the multi-frequency and multi-polarization Global SAR data have been used to study the classification of land use, especially in southern tropic China (Chen S.P. and Chen Y.F., 1998).

Urbanization: Under the support of the Central Government, 100 cities were monitored using TM in 1997 and over 600 cities in China will be monitored in detail this year. In addition, collaborative projects for urban environmental assessment supported by UNDP/ESCAP in Shenyang City of Liaoning Province and Shanghai metropolis have been published in 1998. Moreover, the urban geographical information systems of Shenzhen, Xiamen and so on have been established and the urban land use changes have also been evaluated.

Desertificaton: In this field, a lot of exploration and research, led by Prof. Ci Longjun form the center of desertification under of the Ministry of Terrestrial Resources, with the cooperation of UN and many other countries, have been undergoing. Moreover, along term works, led by Prof. Zhu Zhenda, have been continuing in the Landzhou Institute of Desert, CAS since 1950's.

Qinghai-Xizang Plateau: Qinghai-Xizang Plateau, called as "Roof of the world", is one of the most sensitive areas of the Earth to global change and is one driving area to climate change in Asian monsoon areas. The extensive uplift of the plateau in the past could have strong impacts on itself, the neighboring regions and the global change. Since 1980's, the Chinese research community has developed studies of integrated survey and environmental changes of the Qinghai-Xizang Plateau, and has made a great contribution to global change studies, such as: uplift of Plateau and corresponding environmental change; response of glacier, snow deposit, and permafrost on the Plateau to modern climate change; climate characteristics of the Plateau during the last 2000 years; framework of eco-geographical regions on the plateau (Qin et al., 1998: Section 2.7).

5. The eco-physiological studies

China has founded a national wide network, the Chinese Ecosystem Research Network (CERN), including 29 research stations, 5 sub-centers and 1 integrated center. The 29 ecological stations represent major ecosystem types in China, such as farmlands, forests, grasslands, lakes and marine areas. The five specialized sub-centers are composed of hydrogen, soil, atmosphere, lake and biology, together with 29 stations being financially supported by the integrated center. The main function of CERN is to obverse the ecological process of China's main ecosystem, and their response to environmental changes to investigate the structure, function and dynamics of an ecosystem.

Amongst the 233 species investigated that belong to 37 families and 144 genus, 89 species were C_4 photosynthetic pathways. The habitats for C_4 species were mostly dry and salt alkaline, and much more tolerant to heat and barren and alkaline environment than C_3 species.

By applying the method to fuzzy analysis, and the ecological geographical zonalization in the biodiversity studies, it was suggested that a four class system to determine the main biomes in

China, which are biodomain, subbiodomain, biome and bioregion. Accordingly, China's terrestrial ecosystems have been divided into 5 biodomains, 7 subbiodomains and 18 biomes (Qin et al., 1998: Section 2.5).

6. The research on the NECT and the PEP-II

The Northeast China Transect (NECT) is one of the first IGBP transect set in the world, which was suggested by Professor Zhang Xinshi, the former director of Institute of Botany, CAS in 1993. It is the most remarkable and typical showcase for the climate gradient featured with precipitation as a driving factors in influencing climatic changes in the temperate zone of middle latitudes in East Asia. NECT runs along the line of 43° 30' North latitude and is caught between 112° and 130° 30' East longitude. It is nearly 1600km long, featuring a vegetation transition from a temperate timberland of evergreen coniferous forests and broadleaved deciduous forests to a mild temperate steppe.

The Polar-to-Polar profile (PEP-II) is one of three Pole-to-Pole transects in the PANASH project, which was proposed by Professor Liu Tungsheng, Academician of Institute of Geology, CAS. China plays the important role in this transect.

Through the above studies, the relationship between vegetation and climate, greenhouse effects on the terrestrial ecosystems and the land use at different spatial and temporal scales will be studying systematically and continually.

7. GIS-based climate-vegetation modeling for the study on impacts of global climate change

A new climate-vegetation model supported by GIS has been developed by Dr. Chen Yufeng in LREIS, Institute of Geography, CAS, in which soil taken as a limited factor and elevation as an affected factor. The result shows that the total precision of the model is not only improved from former 40% to present 70%, but the precision of each vegetation type is also amended significantly (Chen, 1999).

Using the new climate-vegetation model coupled with GIS, the changes of distribution of vegetation types in China are studies according to the scenarios for doubled CO_2, with the biggest negative change in no vegetation region and the biggest positive change in the cold prata under the scenario produced by GISS GCM. However, as for the relative change of absolute area after CO_2 concentration is doubled, there are great differences between the increase and decrease in the area of each vegetation type. The area of such types as temperate deciduous broadleaf forest and shrub, subtropical and mountainous coniferous forest, tropical broadleaf forest, cold prata, annually double harvested or biannually tripe harvested crops, annually single (double) harvested cold-demanding rice etc., tend to expand, while the areas of such types as cold temperate and temperate mountainous coniferous forest, subtropical evergreen broadleaf and deciduous broadleaf mixed forest and shrub, mountainous shrub, temperate desert, cold desert, temperate prata, temperate marsh, annually single harvested crop, annually double harvested rice or warm-demanding dry crop accompanied with rice tend to shrink (Chen and Li, 1996).

Perspective and Proposal

The East Asia is one of the special regions in the world, with the strong monsoon, complex terrain relief and geomorphy, huge population, and centuries-old civilization. Therefore, more

and more attentions have been attracting to study the vegetation change and land cover change in this area. The Chinese scientists have conceived of the international cooperative research project on this area.

1) to compile a vegetation/land-cover maps of East Asia with NOAA AVHRR and SeaWIFs satellite data, at the scale of 1:1M, to showing the relationship between the terrestrial ecosystem and ocean ecosystem and their mutual influences.
2) These maps may be with three temporal type such as history-reconstruction, current-distribution and future-variety by the remote sensing/geographical information systems-based modeling with the knowledge of phenology, three-dimension geo-belt-regularity.
3) To estimate the terrestrial biomass and terrestrial and marine net primary production in the range of East Asia based on phenology and biogeochemistry under the supports of remote sensed geo-mechanism, GIS modeling and climatological models.
4) To project the tendency of vegetation/land-cover change in East Asia on the basis of the scenarios of global climate change, population increase and socioeconomic development, thus putting forward the option adaptation on regional sustainable development.

References

Chen S.P. and Chen Y.F. (1998), Remote sensing and geo-information system, In Qin D.H., Chen P.Q., Ge Q.S(eds.), Advances in Global Change Studies of China, China Ocean Press, Beijing.

Chen Y.F. (1998), Seasonal patterns of spatial differentiation of land-cover change in China, *Chinese Science Bulletin*. (forthcoming).

Chen Y.F. (1999), China climate-vegetation model based on soil classification, *Progress in Natural Science*, 9(1):1-7.(in press)

Chen Y.F. and Li K.R. (1996), GIS-based Research on possible impacts of global climate change on China's vegetation (*in Chinese*), *Acta Geographica Sinica*, 51 (special issue): 26-39.

Gong P., Shi P.J., Pu R.L., Guo H.D. (1996), Earth Observation Technology and Earth System Science (*in Chinese*), Science Press, Beijing.

Liu J.Y. ed (1996), Macro-scale Remote Sensed Investigation of National Land Resources and Environmental and Typical Change Study (*in Chinese*), China Science and Technology Press, Beijing.

Qin D.H., Chen P.Q., Ge Q.S(eds.) (1998), Advances in Global Change Studies of China, China Ocean Press, Beijing.

Session : Global scale action and East Asia action

Extraction of Wetland Areas in the West Siberian Lowland using NOAA/AVHRR Imagery

Masayuki Tamura[a], Hiroto Shimazaki[a], Mitsuhiro Tomosada[a],
Fumiko Makita[a], Zhao Wenjing[a] and Yoshifumi Yasuoka[b]

[a]National Institute for Environmental Studies, Tsukuba, 305-0053 Japan
[b]Institute of Industrial Science, University of Tokyo, Tokyo, 106-8558 Japan

ABSTRACT

A method is presented for extracting wetland areas in northern high-latitude zones using Normalized Difference Vegetation Index (NDVI) and land surface temperature (T_s) calculated from midday NOAA/AVHRR imagery. Wetland areas have been distinguished from other land-cover types using signatures on a scattergram of NDVI vs. T_s. The method was applied for extracting wetland areas in the basin of the Ob River in the west Siberian lowland. The result has been verified with ground-truth data and land-cover classification results obtained from high-resolution satellite images.

1. INTRODUCTION

The west Siberian lowland is presumed to be a large source of atmospheric methane, which is the most important greenhouse gas after carbon dioxide. The Japan-Russia joint research project conducted since 1991 by the National Institute for Environmental Studies (NIES) and Russian researchers has produced results confirming this presumption[1]. As basic data for estimating regional-scale methane fluxes from the west Siberian lowland, it is necessary to measure the distribution and areal extent of wetlands and to monitor seasonal changes of vegetation and surface conditions such as surface temperature and water level. Since detailed geographic information is not available in west Siberia and it is often difficult to access wetlands by ground vehicles, satellite or aerial images are necessary for investigating wetland ecosystems and mapping the geographic distribution of wetlands. In this study we present a method for extracting wetland areas in west Siberia using midday NOAA/AVHRR imagery. Use of AVHRR data makes it possible to map the geographic distribution of wetlands with 1-km ground resolution.

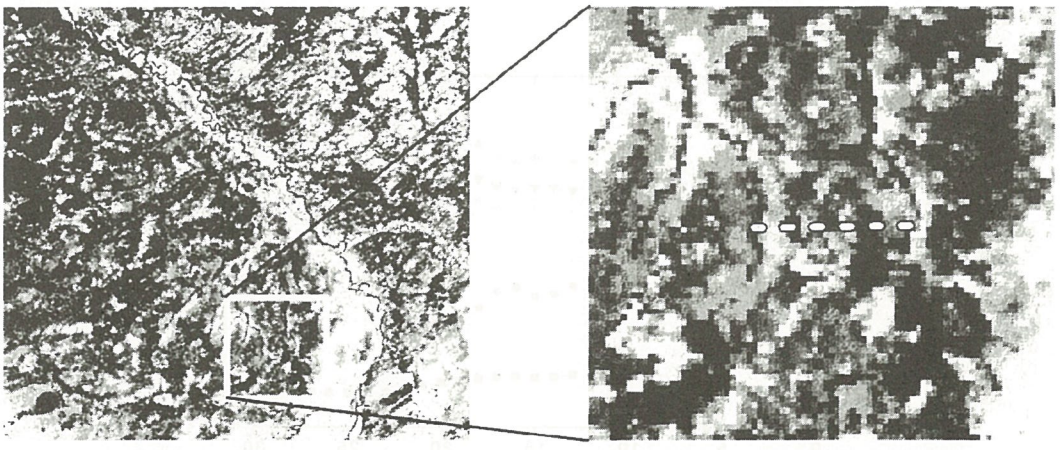

Fig. 1. (a) AVHRR image (in Band 1) obtained on 8th July 1995 in the Obi Basin. Area size: 450 km wide and 415 km long. Scene center: (82°E, 58°N). (b) Ground-observation site.

2. STUDY AREA

Fig. 1 (a) shows the AVHRR image taken at 7:21 GMT (around 13:00 in local solar time) on 8th July 1995 in the basin of the Ob River. It covers a rectangular area centered at (82°E, 58°N) with a width 450 km and a height 415 km. The Ob River flows from bottom right to top left. Wetlands and forests occupy most part of the image area, and there are also several villages and agricultural lands along rivers. The bright spots near the bottom right corner show the city of Tomsk. The wetlands are mainly covered with sphagnum mosses, sedges, cotton grasses, reeds, dwarf shrubs and low pine trees. The forest vegetation consists of both deciduous trees (birches and aspens) and coniferous trees (pines and larches).

The image includes the mires where the NIES and Russian researches are making ground observations of wetland vegetation, methane fluxes, surface temperatures and water levels. The location of the ground-observation site is indicated by the white rectangle in Fig. 1 (a), and its enlarged image is shown in Fig. 1 (b).

3. EXTRACTION OF WETLAND AREAS

3.1 SPATIAL PROFILES OF AVHRR DATA

Fig. 2 shows the spatial profiles of AVHRR data along the transect line (white dotted line) indicated in Fig. 1 (b). The abscissa denotes distance in a pixel unit; the ordinate denotes reflectance (%) for visible and near infrared bands (bands 1 and 2), and radiometric brightness temperature (°C) for thermal bands (bands 3-5). The interval between 6 to 22 pixel distances corresponds to a wetland area; the rest parts correspond to forest areas. We see that from the spatial profile characteristics, AVHRR spectral band data can be classified into three groups, i.e. band 1, band 2, and bands 3-5. Band 1 reflectance is higher in wetlands than in forests. It can be explained by the fact that majority of sphagnum mosses found in this region take on brownish color, having higher reflectance in red band than forest green leaves. Band 2 data have higher values in forests than in wetlands, which demonstrates that green leaves have higher reflectance than sphagnum mosses in near infrared band. The dip from 18 to 21 pixel distances corresponds to the place where wetlands have been dried by digging trenches. The bands 3-5 have more or less the same spatial profiles, having higher brightness temperatures in wetlands than in forests. This temperature difference may be explained by two mechanisms. First, forests may have a greater transpiration rate than wetlands; thus, forests have lower surface temperature in midday due to greater latent heat transfer. Second, forest leaves may be cooled by air until leaf temperatures are in close adjustment with air temperatures[2]; on the other hand wetland plants represented by sphagnum mosses may be less cooled by air because they grow in dense clusters near or at the ground surface. We note that surface temperatures have highest values in dried parts of wetlands.

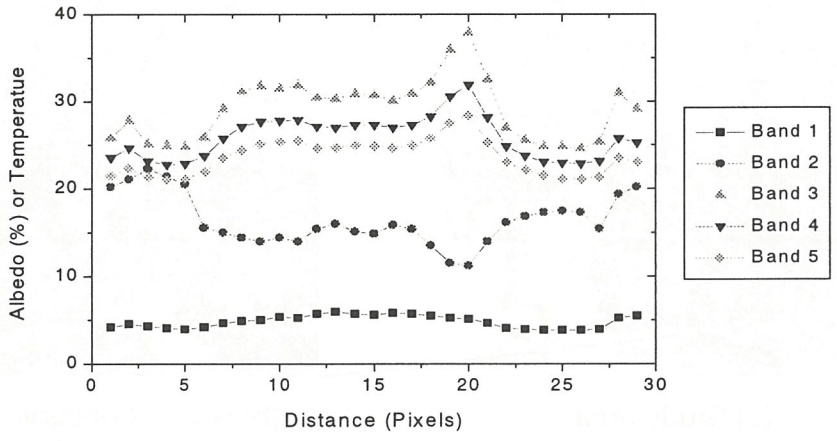

Fig. 2. Spatial profiles of AVHRR data along the transect line in Fig. 1 (b).

From the observation of the spatial profiles of AVHRR data, we have chosen two indices for delineating land cover types in the study area. One is the Normalized Difference Vegetation Index (NDVI) :

$$NDVI = \frac{NIR - RED}{NIR + RED}$$

where RED and NIR are reflectance values of bands 1 and 2 of the AVHRR. The other is surface temperature (T_s) computed by the split-window method[3]:

$$T_s = 1.764T_4 - 0.764T_5 + 0.78$$

where T_4 and T_5 are radiometric brightness temperatures derived from AVHRR bands 4 and 5 respectively. Fig. 3 shows the spatial profiles of NDVI and T_s along the same transect line as in Fig. 2. We can see there is a negative correlation between NDVI and T_s, which has been observed by several researchers for various types of ecosystems[4,5,6,7]. NDVI expresses spectral reflectance properties and density of vegetation; surface temperature, on the other hand, is related to water and energy balance determined by moisture availability, amount of evapotranspiration and local climate factors. Since wetland vegetation has different features from other land-cover types in vegetation properties and moisture status, we can expect that wetland areas can be differentiated from other land-cover types by using NDVI and surface temperature as feature-extraction axes.

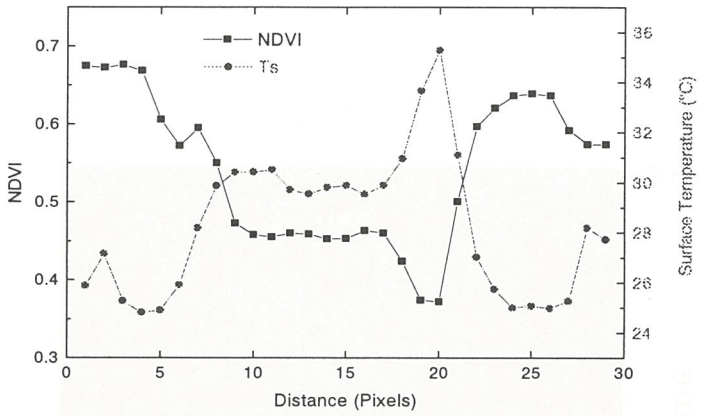

Fig. 3. Spatial profiles of NDVI and surface temperature along the transect line in Fig. 1 (b).

3.2 LAND-COVER CLASSIFICATION BY NDVI AND SURFACE TEMPERATURE

Figs. 4 (a) and (b) illustrate NDVI and surface temperature for the study area respectively. The relation between NDVI and surface temperature can be visualized by a two-dimensional scattergram of NDVI vs. T_s. (Fig. 5). The location of each pixel on the scattergram is determined by the status of vegetation cover and moisture availability. We can hence expect that ecosystems having different properties in vegetation cover and moisture conditions occupy different places on the scattergram.

Signatures of eight land-cover types typically found in this region were drawn on the scattergram: wetlands, birch forests, conifer forests, grasses, soils, rivers, lakes and clouds. The rectangles and '+' signs in Fig. 5 indicate the boundaries and means of training samples of the signatures. Signatures of birch forests, conifer forests, wetlands and soils are placed along a line of a negative slope in descending order of NDVI and in ascending order of T_s. The signature of grasses is located above this line, having higher surface temperatures than wetlands and forests. Lakes and rivers have almost the same surface temperature, but have different NDVI values due to the turbidity of river water. We note that existence of water surface in a pixel tend to shift the location of its scatterplot toward the signature of lake or river water. Clouds are characterized by their low surface temperatures and relatively low NDVI values. Pixels partly contaminated by clouds are shifted toward the signature of clouds.

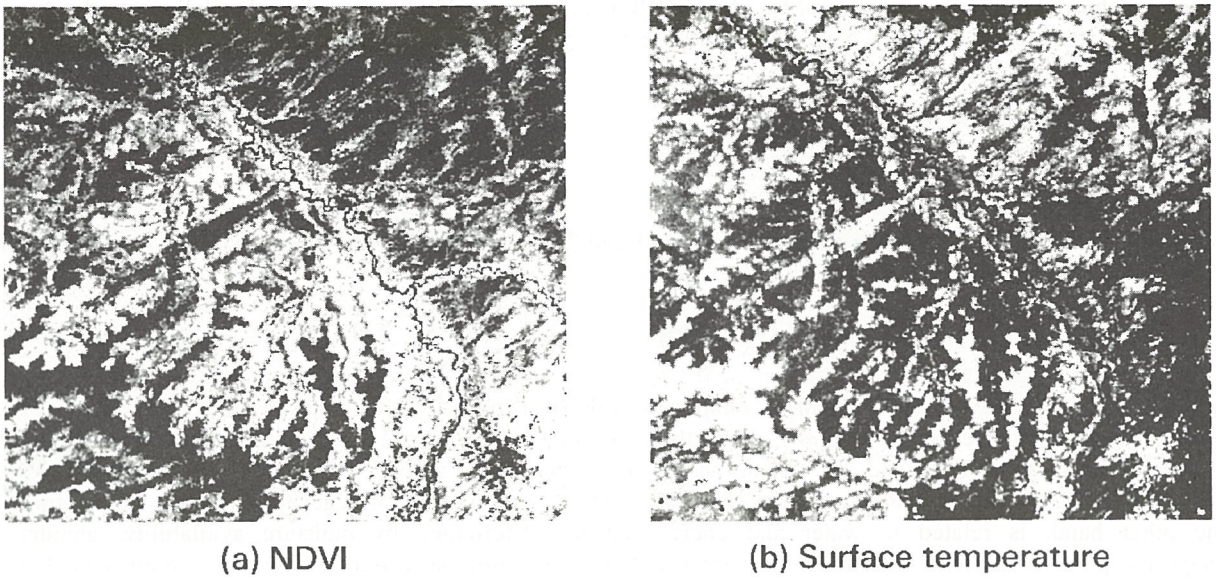

Fig. 4. Study area seen in (a) NDVI and (b) surface temperature.

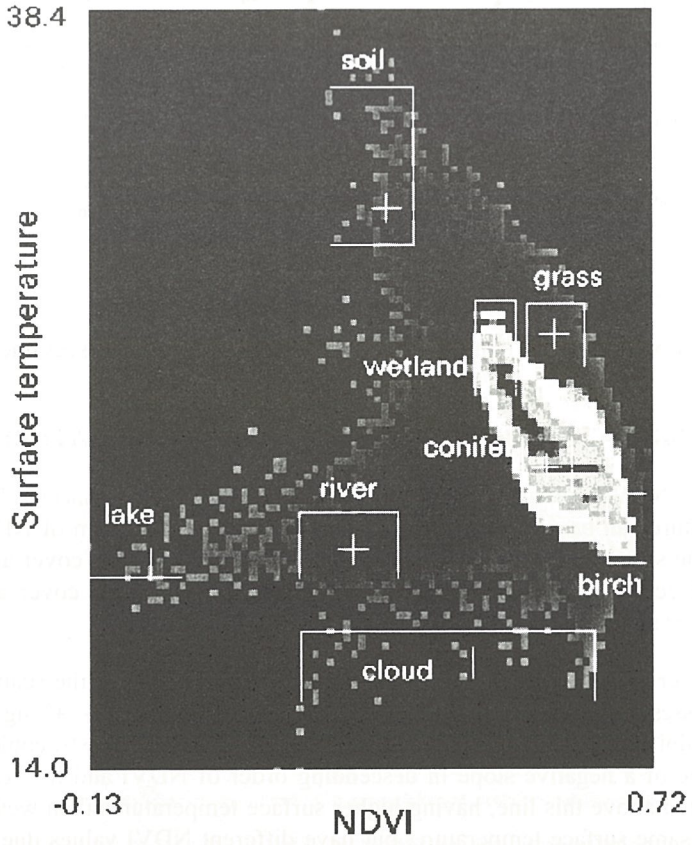

Fig. 5. Scattergram of NDVI vs. T_s. The rectangles and '+' signs show the boundaries and means of signatures.

Using these signatures we classified land-cover types by combined use of parallelepiped decision rule and minimum-distance decision rule. Fig. 6 shows the result of classification. From this result wetlands were estimated to cover 29 % of the entire image area, and forests cover 67 %. For verification, this result was compared with results of land-cover classification obtained from high-resolution satellite images (SPOT/HRV and JERS-1/OPS). For example Fig. 7 (a) shows the result of land-cover classification by SPOT/HRV. Fig. 7 (b) shows the area in Fig. 6 corresponding to the SPOT/HRV image. In both figures wetland areas are indicated by white colors. We can say both results are in fairly good agreement.

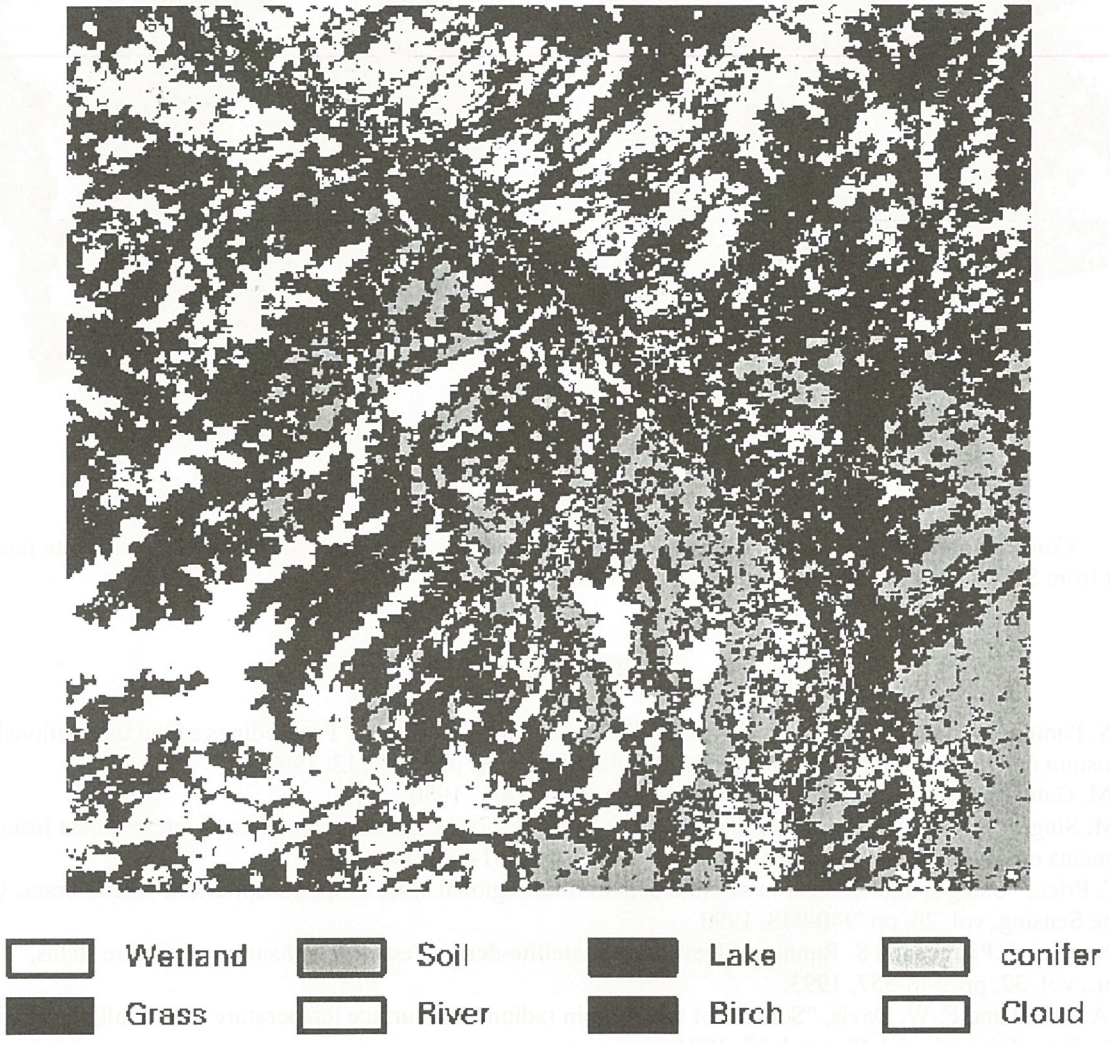

Fig. 6. Result of land-cover classification using NDVI and surface temperature.

4. SUMMARY

Two indices calculated from midday NOAA/AVHRR data (NDVI and surface temperature T_s) have been used to extract wetland areas in the basin of Ob River in the west Siberian lowland. From the observation of the spatial profiles of AVHRR data, we have chosen NDVI and T_s to be suitable for differentiating wetlands from other land-cover types. NDVI reflects properties of vegetation cover. Surface temperature is related to surface energy balance determined by moisture availability and evapotranspiration. A scattergram of NDVI vs. T_s has shown a negative correlation between these indices. NDVI is high in forests and low in wetlands, whereas surface temperature is low in forests and high in wetlands. Signatures of eight typical land-covers (wetlands, birch forests, conifer forests, grasslands, soils, lakes, rivers and clouds) have been drawn on the scattergram of NDVI vs. T_s. Based on these signatures wetland areas have been distinguished from other land cover types by combined use of parallelepiped

decision rule and minimum-distance decision rule. The results have been verified by ground-truth data and by comparison with the results of land-cover classification obtained from high-resolution satellite images.

Fig. 7. Comparison with the result of land-cover classification obtained from a high-resolution satellite image. (a) Result from SPOT/HRV. (b) Result from NOAA/AVHRR.

5. REFERENCES

1. N. S. Panikov, "CH_4 and CO_2 emission from northern wetlands of Russia," Proceedings of the International Symposium on Global Cycles of Atmospheric Greenhouse Gases, pp. 100-112, 1994.
2. D. M. Gate, *Biophysical Ecology*, Springer-Verlag, New York, 1980.
3. S. M. Singh, "Removal of atmospheric effects on a pixel by pixel basis from the thermal infrared data from instruments on satellites," Int. J. Remote Sensing, vol. 5, pp. 161-183, 1984.
4. J. C. Price, "Using spatial context in satellite data to infer regional scale evapotranspiration," IEEE Trans. Geosci. Remote Sensing, vol. 28, pp. 940-948, 1990.
5. R. Nemani, L.Pierce, and S. Running, "Developing satellite-derived estimates of surface moisture status," J. Appl. Meteor., vol. 32, pp. 548-557, 1993.
6. M. A. Friedl and F. W. Davis, "Sources of variation in radiometric surface temperature over a tallgrass prairie," Remote Sens. Environ., vol 48, pp. 1-17, 1994.
7. E. F. Lambin and D. Ehrlich, "The surface temperature-vegetation index space for land cover and land-cover change analysis," Int. J. Remote Sensing, vol. 17, pp. 463-487, 1996.

Present Status of the Global Map Development

Yoshikazu Fukushima, Hiromichi Maruyama
Geographical Survey Institute

1. Introduction

Since the 1972 United Nations Conference on the Human Environment, there has been a growing concern, commonly shared by the people in the world, for the global environment. Contrary to this people's concern, little improvement has been made on the global environment. The 1992 United Nations Conference on Environment and Development (UNCED) recognized that the increasingly serious environmental and developmental problems facing the world require global solutions, and that solutions to these problems require cooperation between nations and between all sectors of society. One of the outcomes of UNCED was Agenda 21 which specifies an action plan for all countries to achieve sustainable development. Eight chapters of Agenda 21, especially Chapter 40 on "Information for Decision Making," describe the need of geographic information for sustainable development.

However, currently available geographic information of scientific quality is still insufficient to provide adequate understanding of actual state of the global environment (Estes and Mooneyhan, 1994). Because of the availability of road maps, colorful pictures of world maps with topographic information and other cartographic products, people tend to think that important, accurate geographic information must have been developed by somebody else and such information must be available somewhere and easily accessible.

Thanks to advances in technologies like satellite remote sensing, geographic information systems, and global positioning systems including computers for large data processing and storage in recent years, development of consistent global geospatial information has become realistic. Actually, some organizations, in cooperation with other countries, have been successful in developing global geospatial information in a relatively short period of time (Geographical Survey Institute, 1996; ISCGM, 1996b). Yet only a limited number of countries and organizations are involved in these activities, and there is still no mechanism to ensure the development and maintenance of consistent, accurate, global geospatial information, and to make such information available and accessible to the public. Without such a mechanism, monitoring the global environment and detecting global change as well as encouraging economic growth within the context of sustainable development would not be attainable.

In order to realize the mechanism, the concept of Global Mapping was developed in 1992 by the Ministry of Construction (MOC) and the Geographical Survey Institute (GSI) of Japan (Geographical Survey Institute, 1996). This paper first summarizes the concept of Global Mapping and the related activities conducted by the GSI, then describes the present status of the Global Map Development including the specifications of the Global Map and data development in South East Asia.

2. Global Map Concept

The International Steering Committee for Global Mapping (ISCGM) defined Global Map as a group of global geographic data sets of known and verified quality, with consistent specifications which will be open to the public, considered a common asset of mankind and distributed worldwide at marginal cost (ISCGM, 1996a). This definition clarifies three basic and important ideas about Global Map: i) global coverage; ii) consistent specifications; and iii)

open to the public and distributed worldwide at marginal cost.

i) Global coverage

Most countries have national mapping organizations for national mapping programs to ensure base map coverage of their countries. Likewise, it is necessary to have global coverage of geospatial information to provide a baseline data sets of our planet.

i) Consistent specifications

Better understanding of the earth sometimes requires direct comparison between different parts of the world. However, if the geodetic datum, mapping accuracy, classification criteria, etc. are not consistent worldwide, accurate understanding of the state of the earth may not be realized. For example, total area of forest or desert would be different, if the classification criteria are not consistent between countries or regions. To detect changes of the earth, frequent update of the data is also important. As for spatial resolution, Global Map has one kilometer resolution on the ground.

iii) Open to the public and distributed worldwide at marginal cost

Even though global geospatial information is developed with consistent specifications, it would be almost useless unless it is made widely available to the international community and used among different sectors of the society. There exist a few data sets whose distribution is prohibited or limited to a specific community due to national security, political sensitivities and other reasons. Similar to the idea of national digital geospatial data framework, Global Map should be open to the public and distributed at marginal cost. The spatial resolution of one kilometer on the ground would cause little concern for national security, as we are anticipating sub-meter pixel resolution imagery from commercial high resolution satellites.

3. History of the Concept and Activities

The idea of Global Mapping, including the establishment of an international body for Global Mapping, was first conceived by MOC and GSI in 1992 as one of the measures of the Ministry for global issues (Geographical Survey Institute, 1996). Since cooperation between all countries and related international organizations in the world are needed for the Global Map development, MOC and GSI have been promoting this Global Map concept at the following academic and UN conferences:

1992 - the Thirteenth Asian Conference on Remote Sensing.
- the Working Group on Data Use of the Committee on Earth Observation Satellites (CEOS).

1993 - the Fifth United Nations Regional Cartographic Conference for the Americas.

1994 - the U.S.-Japan Framework for New Economic Partnership.
- the Thirteenth United Nations Regional Cartographic Conference for Asia and the Pacific. Promotion of geographical information exchange was resolved.
- the International Symposium on Core Data Needs for Environmental Assessment and Sustainable Development Strategies organized by the United Nations Environmental Programme and the United Nations Development Programme. Ten "core" geospatial data types were listed at this Symposium to be developed with top priority (Estes, et al., 1994).
- the Cambridge Conference for National Mapping Organizations (Cambridge Conference).
- the International Conference Concerning the Establishment of the Permanent Committee on GIS Infrastructure for Asia and the Pacific.
- the Seventeenth Conference of International Cartographic Association (ICA).

1997 - the Fourteenth UN Regional Cartographic Conference for Asia and the Pacific. Development of the Global Map was resolved.
- the Sixth United Nations Regional Cartographic Conference for the Americas. Development of the Global Map was resolved.
- the Fifth session of Committee on Sustainable Development. The executive summary of "Interregional Seminar on Global Mapping for the Implementation of Multinational Environmental Agreements" was submitted.
- the Special Session of the United Nations General Assembly. The executive summary of the above seminar was submitted. The adopted document of the Special Session "Programme for the Further Implementation of Agenda 21" refers to Global Mapping in its Paragraph 112.

In addition, GSI organized the First International Workshop on Global Mapping in Izumo, Japan (Izumo Workshop) in November 1994. At this workshop, delegates from mapping organizations from fourteen countries and one international organization reached a number of resolutions regarding ways to promote international cooperation in the development of Global Mapping. Delegates agreed that:

- Action should be taken to achieve the development of Global Mapping by the year 2000;
- Ways must be found to encourage scientific and technological development needed to use data more efficiently;
- A need exists for and ways must be found to provide technical and economic support to developing countries; and,
- There is a need to establish an international steering committee to coordinate the Global Map development preparatory activities and the development and encouragement of this work.

To advance and implement the resolutions of the Izumo Workshop, the Second International Workshop on Global Mapping was held in Tsukuba in February 1996. During the Second Workshop, the International Steering Committee for Global Mapping (ISCGM), which consists of heads and experts of National Mapping Organizations and related international organizations, was established. The primary purpose of ISCGM is to examine measures that concerned national, regional and international organizations can take to foster the development of Global Mapping in order to facilitate the implementation of global agreements and conventions for environmental protection as well as the mitigation of natural disasters and to encourage economic growth within the context of sustainable development (ISCGM, 1996). GSI was designated as the Secretariat of ISCGM.

Based on the resolution of the Izumo Workshop regarding the Global Map development by the year 2000, an idea of phased approach was introduced at the First ISCGM meeting held during the Second Workshop (Geographical Survey Institute, 1996). The first phase of the data development focuses on employing existing global or regional geographic information through mutual information exchange between international agencies and organizations in different countries, and by voluntary efforts of filling in blank areas to complete the Global Map by 2000. In this case, the three basic principles of the Global Map, (i) total global coverage, (ii) consistent specifications, and (iii) open availability (no restrictions, marginal cost) may not be completely realized, but this approach is considered most realistic. Subsequent phases of the Global Map development will include revisions to detect/highlight environmental changes.

To further advance the idea of Global Mapping, "Interregional Seminar on Global Mapping for the Implementation of Multinational Environmental Agreements" was held in Santa Barbara, California in November 1996 under the joint auspices of the United Nations, the University of California at Santa Barbara and GSI. The

Seminar adopted "Santa Barbara Statement on Global Mapping for Implementation of Agenda 21" (Santa Barbara Statement) with nine recommendations including the following items (ISCGM, 1996c):

i) A Global Mapping Forum must be created bringing data users and providers together to facilitate creation of Global Spatial Data Infrastructure (GSDI);

ii) Agencies implementing Agenda 21 accords should precisely define their spatial data and information requirements for implementation, compliance, and monitoring with the assistance of expert groups (e.g. ISCGM). These requirements should be included as priorities of the GSDI;

iii) Overall Global Map development should be fostered under the umbrella of the United Nations and should recognize initiatives being taken at national, regional and global levels; and

iv) These recommendations should be embodied in a report to be presented to the Special Session of the United Nations General Assembly on the Implementation of Agenda 21 in 1997.

Regarding the last item, the executive summary of this Seminar, including the Santa Barbara Statement, was actually submitted jointly by the United States and Japan to the Special Session of the United Nations General Assembly on the Implementation of Agenda 21, as written already.

Global Mapping Forum, which was recommended in the Santa Barbara Statement, was held in Gifu, Japan in November 1997, and in Sioux Falls in June 1998. These forums gave good opportunities to exchange views and opinions on the Global Map between data users and providers. The meetings of the ISCGM were held just after the forums, and the specifications of the Global Map and the invitation to the Global Mapping Project for the national mapping agencies in the world were discussed (ISCGM, 1997,1998). These issues are the first issues to be determined in the implementation stage of the project.

4. Specifications of the Global Map

It is necessary to determine the specifications for starting the development of global mapping data. The specifications were focused on the implementation of the first phase of the data development where existing global or regional geographic information is used as much as possible.

4.1 Data Sources

The following data are used as data sources for the Global Map development.

i) Global 30 Arc Second Elevation Data Set (GTOPO30), which has prepared by USGS, EROS Data Center and other organizations : elevation.

ii) Global Land Cover Characterization Database, which has prepared by USGS, EROS Data Center, Univ. of Nebraska-Lincoln, and EC Joint Research Center : land use / cover and vegetation.

iii) VMAP Level 0, which has prepared by NIMA : drainage system, transportation, boundaries, etc.

Besides these, existing small scale topographic maps are important data source.

4.2 Data Model

The Global Map covers whole land area of the earth at the scale of 1:1 million, or equivalently one km resolution. It consists of both vector layers and raster layers. Vector layers are "Transportation", "Boundaries", "Drainage", and "Population Centers." "Transportation" layer include railroad, road and trail as mandatory. "Boundaries" includes administrative boundaries under international boundaries as mandatory. "Drainage" includes rivers and lakes as mandatory. "Population centers" includes Built-up area, but all features are optional. Elevation, land use / cover and vegetation are stored as raster layers

Data in the both vector and raster layers are described based on the horizontal coordinate system in latitude and longitude referenced to ITRF1994 and GRS80.

4.3 Tiling

The Global Map covers the land area extending entire globe, thus tiling is required to deal with it efficiently. The tiling system is that used for VMAP Level 0. Tile size in longitude direction increases as latitude increases in order to avoid the big difference in the dimension of the tile on the ground among tiles. If the latitude is less than 40 degree, the tile size is 5 degrees by 5 degrees in latitude and longitude direction. If latitude is between 40 degree and 50 degree, the tile size is 5 degree in latitude direction and 6 degree in longitude direction.

4.4 Metadata

The contents of metadata follow the ISO standard of metadata (ISO 15046) which is being discussed at the ISO /TC211. Metadata at conformance level 1 is mandate, and those at conformance level 2 is optional in the Global Map.

4.5 File Format

The vector layers is described by Vector Product Format(VPF), which has been determined by NIMA. The raster data are described in Band Interleaved (BIL) format with a separate header file.

5. The Implementation of the Global Mapping Project

In order to increase the number of national mapping organizations participating in the Global Mapping Project, the invitation letter to the project has sent through UN to the NMOs of Member States. GSI, as the advocator of this project, has started the data development in parts of Asia in cooperation with the countries of the area, which is expected to encourage as many as countries to participate in the project.

In the data development in parts of Asia, source data of vector layers are not VMAP Level 0, but topographic maps prepared by national mapping organization in respective countries. Satellite imagery is also used for updating recent changes on the earth surface related to the contents of the Global Map. The countries involved in this data development are now Philippines, Thailand and Vietnam. GSI plans to extend this cooperative work to other Asian countries.

It is important to make it possible for anybody to access the Global Map easily. The first product developed based on the specifications of the Global Map will be appear next year. Therefore, GSI, as the Secretariat of the ISCGM, is now demanding the budget of the distribute system of the Global Map through Internet as a part of the Budget of GSI in fiscal 1999. It is also important to integrate other global thematic data set, such as soil and population, on the Global Map, which will increase the extent of the application of the Global Map largely.

6. References

Estes, J. E., and D. W. Mooneyhan (1994), Of Maps and Myths, *Photogrammetric Engineering and Remote Sensing, Vol. 60, No. 5, pp. 517-524.*

Estes, J. E., J. Lawless and D. W. Mooneyhan (1994), *Report of the International Symposium on Core Data Needs for Environmental Assessment and Sustainable Development Strategies, Bangkok, Thailand, Nov. 1994, Vols. I & II, Washington D. C.; U. S. Geological Survey, National Mapping Division, Vol. 59p.; Vol. II, 130p.*

Geographical Survey Institute (1996), Present Status and Future Prospects of Global Map Development: A Background Paper for the First Meeting of the International Steering Committee for Global Mapping, *Report of the First Meeting of the International Steering Committee for Global Mapping, Tsukuba, Japan, Feb. 1996.*

ISCGM (1996a), Rules of the International Steering Committee for Global Mapping, *Report of the First Meeting of the International Steering Committee for Global Mapping, Tsukuba, Japan, Feb. 1996.*

ISCGM (1996b), A Survey of Global Mapping Related Activities, *Report of the Second Meeting of the International Steering Committee for Global Mapping, Santa Barbara, California, U.S.A., Nov. 1996.*

ISCGM (1996c), Santa Barbara Statement on Global Mapping for Implementation of Agenda 21, *Report of the Second Meeting of the International Steering Committee for Global Mapping, Santa Barbara, California, U.S.A., Nov. 1996.*

ISCGM(1997), *Report of the Third Meeting of the International Steering Committee for Global Mapping, Gifu, Japan, Nov. 1997,68p.*

ISCGM(1998), *Report of the Fourth Meeting of the International Steering Committee for Global Mapping, Sioux Falls, South Dakota, U.S.A., June. 1998, 128p.*

Kline, K., J. Estes and T. Loveland (1996), The Need for Global Mapping, A background paper prepared for the Interregional Seminar on Global Mapping for Implementation of Multinational Environmental Agreements, *Proceedings of the Interregional Seminar on Global Mapping for Implementation of Multinational Environmental Agreements, Santa Barbara, CA, USA, November 13-16, 1996.*

Murkami, H. (1993), Global Mapping – Global Geographic Data Set for Global Environment Studies, *Proceedings of the International Workshop of Global GIS, Tokyo, Japan, Aug. 1993.*

Nonomura, Kunio (1996), History and Future Prospect of Global Map Concept, *Proceedings of the Interregional Seminar on Global Mapping for Implementation of Multinational Environmental Agreements, Santa Barbara, CA, USA, November 13-16, 1996.*

URL:http://edcwww.cr.usgs.gov/landdaac/glcc/glcc.html, Global Land Cover Characterization Database.

URL:http://edcwww.cr.usgs.gov/landdaac/gtopo30/gtopo30.html, Global 30Arc Second Elevation Data Set.

URL:http://164.214.2.59/publications/specs/printed/VMAP0/vmap0.html, VMAP Level 0.

A Japanese study on carbon cycling: its outline

Yoshio Awaya
Tohoku Research Center,
Forestry and Forest Products Research Institute

1. Background

Although there is uncertainty, global warming will be the most serious problem for us. Increasing of carbon dioxide (CO2) in the atmosphere is outstanding for these several ten years and it is one of the causes (green house gases) of global warming. The global warming will cause very drastic environment changes, which never happened before on the earth, and serious changes on the terrestrial ecosystem. Therefore monitoring of CO2 flux or carbon balance is one of most important problem, and its reality must be made clear urgently. Necessity of carbon balance evaluation was pointed out in the second meeting of Inter-governmental Panel on Climate Change (IPCC) in 1990, and CO2 emission control was discussed in the Kyoto COP3 summit in last December.

On the other hand, progress of earth observation and computer technology is going to improve accuracy of land cover mapping spectrally and spatially. Although the global vegetation index (GVI) of NOAA AVHRR data has been used for global study, there were several problems with GVI data due to its data processing procedure (Goward et.al. 1993). However, finer resolution mosaics has been created by improved data processing procedure, and the problems with GVI is going to be removed. There are some international plans for satellite launches with earth observation sensors such as MODIS on EOS-AM, GLI on ADEOS-II. They have more channels and finer resolution than AVHRR. It would be possible to improve global land cover maps using those data. The data would be also helpful for carbon flux estimation. Therefore, it is an urgent requirement to understand the carbon circulation mechanism and patterns in global scale using updating technology.

Although carbon balance has been studied intensively comparing with other elements such as nitrogen, it is not very clear still now. It was recognized that the ocean was very huge sink of CO2, but carbon balance estimation couldn't tell unknown sink of CO2 at that time. On the other hand, a role of temperate and boreal forests in the northern hemisphere as CO2 sink is becoming clear nowadays, and they say that it may absorb big amount of carbon, which can compensate the missing sink. As seen in the history of carbon balance study, it must be very important to evaluate land and ocean at the same time.

A Japanese carbon flux mapping study, which is called 'Study on global carbon cycle and the

related global mapping' (tentative English title), has been organized sponsored by the Science and Technology Agency of Japan under such backgrounds. It covers both the terrestrial and ocean ecosystems.

2. Outline of the study

The land part of study is explained hereafter. The study is composed of 2 phases, the productivity mapping phase and the carbon flux mapping phase. The objective is global mapping of net primary production (NPP) and some parameters, which affect on NPP, with satellite remote sensing in the first 3-year phase. It will be basic information about carbon cycling. We will execute field surveys to understand mechanism of carbon cycling and to improve mapping accuracy in the eastern Eurasia and Oceania, where we selected as intensive test sites.

2.1 Flow of the study

We take two approaches to estimate global NPP patterns (Fig. 1). There may be some methods for global mapping of NPP. Most promising and simple method is classifying terrestrial ecosystem in detail and allocate an unit value, which would be determined based on past study or results of the project, to each vegetation types. It is called as bulk method in this study and will be utilized to know rough patterns of NPP distribution.

Satellite remote sensing is very effective for large area mapping and many vegetation maps have been produced. Advanced multi-channel satellite data would make global vegetation map more accurate. However, spectral similarity of different vegetation types and variation of phenological-sepctral patterns year by year will cause inconsistency in classification results. And this method cannot show effects of climate changes on NPP.

Due to such problems, we also study a precise method based on process studies of carbon flux in different major vegetation. Continuous measurements of carbon flux will be executed to understand the process, and measurement methods will be improved and systematized. One of primary objective is to develop any process models, which use satellite data directly or indirectly. Vegetation changes would be monitored by satellite data, effects of environmental changes will be monitored by process models. Although basic models have been produced, it would be a hard task to improve models.

2.2 Production and Carbon Flux

Green plants fix CO2 in the air by photosynthesis to their body, and emit CO2 by respiration. CO2 is also released from soils as the result of respiration by roots and bacteria (soil respiration). Total photosynthesis is called gross primary production (GPP) and plants

consume the production for respiration (PR). Difference of GPP and PR is called net primary production (NPP). NPP shows uptake of CO2 by plants, and it can be measured as follows.

$$NPP = \Delta W + L \quad (1)$$

where ΔW is biomass growth of plants and L is litters from plants to soil in a year.

On the other hand, it is necessary to take into account of soil respiration (SR) to know CO2 flux and it is shown as follows.

$$NEP = NPP - SR \quad (2)$$

NEP is called net ecosystem productivity, and it shows CO2 flux (Oikawa, 1991). Therefore it is very important to estimate the amount of CO2 uptake by plants and release by soil to estimate CO2 flux in the terrestrial ecosystems.

We classifies terrestrial vegetation into 3 major groups as follows. Terrestrial vegetation would be classified into 2 types by its structure, trees and herbs. Herbs would be classified into two types, natural herbs and agricultural crops by difference of human interaction. The biggest difference between trees and herbs is that trees have woody parts, which are large in volume and non-assimilatory. Trees and many of natural herbs are perennial plants, and they start growing drastically using nutrient in their roots in early spring in temperate and boreal zones. On the other hand, many of crops are replanted and harvested year by year by human. Thus those would cause big differences in the process of carbon cycling. Therefore we separate terrestrial ecosystems into forest, natural herbs (grasslands and wetlands) and crops (Fig. 2).

It is pointed out that classifying vegetation into same functional types is favorable for ecosystem modeling (Gitay and Noble, 1997). Such classification using satellite data would be necessary, however we have to remind that classification, which based on production types, would be very difficult by satellite data alone. Combination of satellite and environmental information would be necessary to derive better vegetation type maps.

2.3 Classification of vegetation

Ground truth collection is one of hard task for global classification. Vegetation type maps are necessary, but each map would be produced by different classification system. There may be inconsistency of categories among maps, and then high-resolution satellite imagery will become an important ground truth data.

As pointed out widely, the idea of scaling up would be important (Ehleringer and Field, 1993). Since Landsat TM covers important spectral channels, its data could be used to produce simulation data of low resolution imagery of advanced sensors. If it is so, any analysis methodology for TM data could be applied to low resolution data. We would employ 2 level

categories in the global vegetation classification (Fig. 3). The level 1 categories may be classified using low-resolution satellite data alone, and idea of scaling-up would be utilized there.

Although satellite data is effective for large area classification, it would be very difficult to classify vegetation types in detail. Since each plant grows in its ideal environment, and environmental information will be mandatory for level 2 classification.

2.4 Linkage of satellite data and process

Optical satellite sensors measure reflectance from the ground and their data include information about plant biological status, which has close relationship with photosynthesis or productivity. Thus satellite data may be very effective for NPP estimation. It has been recognized that there is a near linear relationship between sum of the normalized vegetation index (NDVI) and productivity of different ecosystems in the continental scale.

NDVI is very well studied, and it was demonstrated that NDVI had a linear relationship with fAPAR and curvilinear relationship with LAI. Although many ecological models use LAI to describe production, this fact shows disadvantage of utilizing satellite data to estimate LAI. On the other hand, sunny and shade leaves have different photosynthetic capacity, LAI may not be a suitable parameter for production modeling. There would be any possibility to utilize fAPAR as an input parameter in production models.

It is impossible to measure soils under dense vegetation canopy directory by remote sensing. therefore it is necessary to know the relationships between soil respiration and environmental factors in global scales. Even soil cannot be observed, decomposition speeds of leaves are relating with not only climate but also leaf materials, vegetation types are very important information for soil respiration study.

We selected at least one measurement site for the 3 major ecosystems to measure reflectance spectra and biological parameters, which relating with production, respiration and carbon flux (Fig. 4). Various parameters, which relate on production and respiration, will be measured. Relationships between seasonal variation of reflectance spectra and productivity are one of interest to use satellite data for process models.

2.5 Process study

Some process models describe carbon flux as movements of carbon between compartments. There are some methods to measure total carbon flux and movement of carbon between compartments as shown in Fig. 5. Each method has its own advantages and disadvantages,

and they may give different outputs. Thus it is very important to improve methods and to systematize community level measurements for accurate measurements. On the other hand, since biological process is controlled by environment, environmental effects on carbon flux must be analyzed in not only compartment level but also community level. Measured flux between compartments will be used as a basic information to understand process and to improve process models. Those measurements are basics for modeling.

2.6 Global mapping

Developed algorithms will be modified and combined for global mapping of NPP and carbon flux at the end of the first 3-year and second 2-year term respectively. As described before, we have selected two approaches for NPP mapping, and the bulk method is much promising to derive any results, although there is hard limitation for improving accuracy. The precise method is much favorable due to its flexibility and reality description. However, there are many problems to be solved before applying the precise method in the global scale.

Key points for the mapping are summarized as follows.

Remote Sensing:

1) Reasonable classification by functional types of production.
2) Estimation of photosynthetic parameters.
   PAR, light use efficiency, LAI etc.

Process:

1) Determination for unit values for the bulk method.
2) Establishment of systematic measurement methods especially for forest community.
3) Analysis of relationship between parameters.
4) Improvement and simplification of models.

To make utilize remote sensing data successful, basic corrections such as geometric correction and atmospheric correction are very important. Although the former will be study and improve correction method in this project, the latter is out of scope at the moment.

Finally, the results will be merged with the ocean group result to make clear global carbon flux. The map will be produced with 8 km resolution.

2.7 Frame

Ten institutions are involved in the land group of this project. Roles of those institutions are briefly summarized in Fig. 6. This study has cooperation with IGBP DIS and TEMA. Most institutes have any international cooperative institution in China, Mongolia, Korea and

Australia. There is an international flux network to exchange information, and we are planning to contribute on it.

3. Conclusion

As described above, current technological improvements make global analysis possible. There are many activities to understand global ecosystem using advanced technologies. However, we still needs ground measurements over the world for validation of study. It is very hard task for each research group to derive ground data in various places. Thus international cooperation is already mandatory in global studies.

Global warming causes drastic environment changes, which never happened in the earth history. The human society needs various efforts to prevent global warming to keep sustainable development. It would be our duty to observe and record current earth for the future.

Acknowledgement

The author appreciates for the hearty supports and efforts of Professor Haruhisa Shimoda (Tokai University) and Professor Yoshifumi Yasuoka (the University of Tokyo) at the setting up of this project. The author also appreciate for the financial support of the Science and Technology Agency of Japan.

References

Ehleringer, J.R. and Field, C.B., 1993, Scaling physiological processes. Academic Press, pp.388.

Gitary, H. and Noble, I.R., 1997, What are functional types and how should we seek them? (in Plant functional types, Smith T.M. and Shugart, H.H. (edts.) Cambridge University Press, p.3-19.

Goward, S.N., Dye, D.G., Turner, S. and Yang, J., 1993, Objective assessment of the NOAA global vegetation index data product. Int. J. Remote Sensing, 14, 3365-3394.

Oikawa, T., 1991, Climate change and biological carrying capacity. Journal of Geography, 100, 843-850 (in Japanese).

Flow of carbon flux mapping

Objectives :

1. Development of classification method based on the functional type.
2. Estimation of terrestrial NPP.
3. Improvement of carbon flux measurement methods.
4. Understanding relationships between satellite data and vegetation activity, and development of process models using satellite data as inputs.
5. Understanding process relating with carbon flux, and improving process models.

-> mapping of net primary production and carbo flux.

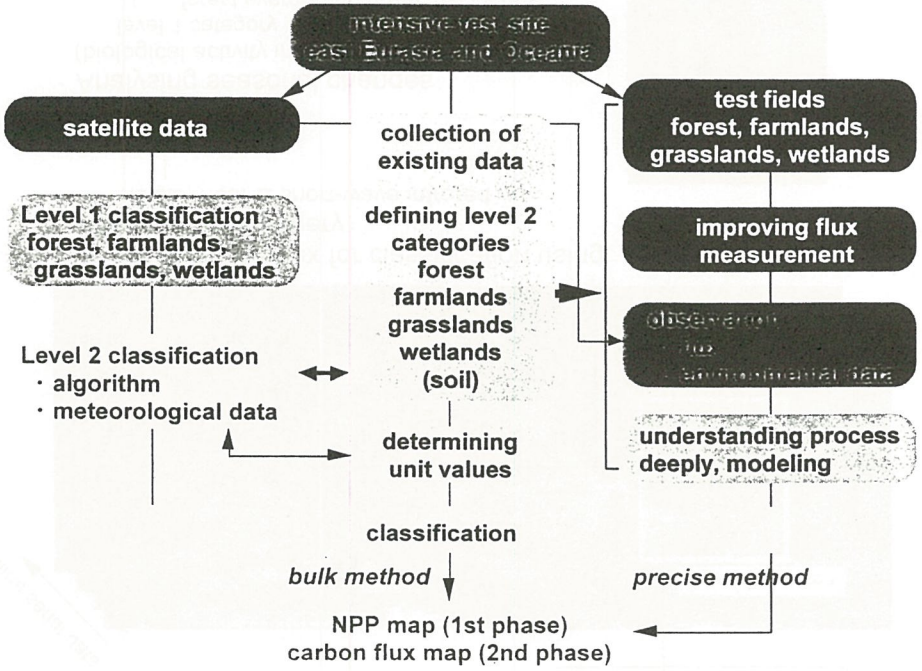

Fig. 1 flow of the study.

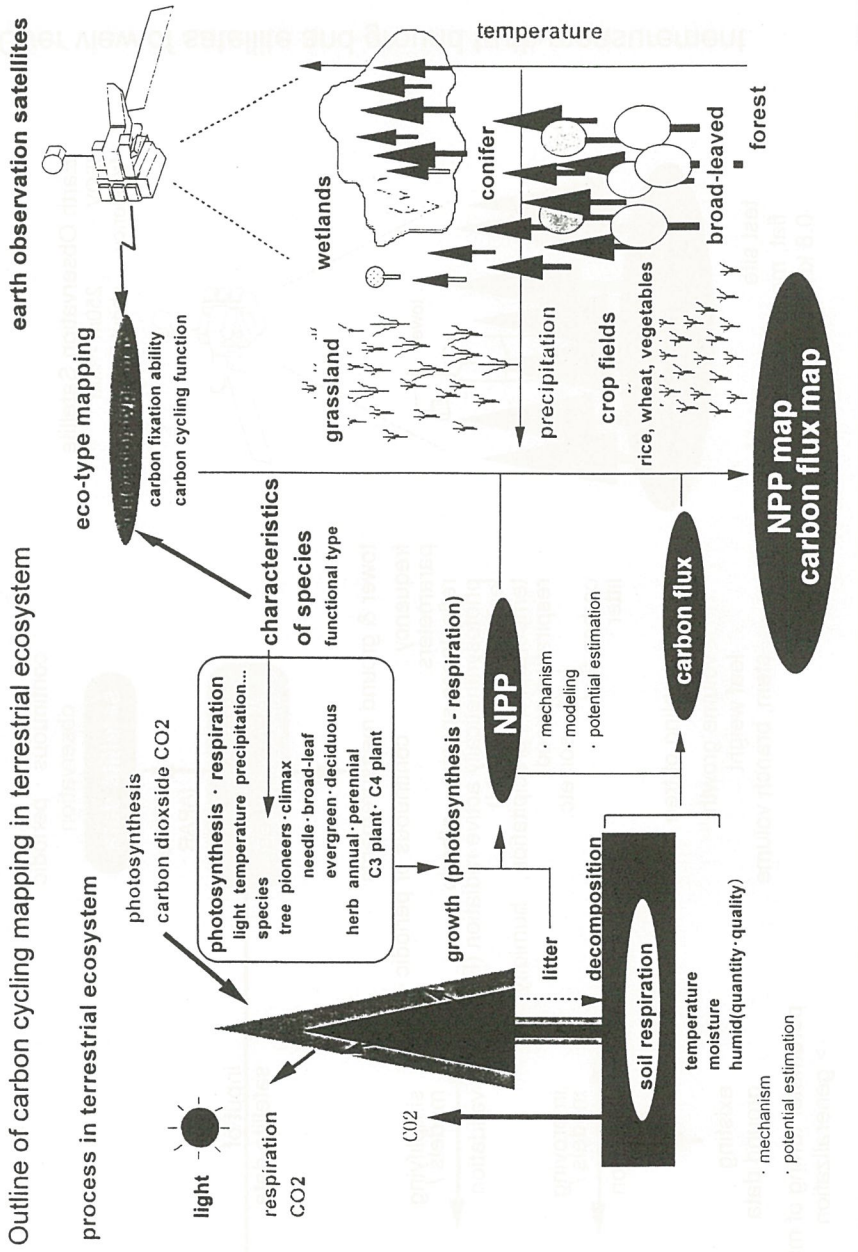

Fig. 2 Out line of carbon cycle mapping in the terrestrial ecosystem.

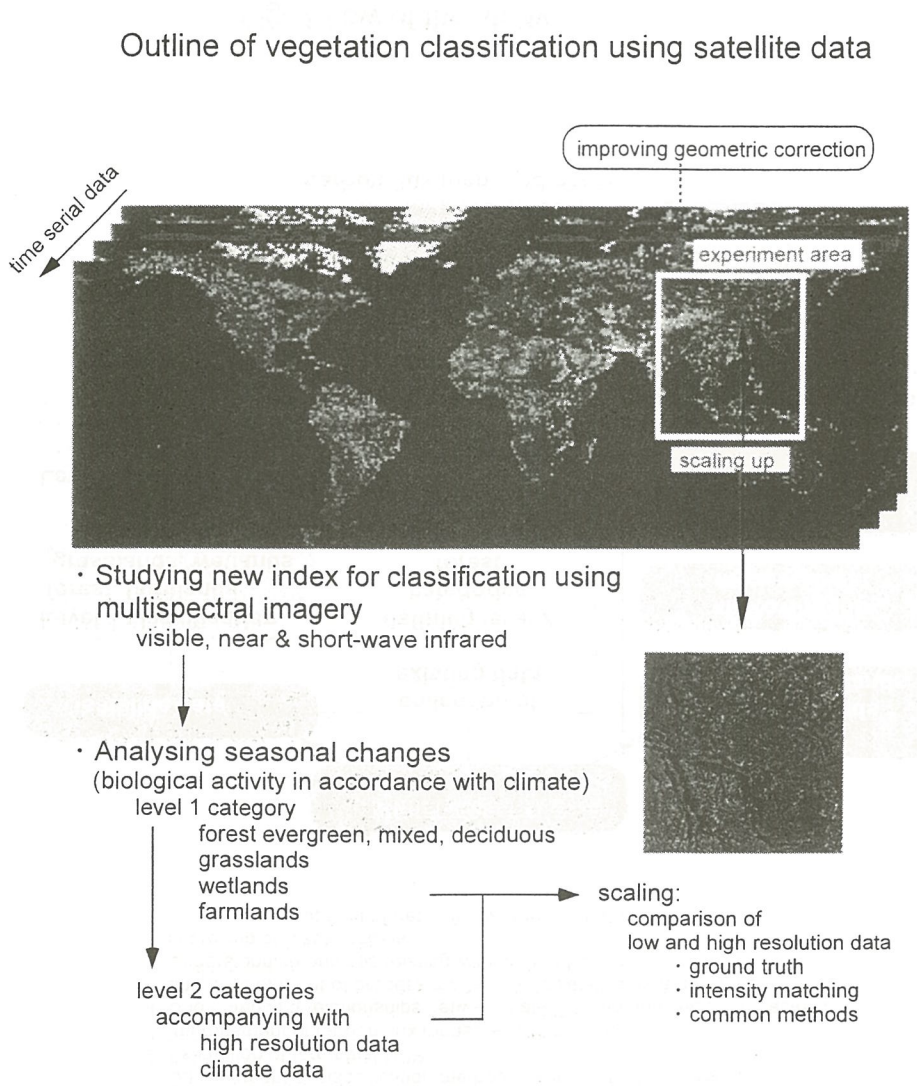

Fig. 3 Outline of vegetation classification using satellite data.

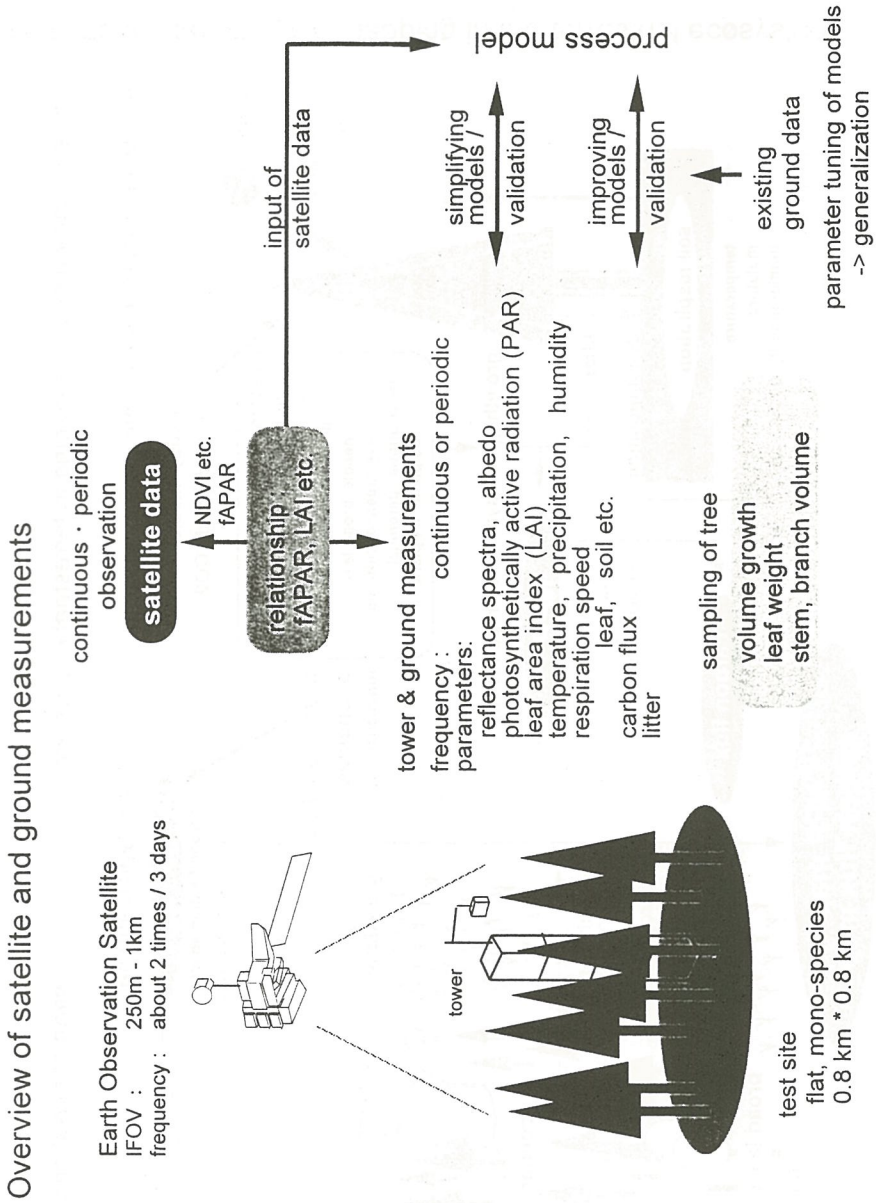

Fig. 4 Over view of satellite and ground truth measurement.

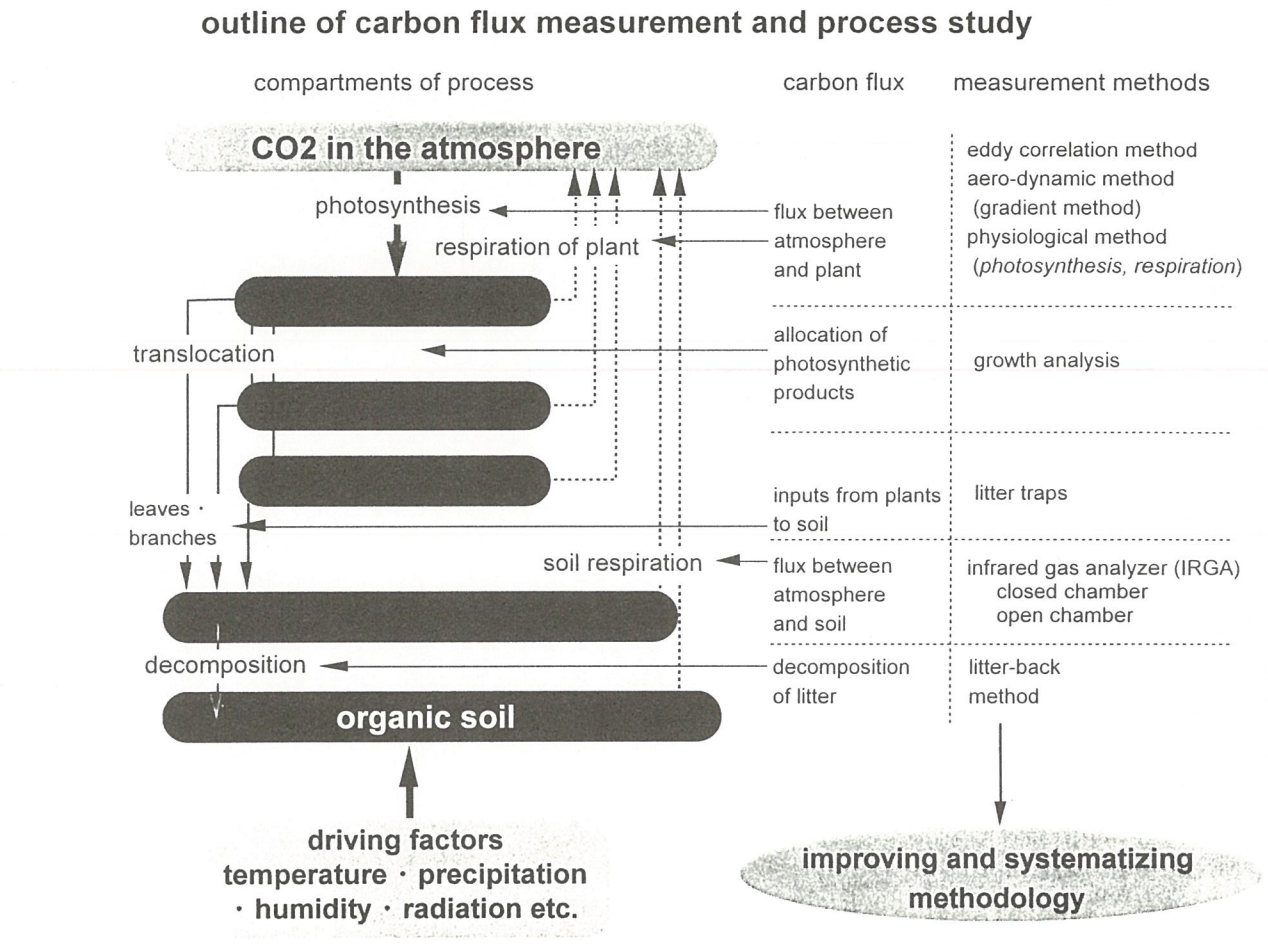

Fig. 5 Outline of carbon flux measurement and process study.

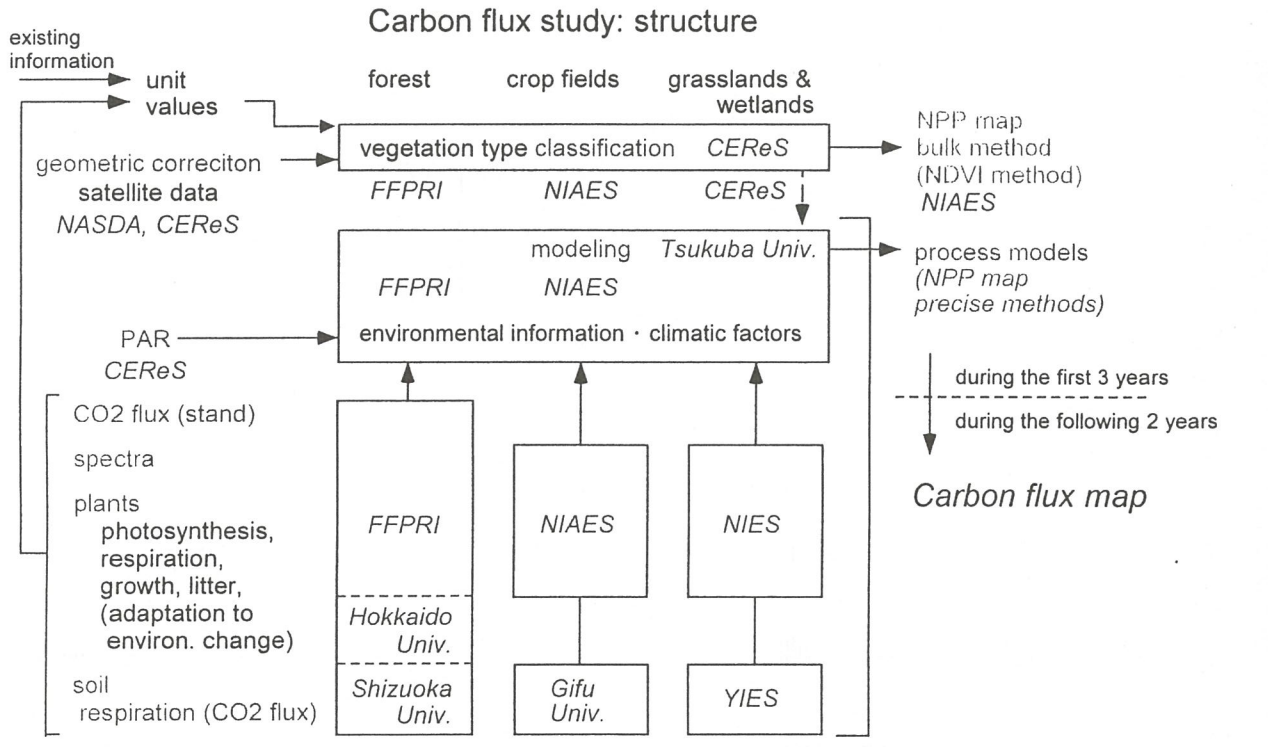

Fig. 6 Carbon study: structure.

Institutions:

FFPRI: Forestry and Forest Products Research Institute
NIAES: National Institute of Agro-Environmental Sciences
NIES: National Institute for Environmental Studies
NASDA: National Space Development Agency of Japan
YIES: Yamanashi Institute of Environmental Sciences
CEReS: Center for Environmental Remote Sensing
Gifu University
Hokkaido University
Shizuoka University
Tsukuba University

Session : East Asia regional projects

Land-cover classification based on AVHRR and Geo-spatial data analysis

(Liu jiyuan, Luo Di, Zhuang Dafang)

Institute of Remote Sensing Applications, C.A.S. Beijing, 100101,China

Abstract

Information regarding the characteristics and spatial distribution of Earth's land cover is critical to global environment research. AVHRR data have been increasingly used in land-cover characterization for large area. Although there have been great progresses in improving the result of classification with geographical knowledge, how to make the best of geo-spatial data remains an open question. As the distribution of land-cover types is the combination of many geo-factors such as terrain, soil, climate and wind, the comprehensive influence of these factors should be taken into account when employing ancillary geo-spatial data for better result of characterization. In this study, effort was made to develop an innovative strategy for land-cover classification of China. By using geo-spatial data such as elevation, precipitation and temperature, a geo-environment image was generated as a band to composite with remotely sensed data for supervised classification. A sample area—Northeast China was used to test the feasibility of this method.

Keywords: NOAA-AVHRR, geo-spatial data, Geo-environment image, Supervised classification

1. Introduction and objectives:

With the growing concern about global change, regional to global land-cover mapping has become an increasingly important data source in a variety of studies such as land-use change, biogeochemical cycle modeling , and climate modeling .

Compared with TM、SPOT imagery，National Oceanic and Atmospheric Administration（NOAA）Advanced Very High Resolution Radiometer（AVHRR）imagery has become a popular alternative for land mapping for large area, because it is relatively inexpensive, has high temporal frequency for avoiding cloud cover，and has moderate data volume for collecting，storing and processing. As AVHRR "Greeness data" such as NDVI are useful for depicting change in vegetative activity over time，we can perform land-cover classification and characterization with AVHRR data based on associations between land-cover types and variations in periodic observance of greeness.

Although during the last decade，substantial progress has been made in using AVHRR data for land-cover characterizations，the result of classification is yet to be further improved. The low accuracy on one hand is due to the coarse spatial resolution and constrained spectral resolution；on the other hand it is also because some disparate land-cover types share spectral reflectance characteristics on the image. When we performing land-cover classification，problems exist in discriminating between land-cover types exhibiting similar phenologies. Such land-cover types often have similar spectral signature on the image，which make it difficult for computer to discriminate different types only based on colorimetry, luminance and the statistic information recorded on the image.

Remote sensing specialists have long recognized the importance of geo-spatial data for land-cover characterization. Significant advances have been made in developing techniques and strategies for using geo-spatial data as ancillary information to improve the result of the land-cover classification. Pettinger（1982）used agricultural，upland，lowland environmental strata and decision rules based on field research to adjust a landsat MSS land-cover classification in Idaho. He showed that the stratification improved both the detail and the accuracy of the map. Cbula and Nyquist（1987）used terrain data and climatological data

(precipitation and climate regimes)in a Landsat Mss classification of Olympic National Park, Washington, resulting in an increased land-cover classes from 9 to 21 as well as an overall accuracy of 91.7 percent.

As geographic information system(GIS)technology has developed, and integrated GIS-Image analysis software has become more common, opportunities for using geo-spatial data and remotely sensed data in concert have expanded. Innovations in data analysis based on expert systems and related techniques facilitate implementation of complex multi-source data analysis strategies. Jesslyn .F. (1994), with the support of remote sensing and GIS, performed land cover classification for the conterminous U.S.. Then she used ancillary data including digital elevation, temperature, precipitation and frost-free-period in post-classification refinement, and got good result.

Although progresses have been made in employing geographic knowledge for land-cover characterization, how to make the best of geo-spatial data remains an open question. What should be kept in mind is that the distribution of land-cover types, especially vegetation types, is limited not by a single factor, but the combination of many environmental factors. How to choose the most influential geo-spatial data and then to exhibit their comprehensive influence on land-cover distribution is important for the further improvement of land-cover characterization.

In this research, an innovative strategy is developed for land-cover characterization for People's Republic of China, geo-spatial data, including temperature, precipitation and elevation was used as a band to corporate with remote sensing data. The objective of this paper is to present this technique. An example area, Northeast China, was used to test the feasibility of this approach.

2. Method

Any object on the earth surface is closely connected with its environment. The variance on earth surface, especially the natural and physical characteristics of the earth surface, is the main limitation for the distribution of different land-cover types. In many cases, land-cover types which have similar spectral structure on the image, often exhibit variance in their environment. This is why geo-spatial data are required for better accuracy of classification.

In this research, we try to add some environmental information into the image and thus to improve the discriminability of the image. The environmental information here refers to those geo-spatial data that are well-associated with the distribution of vegetation. As previous studies suggest that terrain, moisture and temperature have great influence on the distribution of vegetation in China, we chose these three factors as ancillary data in our land-cover characterization. On the basis of comprehensive analyzing their contribution to vegetation allocation in different areas, a geographical environmental image is made as a "band" to composite with remote sensing data. The image we ultimately for classification is an comprehensive image containing both spectral and geographical environment information.

2.1 Processing flow

The strategy developed to characterize land-cover types employed both geo-spatial and AVHRR data is in a structured manner(Figure 1.)

2.2 Regionalization

Land-cover mapping for large area has unique analysis problem: Continental area typically exhibit greater variation in climate, terrain, vegetation, soil than they are encountered in analysis of small area. Such problem can be dealt with in two ways: first, the study area could be treated as a single one, This

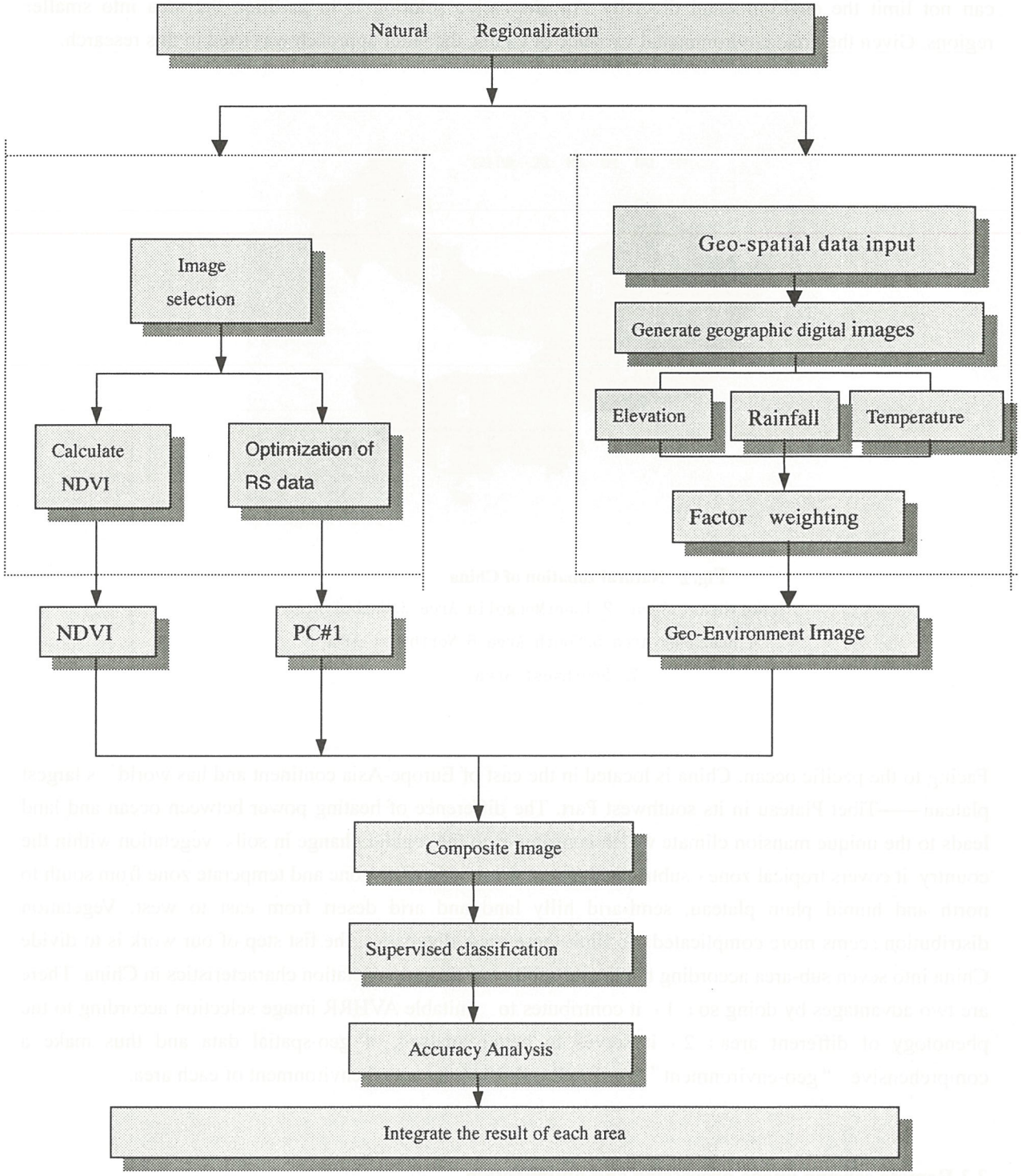

Figure 1. Processing Flow

would serve to avoid the post-classification mosaicing and interregional class correlation problems, but can not limit the environmental diversity. An alternative solution is to partition the area into smaller regions. Given the great environmental variance of China, the latter approach was used in this research.

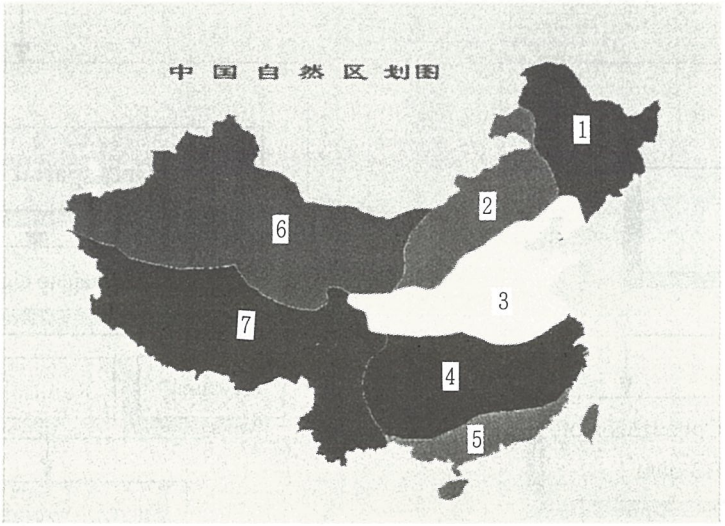

Fig. 2 Natural zonation of China

1. Northeast Area 2. InnerMongolia Area 3. Huabei Area
4. Huazhong Area 5. South Area 6. Northwest Area
7. Southwest Area

Facing to the pacific ocean, China is located in the east of Europe-Asia continent and has world' s largest plateau——Tibet Plateau in its southwest Part. The difference of heating power between ocean and land leads to the unique mansion climate which contributes to the regular change in soil、vegetation within the country. it covers tropical zone，subtropical zone，warm temperate zone and temperate zone from south to north and humid plain plateau, semi-arid hilly land and arid desert from east to west. Vegetation distribution seems more complicated. To limit these great diversities, the fist step of our work is to divide China into seven sub-area according to climate、soil、terrain and vegetation characteristics in China. There are two advantages by doing so：1，it contributes to suitable AVHRR image selection according to the phenology of different area；2，it serves to better analysis of geo-spatial data and thus make a comprehensive "geo-environment" band well reflecting the actual environment of each area.

2.3 Remote sensing image processing and optimization

2.3.1Selection of suitable images

Phenology is indispensable for image interpretation because it can help to select an image on which disparate vegetation types could be relatively easy to discriminate. There is great phenological variance in China due to its different climate zones; thus it is necessary to select suitable temporal image before classification. As single-data image is often inadequate for land-cover type characterization，multi-date composite images are required.

2.3.2Calculating NDVI

Vegetation indices are commonly calculated to depicting the growth, coverage and biomass of vegetation on earth surface. Many vegetation indices have been developed for remotely Vegetation monitoring, one of which is Normalized Difference Vegetation Index(NDVI)Derived from the reflectance values of NIR and Visible band, NDVI widely used in studies on soil moisture, crop growth monitoring and vegetation classification.

It is the deference of near-infrared(NIR) and visible(VIS)reflectance values normalized over the sum of those values, as for AVHRR, simply:

$$NDVI = \frac{ch_2 - ch_1}{ch_2 + ch_1}$$

Where ch_2 is the near-infrared band and ch_1 is the visible band.

As a useful vegetation dynamic indicator, NDVI reflects plants' intrinsic biophysichemical characteristic such as biomass、coverage and content of chlorophyll. The definition of NDVI as a ratio helps to suppress the differential solar illumination effect due to surface topography and aspect, and simultaneously emphasize the useful vegetation information. Many researches have showed that NVDI can well capture the dynamic change of vegetation. Goward et al. (1985) used NDVI images from April through November 1982 to map regions of net primary productivity. They show that seasonal NDVI patterns could be associated with major land-cover regions, and that multi-date greeness images could be used to observe patterns of vegetation growth and senescence. In later work, he compared the vegetation characteristics of North and South American biomes by analyzing GVI data using methods developed in Goward's 1985 research. They found that the differential timing and longer duration of the South American growing season was well captured. Biome distributions appeared, qualitatively, well associated with published maps.

In this research, NDVI is calculated for multi-temporal images of each sub-area to represent temporal activities of Vegetation.

2.3.3 Optimization of NOAA-AVHRR data

NOAA-AVHRR has five bands from red to thermal bands. To improve visual effect, we often use colored or false colored image in data processing: choose three bands or channels from multi-band data as red, green and blue channel after data processing. In this study, we intended to integrate temperature, precipitation and elevation data as one band, NDVI MVC image as the second band. Therefore, we could only employ one band from NOAA-AVHRR for false-colored image processing. Because principal components analysis (PCA) can be used to simplify data processing and compress satellite multi-spectral imagery (Richard, 1986), and one of the most important results of PCA is its ability to change pixel definition from M channel sets of number (counts) to K-principal-component (PC) sets (K<M) without remarkable loss of (relative) information, we use principal components analysis (PCA) to compress multi-spectral NOAA-AVHRR data.

At the image analysis system, principal component analysis of NOAA-AVHRR data acquired during June 1995 in test site was performed after digitally co-registering and merging. eigenvalues and eigenvectors were subsequently computed. For convenience, comparison of the information content in each principal component (PC) have been titled in ascending order (table1).

A close look at table1 reveals that the first principal component (PC#1) account for 84.8 percent of the total scene variance. In other word, PC#1 contained 84.8 percent information of NOAA-AVHRR data.

Table1. Eigenvalues and eigenvectors of Principal Component Analysis

		PC#1	PC#2	PC#3	PC#4	PC#5
bands	1	0.448	-0.472	0.498	-0.186	0.543
	2	0.369	-0.223	0.246	0.728	0.473
	3	0.320	0.260	-0.508	0.473	0.590
	4	0.727	0.091	0.345	-0.460	-0.363
	5	0.170	0.808	0.561	-0.090	0.037
Eigenvalues		2880.2	297.2	151.3	62.4	32.j
Information capacity		84.8%	.8%	3.7%	1.8%	0.9%
Information accumulation		84.8%	93.6%	97.3%	99.1%	100%

Table2. Correlation matrix from five bands of NOAA--AVHRR

	1	2	3	4	5
1	1.00				
2	0.73	1.00			
3	0.42	0.75	1.00		
4	0.71	0.89	0.82	1.00	
5	0.75	0.90	0.81	0.95	1.00

Therefore, PC#1 has represented the main information of the five bands of NOAA-AVHRR and the humidity and thermal distribution of the ground. It can be used as a representative band for vegetation interpretation and we can use it to co-register with digital image of geographic data and NDVI data.

2. 4 geo-spatial data processing and geo-environment image generation

2.4.1Generating geographic digital image from geo-spatial data

Average monthly precipitation and monthly mean temperature have been collected from meteorological stations all over the country. At the same time, elevation data were digitized from topology map at a scale of 1 to 1 million. The processing of digital image with geo-spatial data is performed in ARC/INFO system. For each geo-spatial data，we acquired isogram from separated pointed value with grid cell of 1 km, which is suitable for co-registering with AVHRR image；then, process the isogram by interpolation and digital quantifying. After transfer the vector data to raster image, we can get three geographical digital images for terrain(E(x,y)), precipitation(R(x,y)) and temperature(T(x,y)), as presented in figure 3,4,5 respectively.

2.4.2 digital geo-spatial data Weighting and geo-environment image generation

The geo-spatial data mentioned above are used to generate a "geo-environment" image to composite as a band with NDVI and PC#1 data. To get this image，method of weighted-summing was utilized. More specifics，after giving weights to geo-spatial data by analyzing their influence on vegetation distribution, each image will be added together by their weights.

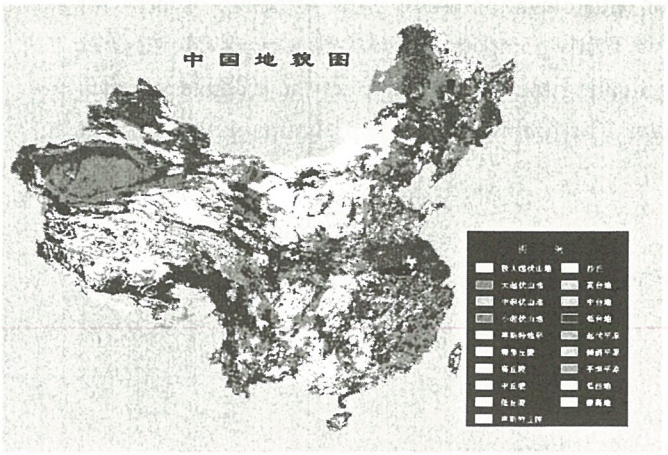

Fig. 3 Geomophology of China

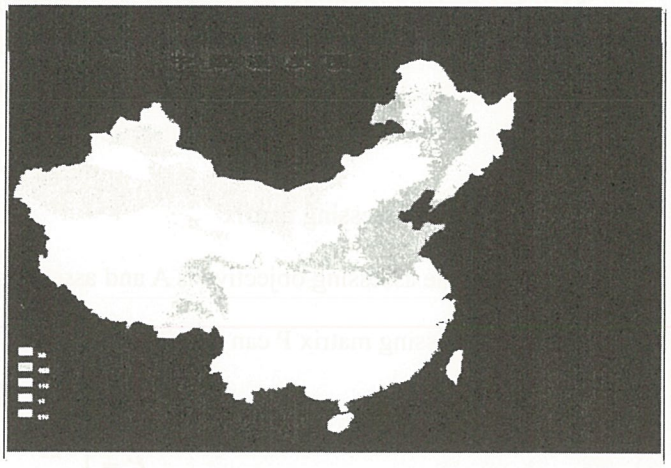

Fig.4 Moisture zone of China

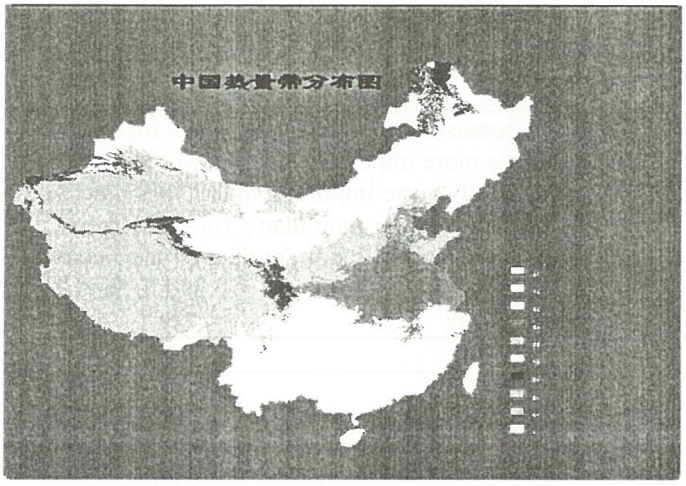

Fig.5 Temperature zone of China

As we know, the distribution of Vegetation results from the combination of many factors, the comprehensive influence of these factors should be given full consideration in analysis of geo-spatial data. Factor weighting is regarded as a crucial step in this research. Although temperature, precipitation and elevation constrict the distribution of vegetation, their contributions to the constriction are not the same. The purpose of weighting is to exhibit the different influence of each factor(In this study, the more the factor has the influence on land-cover distribution, the higher weight it will have).Reasonably weighting means better reflection the actual geographical background by the and thus leads to better result of classification.

Because of the environmental diversity in China, weighting must be based on the particularity of different areas. Driving factor (the geo-spectral –factor which has the highest weigh) can vary by areas. For example, in InnerMongolia Area, the vegetation distribution is constrained dominantly by rainfall, and we can give a high weight to Precipitation to emphasis its importance in this area; while in south China area which has plenty rainfall, precipitation is not the limitation of plant growth. In other words, it should have a relatively low weight.

There are many mathematical processes such as Analytical Hierarchy Process (AHP) and Sequence Synthetically Process for factor weighting in regional resources evaluation. In this study, we employed

AHP for factor weighting of temperature, precipitation and elevation. AHP is an effective process for quantitatively analyzing un-quantitive factors. In AHP, we firstly compute the maximum eigenvalue and its corresponding eigenvector from assessing matrix of evaluating factors and then get the weights for each factor by means of normalizing the maximum eigenvector. The following list the preliminary procedure of AHP:

1). To construct assessing matrix

Given the assessing objective is A and assessing factors are $F = \{f_1, f_2, \cdots, f_n\}$,

Then the assessing matrix P can be set as:

$$P = \begin{bmatrix} f_{11} & f_{12} & \cdots & f_{1n} \\ f_{21} & f_{22} & \cdots & f_{2n} \\ \vdots & \vdots & \vdots & \vdots \\ f_{n1} & f_{n2} & \cdots & f_{nn} \end{bmatrix}$$

Where f_{ij} is the value that accounts for the relative importance of f_i compared with f_j, the meaning of the value listed in table 3.

Table 3. The value of f_{ij} and its meaning:

value of f_{ij}	meaning
j	f_i and f_j possessed the same importance for objective A.
3	f_i is a little more important than f_j for objective A.
5	f_i is obviously more important than f_j for objective A
7	f_i is much more important than f_j for objective A
9	f_i is extremely more important than f_j for objective A
2，4，6，8	the mean value between 1 and 3, 3 and 5, 5and 7, 7and 9 respectively.
$f_{ji} = 1/f_{ij}$	

2.5 Classification

For accurate integration of remote sensing image and geo-spatial data, the strict registration of multi-source data of different measurement scales is important. In this experiment, a projection transformation is applied to the composite geo-spatial data and remotely sensed data, and we use the same Longitude and Latitude reference frame for registration. Then use the registered geo-environment band with NDVI image and the first Principal Component of AVHRR data to produce the composite image (figure 6).

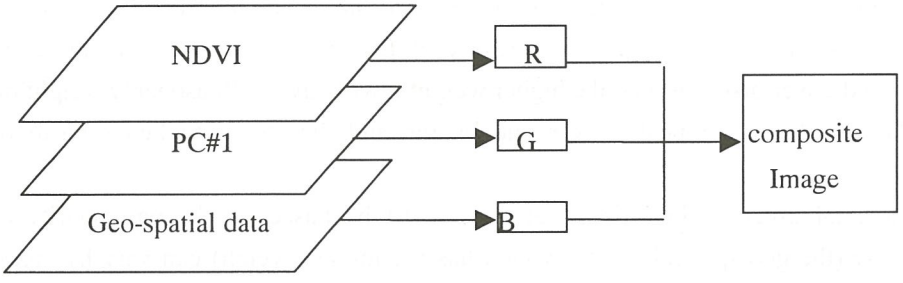

figure 6. Remote sensing and geo-spatial data integration

The composite image, containing both the spectral and the geographic information, is an integrated reflection of physical entity. As we used supervised clustering algorithm and maximum likelihood classification to characterize the land-cover types. Ground samples and published maps in test area have been referred to select training spot in the image.

3. Case study- land-cover classification of Northeastern China

3.1 Description of study area

Northeastern China, the typical vegetation types of which are larch, broad-leaf forest and meadow, covers Arctic-temperate, Temperate-moist and Semi-moist area. According to bio-regions, this region can be divided into three sub-areas： Dawuli, Changbai and Mongolia, corresponding to such land-cover types as conifer, conifer-broadleaf mixed forest and prairie respectively. In this area, winter is cold and long lasting in Northeastern China while summer is temperate but rather short. The average frost-free period is about 100-150 days. Of the whole year, there are 180~190 days (from early April to October) with the mean daily temperature (MDT) above 5 and 120~170 days on which MDT is above 10. Greater than evaporation in the mountain area while a little lower than evaporation in the plain, the precipitation of this area is moderate and decreases from southeast to northwest, from plain to mountain, with the least rainfall mostly in the winter month January and the most in July or August. About sixty percent of total year precipitation concentrates in June to September. Affected by the Southeast Monsoon, precipitation variations are evident among years with average variational rate of 15~20 percent.

3.2 Data collection

The following data are collected:

1. AVHRR data

High temporal density 1 km NOAA-AVHRR images of June 1995 are used in this experiment. After geometric correction, cloud-free processing, projection transformation, we have the NOAA-AVHRR image of Northeastern China (figure 6).

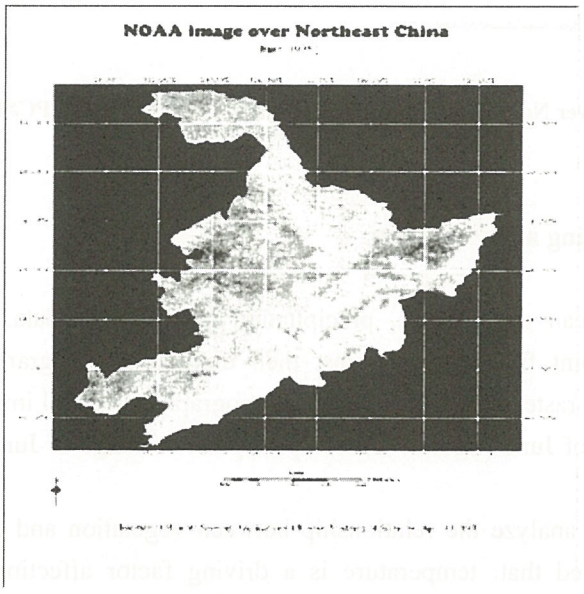

Fig.6 NOAA_AVHRR Image of Northeast China

2. Terrain data

Elevation data recorded by National Observatories.

3. Climate data

Monthly mean precipitation recorded by 361 National Meteorological Observatories.

4. Others

Natural zonation maps, administrative boundary maps, vegetation maps, Land-use maps, etc.

3.3 Remote Sensing data processing

Then process them in ERDAS/IMAGINE to make NDVI images (figure 7) and the first Principal Component image (Fig. 8)

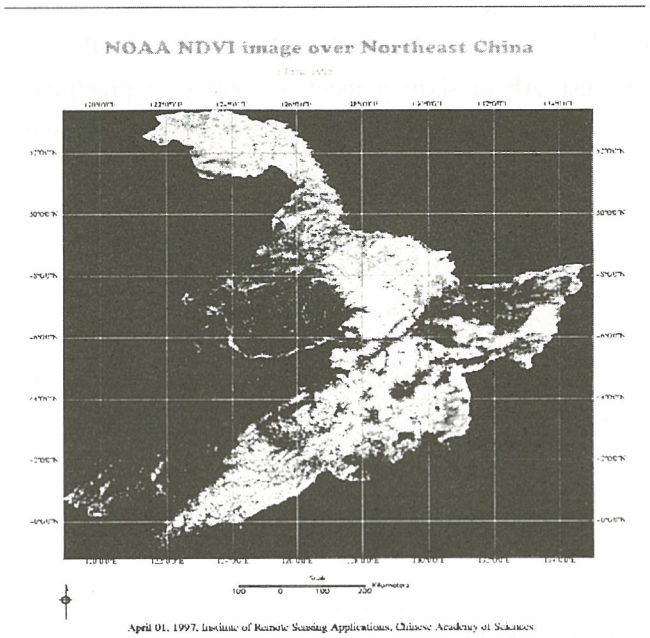

Fig.7 NDVI image over Northeast China

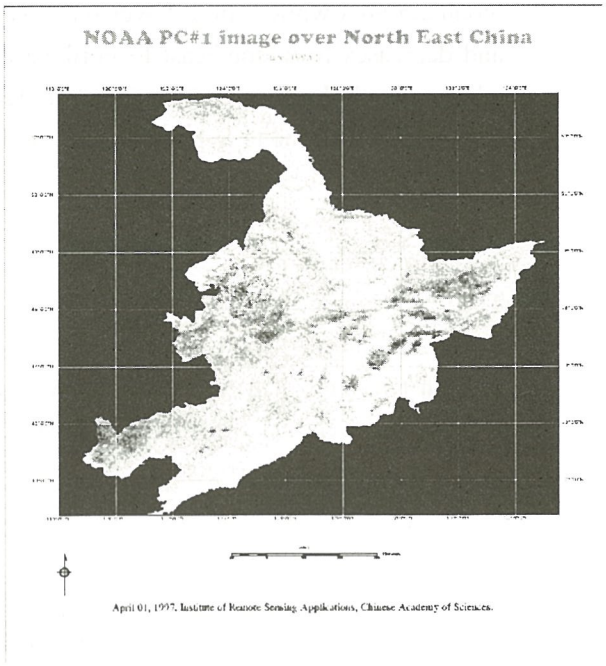

Fig.8 NOAA PC#1image over Northeast China

3.4 Geo-spatial data processing and weighting

Collect the monthly mean temperature, precipitation and altitude data, and input them into the computer. Transform the point file into isograms, then digitize the isogram using interpolation, and transform the vector map into raster image. The resulting geographical digital images of Northeastern China are mean temperature image of June (figure 9), mean precipitation image of June (figure 10) and elevation image (figure 11).

In study area, when we analyze the relationship between vegetation and temperature, precipitation and elevation, we can learned that: temperature is a driving factor affecting the vegetation growth; precipitation affects the vegetation growth coordinated with temperature; the influence on vegetation growth from elevation is not somewhat less important than that of temperature and precipitation.

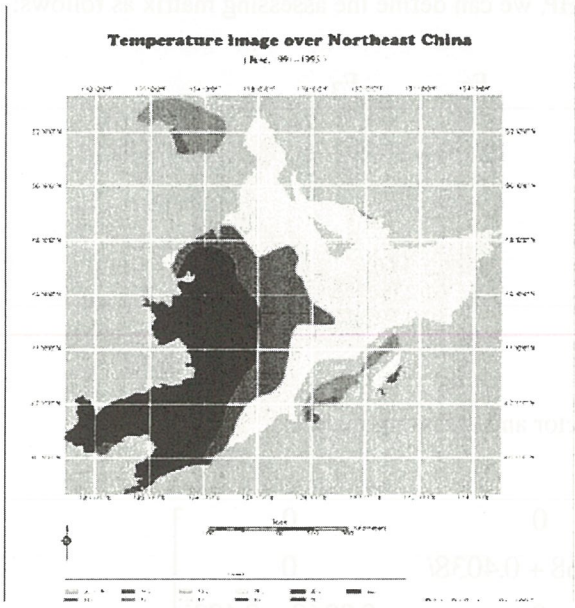

Fig.9 Monthly mean temperature of June

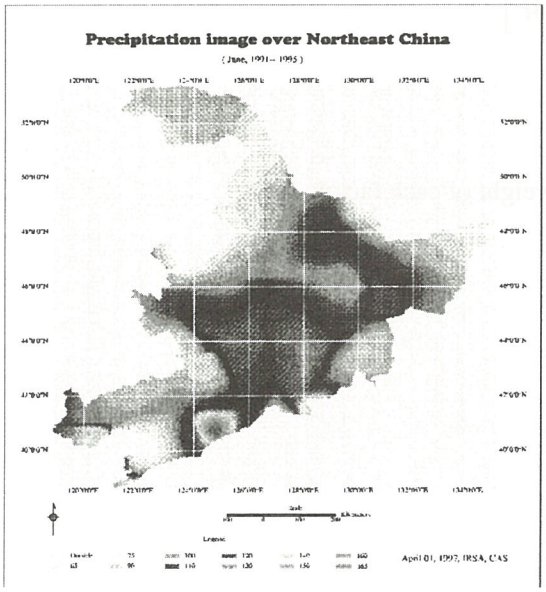

Fig.10 Monthly mean precipitation of June

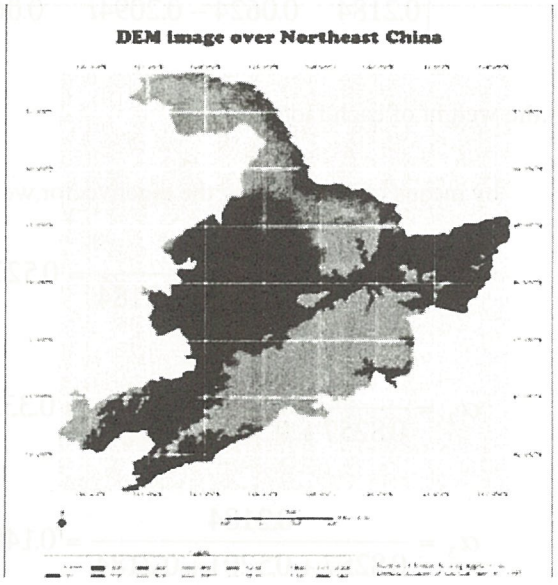

Fig.11 DEM image of Northeast China

Therefore, according to AHP, we can define the assessing matrix as follows:

	F_1	F_2	F_3
F_1(temperature)	1	2	3
F_2(precipitation)	$\frac{1}{2}$	1	3
F_3(elevation)	$\frac{1}{3}$	$\frac{1}{3}$	1

2). Eigenvalue (d) and eigenvector and assessing matrix

$$d = \begin{bmatrix} 3.0536 & 0 & 0 \\ 0 & -0.0268 + 0.4038i & 0 \\ 0 & 0 & -0.0268 - 0.403i \end{bmatrix}$$

$$X = \begin{bmatrix} 0.8257 & 0.5674 + 0.5998i & 0.5674 - 0.5998i \\ 0.5201 & -0.5060 + 0.1206i & -0.5060 - 0.1206i \\ 0.2184 & 0.0624 - 0.2094i & 0.0624 + 0.2094i \end{bmatrix}$$

3).the weight of each factor

by means of normalizing the eigenvector,we can get the weight of each factor:

$$\alpha_1 = \frac{0.8257}{0.8257 + 0.5201 + 0.2184} = 0.527$$

$$\alpha_2 = \frac{0.5201}{0.8257 + 0.5201 + 0.2184} = 0.333$$

$$\alpha_3 = \frac{0.2184}{0.8257 + 0.5201 + 0.2184} = 0.140$$

Now, we can define the integrated geo-environment image as:

$$G(x,y) = 0.527 \times T(x,y) + 0.333 \times P(x,y) + 0.140 \times E(x,y)$$

G (x, y) (Figure 12) then can be used as an independent geographic information "band" to composite with remote sensing data.

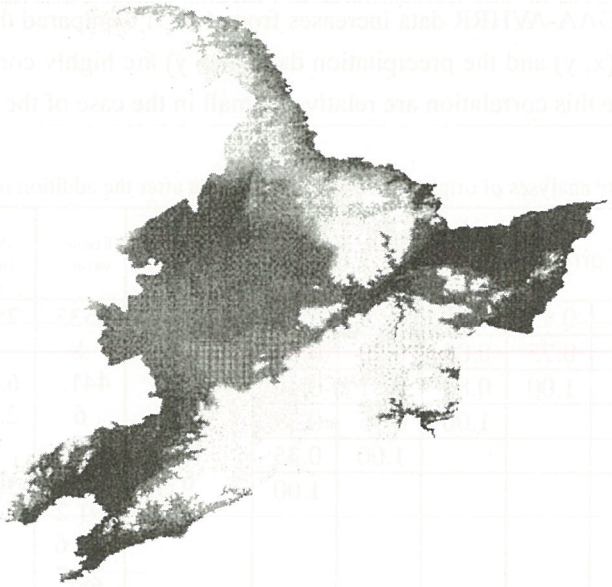

Fig.12 Geo-environment image

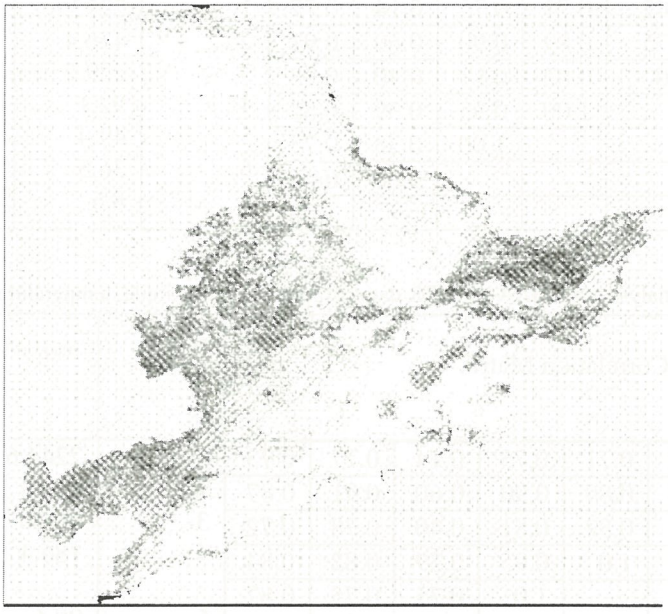

Fig.13 Composite image generated by Geo-spatial data and remotely sensed data

3.5 Integration of geo-spatial data with remote sensing image

After the process of projection transformation and registration of the geo-spatial data and the remote sensing image, we use the geo-environment image, the NDVI image and the PC#1 image of NOVAA-AVH RR as three bands and get a composite image (figure 13).

To test the contribution of geo-spatial data to the new composite image, we analyzed the information capacity of this composite image. The results are showed in chart 4, 5 and 6.

The charts showed that, as a result of incorporating geo-spatial data into remotely sensed data, the

dimension of the original NOAA-AVHRR data increases from 4 to 7. Compared the three chart, we can also find that the climate data T (x, y) and the precipitation data P (x, y) are highly correlated with each NOAA-AVHRR spectral band, while this correlation are relatively small in the case of the altitude data E (x, y).

Chart 4. Information capacity analyses of original NOAA-AVHRR data after the addition of altitude data

Band		Correlation matrix						Principle Component	Eigen-value	Percent of information capacity	Accumulated Percent of Information Capacity
N	1	1.00	0.73	0.42	0.71	0.75	0.14	1	2533	75.3%	75.3%
O	2		1.00	0.75	0.89	0.90	0.60	2	.8	13.1%	88.4%
A	3			1.00	0.82	0.81	0.40	3	441.	6.7%	95.1%
A	4				1.00	0.95	0.39	4	6	2.7%	97.8%
	5					1.00	0.35	5	244.	1.4%	99.2%
E(x, y)							1.00	6	0	0.8%	100%
									91.2		
									48.6		
									26.7		

Chart 5. Information capacity analyses of NOAA-AVHRR data after the addition of altitude and temperature

Band		Correlation Matrix							Principle Component	Eigenvalue	Percentage of information capacity	Accumulated Percent of Information Capacity
N	1	1.00	0.73	0.42	0.71	0.75	0.14	0.77	1	2213.8	71.7%	71.7%
O	2		1.00	0.75	0.89	0.90	0.60	0.91	2	456.4	14.8%	86.5%
A	3			1.00	0.82	0.81	0.40	0.78	3	229.2	7.4%	93.9%
A	4				1.00	0.95	0.39	0.82	4	92.1	3.0%	96.9%
	5					1.00	0.35	0.75	5	49.4	1.6%	98.5%
E(x, y)							1.00	0.46	6	36.5	1.2%	99.7%
T(x, y)								1.00	7	8.6	0.3%	100%

Chart 6. Information capacity analyses of NOAA-AVHRR data corporated with altitude, temperature and precipitation data

波段		Correlation Matrix								Principle Component	Eigenvalue	Percentage of information capacity	Accumulated Percent of Information Capacity
		1.0	0.73	0.42	0.71	0.75	0.14	0.77	0.73	1	2244.6	67.2%	67.2%
	1		1.0	0.75	0.89	0.90	0.60	0.91	0.87	2	422.8	12.7%	79.9%
				1.0	0.82	0.81	0.40	0.78	0.72	3	268.0	8.0%	87.9%
N	2				1.0	0.95	0.39	0.82	0.84	4	186.4	5.6%	93.5%
O						1.0	0.35	0.75	0.87				
A	3									5	98.6	3.0%	96.5%
A													
	4												
	5												
E(x, y)							1.0	0.46	0.38	6	68.8	2.1%	98.6%
T(x, y)								1.0	0.69	7	36	1.0%	99.6%
P(x, y)									1.0	8	16	0.4%	100.%

3.6 Supervised classification

Given the similar spectral character between meadow and some forest, we adopt the method of Binary Tree to divide the composite image into forest and non-forest, then performed supervised classification respectively (Figure 14, Figure 15). In practice, we get forest distribution map of Northeastern from "Resources and Environment Database of China " by GIS to perform the division

From the classification result, the integrated image can be classified as broadleaf forest, mixed needleaf and broadleaf forest, needleaf forest, shrub, miscellaneous forest, poplar and birch, farmland, meadow, marsh, grassland, reed marshes and lake twelve kinds of land-cover types (fig.16). Classification accuracy is 78.72% for forest and 78.9% for non-forest. The overall accuracy is 78.81%.

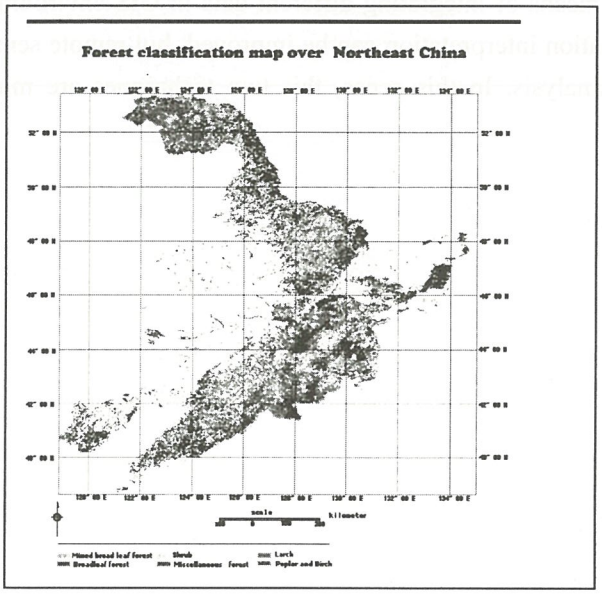

Fig.14 Non-forest classification map

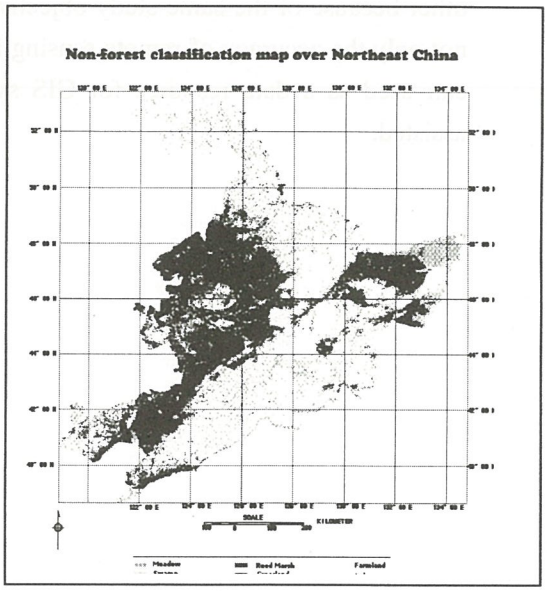

Fig.15 Forest classification map

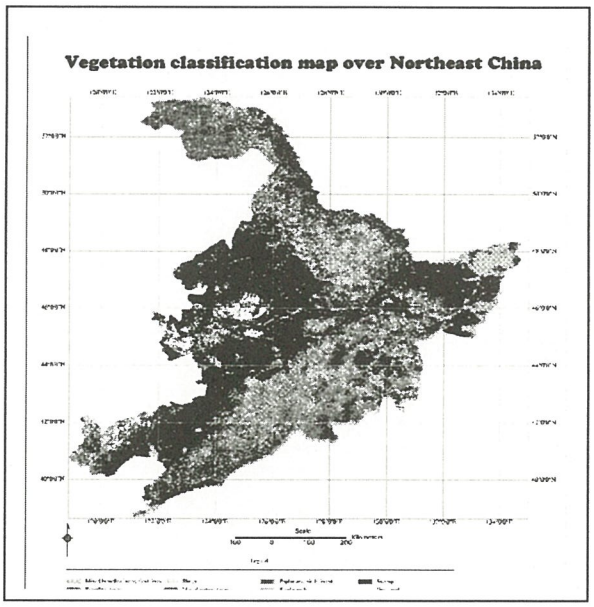

Fig.16 Land-cover classification of Northeast China

4. Conclusion

1). The spectral information structure of remote sensing data can be improved by means of integrating digital geographic data with remote sensing. The integrated image reflected not only the present condition of vegetation but also its internal causes(geographic factors).

2). The methodology of using multi-temporal remote sensing images, coupled with digital geographic image integrated in GIS for vegetation classification proved to be feasible and better than the conventional digital classification method alone. This approach is effective for discriminating land-cover types which have similarity on spectral structure but have relatively more difference in their environment.

3). Although remote sensing and GIS are two relatively independent techniques, they are related to each other because of the same study objective. By means of integrating different data in GIS environment, not only the accuracy of remote sensing information interpretation can be improved, but remote sensing can used as a data resource for GIS system analysis. In this sense, this two techniques are mutual assisted.

References

Zhu qijing, 1991. A Study on Vegetation Classification Using Muti-Temprol NOAA-AVHRR Data: *environment and remote sensing,* vol. 6. No. 2

Wu Bingfang, Huang Xun, Tian Zhigang, 1995. Vegetation Classification Using Remote Sensing And GIS: *environment and remote sensing,* vol. 10, no.1

Gervin, J. C., A. G. Witt, Y. C. Lu, And R. Sekhon, 1989. Comparison of Level 1 Land Cover Classification Accuracy for MSS and AVHRR Data: *International Journal of Remote Sensing*, Vol. 6, No. 1, Pp.47-57

Goward, S. N., D. G. Dye, 1985. North American Vegetation Patterns Observed with the NOAA-7 Advanced Very High Resolution Radiometer: *Vegetatio*,Vol.64,Pp. 3-14

Holben, B., 1988, Characteristics Of Maximum Value Composite Images from Temporal AVHRR Data, *International Journal Of Remote Sensing*, Vol. 7, Pp.1417-1434

James M.E, and Kalluri S.N., 1994,The Pathfinder AVHRR Land Data Set: An Improved Coarse Resolution Data Set for Terrestrial Monitoring. , *International Journal of Remote Sensing Vol1.15, No.17.*

Jesslyn F. Brown, Thomas R. Loveland, James W. Merchant, Bradley C. Reed, Donald O. Ohlen, 1993. Using Mutisource Data in Global Land-Cover Characterization: Concepts, Requirements, And Methods: *Photogrammetric Engineering & Remote Sensing,* Vol. 59, No. 6 Pp.977-987

Justice, C. O., J. R. G. Townshend, B. N. Holben, And C. J. Tucker, 1985 Analysis Of Phenology Of Global Vegetation Using Meteorological Satellite Data: *International Journal of Remote Sensing*, Vol. 6,Pp. 1271-1318

Lloyd, D., 1991, A Phenological Classifiication of Terrestrial Vegetation Using Shortwaye Vegetation Index Imagery: *International Journal of Remote Sensing*, Vol. 11, No. 12, and Pp.2269-2279

Thomas R. Loveland, James W. Merchant, Donald O. Ohlen And Jesslyn F. Brown, 1991. Development of A Land-Cover Characteristics Database for the Conterminous U. S.: *Photogrammetric Engineering & Remote Sensing,* Vol. 57, No. 11, Pp.1453-1463

Townshend, J. R. G., And C. J. Tucker, 1984,Objective Assessment of Advanced Very High Resolution Radiometer Data for Land Cover Mapping: *International Journal of Remote Sensing*, Vol.5, No. 2, and Pp.497-504

Townshend, J. R. G., And C. O. Justice, 1988, selecting The Spatial Resolution for Satellite Sensor Required For Global Monitoring of Land Transformations: *International Journal of Remote Sensing*, Vol. 8, No. 2, Pp. 187-236

Townshend, J. R. G., C. O. Justice, And V. Kalb, 1987, Characterization and Classification of South American Land Cover Types: *International Journal of Remote Sensing*, Vol. 8, No.8, and Pp.1189-1207

Tucker, C. J., J. A. Gatin, And S. R. Schneeider, 1984.Monitoring Vegetation in The Nile Delta with NOAA-6 AND Noaa-7 AVHRR Imagery: *Photogrammetric Engineering & Remote Sensing,* Vol. 50, No. 1, Pp. 53-61

Finding Better Direction of the Development of Global Datasets/Databases

Ryutaro Tateishi
Center for Environmental Remote Sensing(CEReS), Chiba University
1-33 Yayoi-cho Inage-ku Chiba 263-8522 Japan
Fax: +81-43-290-3857
E-mail: tateishi@rsirc.cr.chiba-u.ac.jp

Abstract:
In this short report, two activities by the author are introduced to promote the participation in them. One is the activity by the International Society for Photogrammetry and Remote Sensing(ISPRS) Working Group IV/6 (Global databases supporting environmental monitoring). This activity aims to identify problems in global database development and to find the better direction to go. The working period is until July 2000. The other one is by Data and Information System(DIS) sub-committee of Japan national committee for IGBP. The Asia-Wide Land use and Cover(AWLC) meta-database was developed by this sub-committee. Anyone can access and register land use/land cover data in AWLC meta-database through internet. The AWLC will be the first step to share the local reliable data for continental/global land cover data development.

1. Activity by the ISPRS WG IV/6

1.1 Introduction

Global datasets of geospatial environmental variables are necessary input to global environmental studies. They are also necessary for policy decision making and environmental education. In turn, global data are developed from satellite remote sensing, ground measurement, or social survey like census. Among them, satellite remote sensing is most powerful tool for global data acquisition. Global dataset development is now the main purpose of satellite remote sensing, for example EOS series, ADEOS-II, SPOT-4, ENVISAT. The recently available global datasets are DEM(GLOBE, GTOPO30), population, land cover, in-site observation data(TEMS by GTOS).

1.2 Global datasets or databases of geospatial environmental variables

The ISPRS WG IV/6 deals with global datasets or databases of geospatial environmental variables. The environmental variables consists of physical variables including land variables, ocean variables, and atmospheric variables, and socio-economic variables.They do not include satellite image data. The environmental variables cover, according scientific classification, the following fields: atmosphere, land surface, biosphere, oceans, cryosphere, paleoclimate, human dimensions,

solar physics, hydrosphere, solid earth. The term "Global" means geographic coverage of data. It may be truly global or global land or global ocean. The needs of global datasets/databases come from global change research, political decision making, environmental education.

1.3 Events related to "Global Change"

The main needs for global data is from global change research. The awareness on global change started apparently in 1970s though a part of scientists had noticed before that time. The following events are milestones of the global change related events.

1972 The United Nations Conference on the Human Environment at Stockholm

1985 Global Resource Information Database (GRID)
in the United Nations Environment Programme (UNEP) was established

1986 International Geosphere-Biosphere Program(IGBP)
in the International Council of Scientific Unions'(ICSU)

1987 The idea of "Sustainable Development"
by the UN sponsored Brundtland Commission

1988 Earth system science by NASA, USA

1989-90 the US Global Change Research Program (USGCRP)

1992 Agenda 21 at the United Nations Conference on Environment and Development (UNCED)
A program of international research and policy on global "biodiversity" also began

1999 Launch of EOS AM1 by NASA

2000 Launch of ADEOS II by NASDA

1.4 Examples of global datasets

What global datasets have been produced? The followings are the examples of global datasets.

- basic map data
  - Digital Chart of the World(DCW) Ed.2
  - World Vector Shoreline Plus(WVS+)
- elevation
  - Global Land One-kilometer Base Elevation (GLOBE)
  - Global 30 Arc-second Elevation Data (GTOPO30)

Digital Terrain Elevation Data (DTED) level 1

- land cover

DISCOVER, IGBP

AARS Global 4-minute Land Cover Data Set

- population

Global demography, CIESIN

- soil

SOil and TERrain Digital Database (SOTER), ISSS

- runoff

Global runoff data, the Global Runoff Data Centre

- evapotranspiration

Global land 30-minute evapotranspiration data

- Other data (atmosphere, biosphere, cryosphere, human dimensions, hydrosphere, land surface, oceans, paleoclimate, solar physics, solid earth)

1.5 On-going projects to develop global datasets

There are many on-going projects to develop global datasets. The followings are a few examples.

- Global Observations of Forest Cover(GOFC)

in Committee of Earth Observing System(CEOS)

one of Integrated Global Observation System(IGOS)

5 year project from 1998

cooperation among existing forest related projects

expected data set production

Coarse land cover

Fine land cover

Fire scars

Forest harvest

Forest biomass

Forest functioning(LAI, PAR, FPAR)

Land cover change in areas of rapid change

- DTED level 2

1 arc-second grid

interferometric SAR in shuttle mission between 60N and 60S latitude region

funded by NIMA, launched by NASA in 1999

may be classified or distributed by 3 second grid

- Space Agencies

NASA

EOS AM-1 / MODIS

aerosol concentration and optical properties, cloud properties, vegetation and land

cover, sea ice and snow cover, surface temperature, ocean color,
concentration of chlorophyll-a

NASDA

ADEOS-II / GLI

cloud properties(- optical thickness, - effective particle radius, - top temperature, - top height, column water vapor, aerosol optical thickness)

chlorophyll-a, suspended solid, attenuation coefficient at 490nm, sea ice, snow cover

1.6 What the ISPRS WG IV/6 tries to do

The WG does not aim to develop a specific global dataset. The WG aims to summarize various on-going global dataset development efforts, to identify obstacles for better development and usage of global environmental datasets, to propose measures or methodology to cope with these obstacles, and to disseminate these survey and proposal to researchers and related peoples through publication.

The WG decided to start discussion through virtual and real workshop(15-18 Nov. 1999 at Hawaii) with almost all related key organizations/groups to the development of global datasets such as scientific group(ex. IGBP, IHDP, LUCC), international organizations(ex. UNEP, FAO, World Bank), space agencies under CEOS. Subjects of discussion are divided into thematic subjects and generic subjects. The thematic subjects are obstacles for the development of a specific global data and measures to reduce it. This discussion will be done for each data type such as land surface data, oceanographic data, hydrographic data, etc. The generic subjects are common problems in the development and usage of global datasets. Any person who has an interest in the workshop can contact to the author. The goal of the WG in the term 1996-2000 is to disseminate the WG discussion in a style of book in 2000 to record the present stage of global geospatial environmental database and the state of the art of the technology for global dataset/database development.

(ISPRS WG IV/6 URL http://www.ngdc.noaa.gov/seg/tools/gis/isprs46.html)

2. Asia-Wide Land use and Cover (AWLC) meta-database

--- Request your contribution to global change studies by sending meta-data of your land use/cover and related data ---

DIS(Data and Information System) sub-committee of the Japan National Committee for IGBP (International Geosphere and Bioshere Program) under the Science Council of Japan has developed AWLC(Asia-Wide Land use and Cover) meta-database.

2.1 What is the AWLC meta-database?

The AWLC meta-database is a database of meta-data of land use, land cover, and other land surface

variables in Asia. Land use is a social classification of land which describes how a man utilize land. Land cover is a physical classification of land which describes what type of surface, especially vegetation type, covers a land. Other land surface variables include vegetation cover percentage, forest cover percentage, area of land cover change, area of desertification etc. They are any kinds of variables which describe land surface characteristics. They may be category-type discrete representation of land or continuous variables of land.

2.2 Why do we need the AWLC meta-database?

Land surface characteristics is one of key environmental variables for global change studies and local environmental studies. However we do not have unified detail knowledge about land use and land cover of global area which meets the needs for global change studies. Since land cover of global area varies a lot by continent, land use and land cover of each continent should be investigated first. The AWLC meta-database is focused on Asia. Though we can get land use and land cover information from satellite image, the lack of more reliable information (or ground truth) than satellite extracted one is a common problem. On the other hand, there are many projects and individual studies which provide land use or land cover information as a final product or by-product. But, unfortunately, in most cases, these information can not be accessed by other researchers just because producer of these products think that they are only for their own project, organization or sponsor. The main reason of the development of the AWLC meta-database is to remove barrier which avoid to use the pre-acquired knowledge of land use and land cover of Asia. In other words, the AWLC meta-database changes closed knowledge of land use and land cover to open or common knowledge for Asian scientists. This common knowledge is a common property of Asian scientists and it promotes the understanding of the environment of Asia. Your contribution would be highly appreciated not only by the initiator of this project but also by Asian people who live in Asian environment.

2.3 Web-site address of AWLC meta-database

http://oblbwww.cv.noda.sut.ac.jp/awlc/index2.htm

2.4 Method of registration of your meta-data

You can contribute to the AWLC meta-database by sending meta-data of land use, land cover, or other land surface variables in Asia by the method described below. It would be appreciated if you could send the image data or browse image data of land use/cover or other land surface variable.

Methods to send meta-data or image data:
(Either of the following three methods is acceptable.)

a. **From web site**

Meta-data and image data could be directly registered from the web site:

http://oblbwww.cv.noda.sut.ac.jp/awlc/index2.htm

The file name of image data can be registered at the above web site, but the image data itself should be sent by the method (2) or (3).

b. **By E-mail or ordinary mail**

Meta-data written in English language in a TEXT file (file name: xxxxx.txt) or HTML file (file name: xxxxx.htm) and image data as a GIF file (file name: xxxxx.gif) or a JPEG file (file name: xxxxx.jpg) are acceptable. These data can be sent to the address at the bottom of this page by data media such as a DOS format floppy disk, a 8mm tape, a MO, or a CD-ROM. These data can be also sent by e-mail message or its attached file to the address at the bottom.

c. **From your FTP site**

We can also directly downloaded both meta-data and image data from your FTP site. For this method, please let us know the IP address of your FTP site and the file name of the meta-data and the image data beforehand by e-mail to the bottom address.

Address for sending data and for questions:

Dr. Hirohito Kojima
Remote Sensing Lab., Faculty of Science and Technology
Science University of Tokyo
2641 Yamazaki Noda-City Chiba 278-8510 Japan
Phone : +81-471-24-1501(ext.5014)
Fax : +81-471-23-9766
e-mail : kojima@ir.noda.sut.ac.jp

2.5 Example of meta-data

Example

1. Name of the dataset	(Example) Land cover dataset of Gifu prefecture
2. Location	
Latitude of the north end	(Example) 36 deg 30 min N
Latitude of the south end	(Example) 35 deg 00 min N
Longitude of the west end	(Example)136 deg 15 min E
Longitude of the east end	(Example)137 deg 45 min E
Name of the place	(Example) Gifu prefecture, Japan
3. Attribute	

Land use / land cover class
Land surface variable (Example) Land cover class
Forest, Paddy field, Agricultural field, Grass land,
Urban area, Bare ground, Water
"the detail definition of land cover class" (******.txt)

4. Source information (Example) Landsat TM, 28 July 1995

5. Data
Raster Grid size
Vector Original scale (Example) Grid size : 30 meter and 1 second

6. Any description about the dataset (Example) This dataset was produced as one of the products sponsored by xxxxxx.

7. Availability (Example) Available

8. Contact (Example)
Ryutaro Tateishi
Center for Environmental Remote Sensing(CEReS)
Chiba University
1-33 Yayoi-cho Inage-ku Chiba 263 Japan
Phone: +81-43-290-3850
Fax: +81-43-290-3857
Email: tateishi@rsirc.cr.chiba-u.ac.jp
URL: http://*********

9. Documentation/Web site about this dataset
(Example 1)
Hirohito Kojima, Land cover classification of Gifu prefecture,
International Journal of Remote Sensing,
Vol.xx, No.xx, pp.xx-xx, 1998
(Example 2) "Related report" (http://*********)

10. This dataset is produced by (Example)
Obayashi Shigeyuki
Remote Sensing Laboratory
Science University of Tokyo

11. This meta-data is contributed by (Example)
Hirohito Kojima
Remote Sensing Laboratory
Science University of Tokyo

12. "Browse image of the dataset" (*******.gif)

Fire monitoring from the space

S. KHUDULMUR, M. ERDENETUYA
The Information and Compter Center of the Ministry for Nature and Environment
The National Remote Sensing Center of Mongolia
Tel/Fax: 976-1-326649, Fax: 976-1-329968,Email: mtt@magicnet.mn

1. INTRODUCTION

Mongolia is a country located at the Central Asian highland with an area of 1565000 square kilometres, is bounded on the north by Russia and on south by China. Mongolia located deep within the interior of the Eurasian mainland far from washing it seas and oceans, is a highland country and has a marked continental climates with poor soil fertility, scanty surface water resources, in the harsh natural conditions.

Mongolian nature and geography, its economic and social specific features account for its considerable vulnerability to natural disasters. Winters are cold with zud (severe winter conditions), in springs blizzards and tornadoes, wildfires are common, in summers shower rains, floods, in autumns heavy snowfalls, frosts, blizzards often occur which means that throughout the year the country is under pressure of one of natural disasters.

Many experts from the field of disaster study to estimate how danger it is calculating number of human losses. Most of them did not include such natural hazards like heavy winter, drought and fire to the disaster if there are not so much human death. But in case of Mongolia such hazards are causing direct and indirect way much more losses in livestock beside environmental and ecological damages. Animal husbandry is one of most important field of Mongolian economy and still it is base of our living condition.That is why, for the animal husbandry based on nomadic pastoralism meteorological hazardous phenomena and wildfires, which are affecting on pasture condition, a key influences.

2. FIRE DAMAGES OF LAST 3 YEARS IN MONGOLIA

Forests and grasslands play an important role in the economy development of the country. Forest cover is 12.5 mln.ha or 8.1% mostly with larch, pine, birch, cedar, spruce and saxaul and grassland cover is 70% of all territory. In an average year occur the 50-60 forest fires and 80-100 steppe fires. During last few years Mongolia has a various natural or non natural hazards and one of most dangerous natural hazard is *a Forest and steppe fires.* They damage about 70,000 ha of forest and 700,000 ha of grassland. The economic losses exceed 10 billion tugrigs (Tugrig is Mongolian currency. 800¥ = 1$).

About 90 percent of steppe and forest fires in Mongolia are caused by human. However it is human caused, nature has a burning material. However, the forest resource is 1.3 bln cubic meter, timberland area is 300000ha, 42.1mln cubic meter wood prepared during last 37 years and 70000 ha forest area is damaged by insects every year.

Forest fire and reforestation status:

1993	1994	1995	1996	1997	Total

Burned forest area	205282	117809	34193	2363600	2710000	5430884
Reforested area	4585.7	4934	3970.2	3211.1	5001.1	21702.1

(Areas are in hectares)

According to the statistics since 1963 we can see the frequency of forest and steppe fire and in Mongolia each ten year suffered by high number of fires (Figure 1).

The winter and spring from 1996 to 1998 were extremely dry and lack of snow in most areas. From latest of February to early of June, Mongolia was suffered from large-scale forest and steppe fire, that devastated a large part of the country. In next table we showed the some casualties of these fires.

Year	Aimag	Sum	# of fires	Area	MN¥(mln)
1996	16	120	417	10734178	371.6
1997	14	98	239	14234583	127.4
1998	15	69	132	3641672	93.9
Total			788	28610433	592.9

Casualties are:

29 people died, 82 people had different burn, 11700 livestock died, 218 family house, 1066 communication facilities, 750 fences, 26.3 mln.ha pasture and forest burned

Total cost of properties 820.2mln

Ecological and economical damage estimates 1bln 850.5mln

Figure 1. Fire frequency from 1963-1998*

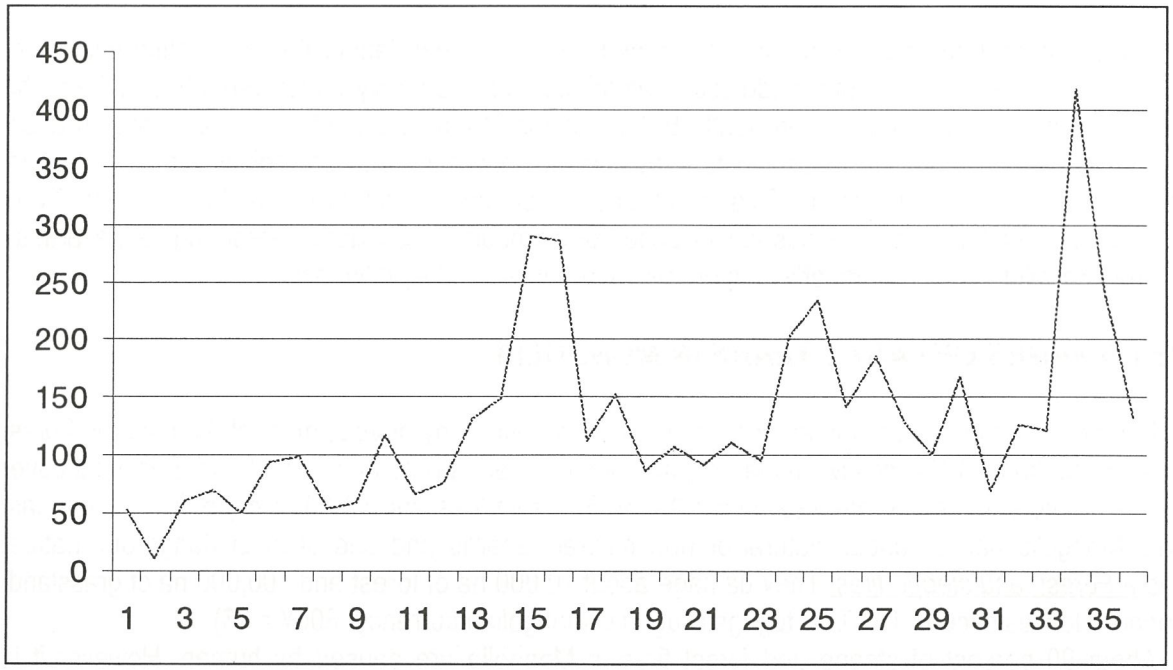

* Data for this graph is provided by N. Erdenesaikhan, officer of the Ministry of Nature and Environment

3. CLIMATE CONDITION IN LAST 3 YEARS

The global warming is one of the reasons of fire. In mountain and steppe zone number of days with 0 and higher degrees increased from 10 to 20 and total temperature increased about 100 degrees. Last 60 years precipitation and temperature are increasing. But precipitation in spring is decreasing. Deepness of frozen soil decreased in 20-60cm. Winter in 1995-1996 was warmest in last 60 years.

4. FIRE DETECTION AND MONITORING BY SATELLITE DATA

The monitoring and establishment of effective early warning system is a key to efficient organization of fire against activities. There are few possibilities of monitroing such as local people, helicopter or airplane patrol and satellite remote sensing.

Local people

Because of low density population and huge territory it is almost impossible to know where what is happening. Distance between 2 families is about 20-30km and distance between 2 sum centres is 50-100km. But if fire location is determined, those local people are the main human resource for the fire against activity.

Helicopter or airplane patrol

Mainly due to economic difficulties it is impossible to establish permanent control using helicopter or airplane. For example for 1h flight by helicopter fuel costs 420$ or flight between Khuvsugul province and Ulaanbaatar city will cost around 2500$. It means to patrol only 4 h per day in spring fuel will cost around 150000USD. But everyday flight between capital city and provinces can used for such purposes.

Satellite remote sensing

This is a most cost effective tool to monitor fires for today. The receiving station, which established in June 1995 at the Information and Computer Centre of Ministry for Nature and Environment, daily receives the AVHRR (Advances Very High Resolution Radiometer) data from NOAA satellites and can be used to detect and monitor the forest and steppe fire. Since 1996 we developed methodology for for detection using AVHRR data and servicing by fire information Mongolian Civil Defence Organization and provicial administrative units.

By above mentioned technology using the daily NOAA satellite data we can monitor and estimate total burned area, as showed on Figures 2-3.

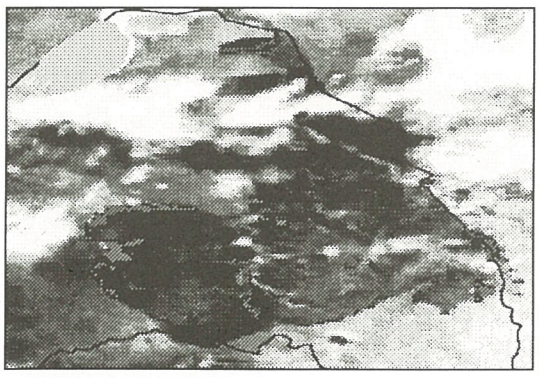

Figure 2. Active fire and burned area

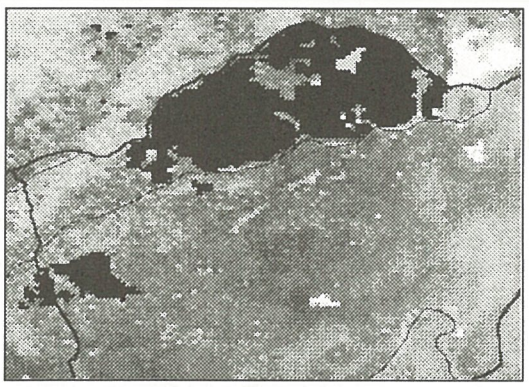

Figure 3. Burned area

Figure 4-6 are showing the summarized burnt area forest and steppe fire over territory of Mongolia, of spring 1996 - 1998 respectively. The total burnt areas calculated as 10734.2, 14234.6 and 3641.7 thousand hectares of forest and steppe respectively.

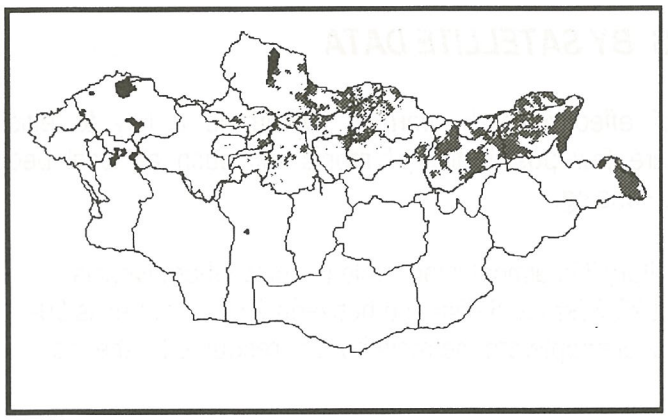

1996,
Total burned area: 10734178ha

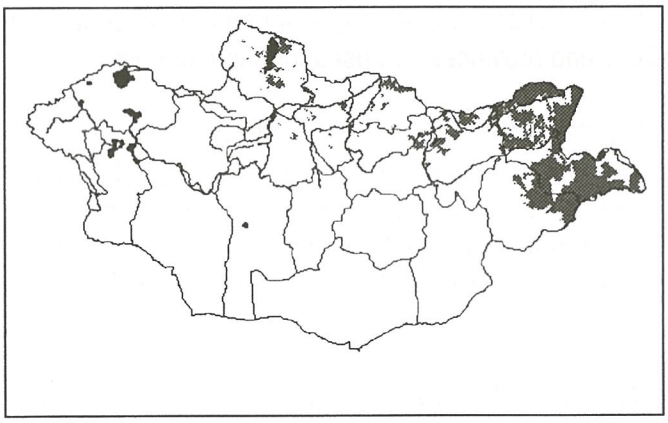

1997
Total burned area: 14234583ha

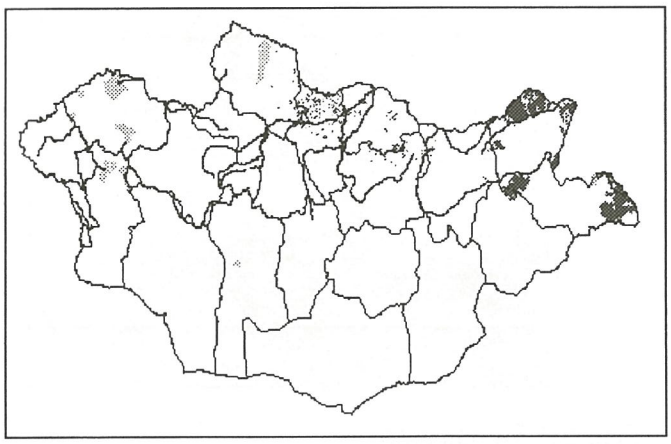

1998
Total burned area: 3641672ha

Figure 4-6. Total burned area maps of 1996, 1997 and 1998

5. CONCLUSION

The remote sensing system is a efficient tool for permanent control for detection and monitoring wildfires. But there are also several difficulties for establishment of early warning mechanism in order to organize effectively fire agains activities. One of them is communication system in Mongolia. Current meteorological and environmental information network reaches all the provincial centres (aimag). It means after receiving and processing of satellite data, producing fire information within 30minuts data can be disseminated to all centres at the aimags and information from the aimag centres to the local places, where is fire, takes many hours. Wild fires, specially in steppe area, are expanding very fast and in many cases information will be useless.

Another problem is a data resolution. NOAA AVHRR data has 1.1km resolution and it is impossible to detect small fires. Specially steppe fires are expanding so quick, and when information reaches the local places, where are fires, it is too late.

Session : Activity of CEReS

Surface climate information from GMS-5 data

I.Okada[1], Y.Takayabu[2], K.Kawamoto[3], T.Inoue[4], T.Takamura[5], H.Tamaru[5] and H.Takemura[5]

1) Japan Science and Technology Corporation, 2) National Institute of Environmental Studies,

3) Center for Climate System Research, University of Tokyo, 4) Meteorological Research Institute,

5) Center for Environmental Remote Sensing, Chiba University

1. Introduction

Cloud is an important component for global and local climate. Its distribution and variation express an integration of atmospheric conditions. Cloud also directly affects to local climate through radiative process. Heat budget at the surface is decided mainly by radiation budget. In daytime, solar radiation dominates the total radiation budget and terrestrial radiation decides it in nighttime. Cloud plays a roll not only on solar radiation but on terrestrial radiation through cloud cover and temperature at cloud bottom. Diurnal change of the radiative flux belongs to the diurnal changes of cloud, atmospheric and surface conditions, and it has large amplitude. The radiative flux at surface is important element for climate condition. Hence it is needed to make properties of the diurnal variation of cloud clear.

In the present study, 1 hourly cloud, clear sky temperature and surface solar radiation data, which are processed from GMS-5 (Geostationary Meteorological Satellite 5), are introduced. Cloud and clear sky radiation temperature data had been stored for 1996. This data covers most of the east Asian continent. Hourly analysis is important because solar radiation changes quickly. Our final purpose is to estimate both of solar and terrestrial radiative fluxes hourly at the surface from geostationary meteorological satellite images. Surface solar radiation for 4 months have been estimated until now, although the research to develop the algorithm for terrestrial radiation is still proceeding.

2. Cloud distribution and clear sky radiation temperature

GMS-5 image data is received at Institute for Industrial Sciences, University of Tokyo, and is processed by Prof. Kikuchi at Kochi University. IR1 (10.5 - 11.5 micro meter), IR2 (11.5 - 12.5 micro meter) and visible channel are used for the present study.

As cloud determination, similar method with infrared analysis part of ISCCP cloud detection (Rossow and Garder, 1993) is applied. The stages are composed of 3 steps.

At first, spatial and temporal variation is analyzed. A pixel is compared with surrounding pixels in the same day and also compared with same pixel (position) in the day before and after. The pixel that has small variation is defined as clear sky. Secondly, clear sky pixels are screened and clear sky radiation temperature for reference is decided. When averaged clear sky radiation temperature for a time series is too lower than maximum among them, the average is assumed to be contaminated by cloud pixels. In such case, maximum is used as clear sky temperature with a negative bias. The biases belongs to surface conditions, open sea, sea ice, high land, snow, and other land covers. The clear sky radiation temperature for reference is decided every 5 days at every hour. Thirdly each pixels are compared with the clear sky radiation temperature. When radiation temperature of a pixel is lower than the clear sky radiation temperature for reference, it is decided as cloudy pixel. The threshold belongs to surface conditions as above.

Detected cloud is classified to cirrus and other cloud. For cirrus detection, the split window method (Inoue, 1987) is applied. When temperature difference between two infrared window channels,

delta T = Brightness temperature (IR1) - Brightness temperature (IR2),

are larger than 1.5 K, the pixel is decided as cirrus.
Then other clouds are classified to 3 layers by its temperature. High layer cloud is defined as that the radiation temperature is lower than atmospheric temperature at 440 hPa. Middle layer is defined between 440 hPa and 680 hPa, and low layer is defined as lower than 680 hPa. ECMWF (European Centre for Medium-range Weather Forecasts) atmospheric data is used for temperature reference. Rest of pixels are classified as clear sky.

The result is stored to 0.5 * 0.5 degree box that has 100 pixels. Hence, cloud amount (%) is expressed as number of pixels in each category. In each box, the median in a category is presented and it is used to calculate cloud optical thickness. The algorithm of estimation for cloud optical thickness in the present study is improved from Nakajima and Nakajima (1995) to adjust for waveband of channels on GMS-5 . Clear sky radiation temperature is also defined as the median in clear sky part in the box.

2-1. Cloud distribution

Fig. 1 shows an example of monthly mean of total cloud amount in July, 1996. It shows very active convection at the Gulf of Bengal, a cloud band from Southern part of China

to Japan islands and clear condition over the Australian continent. Similar maps for 4 cloud categories had been produced for each hour.

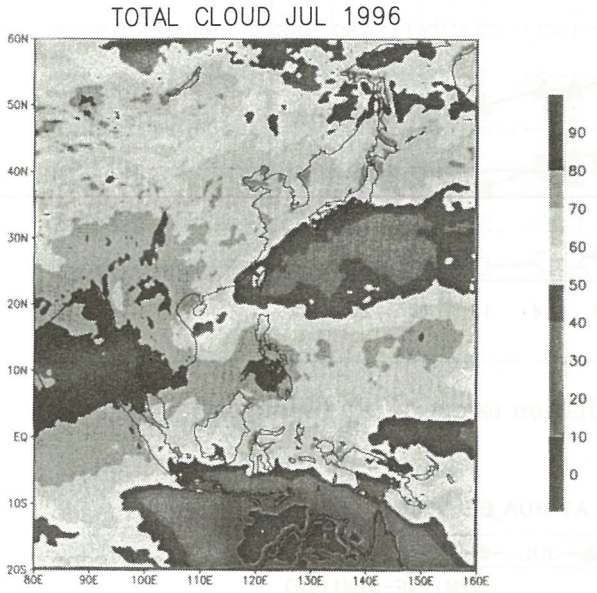

Fig.1. Total cloud cover (%).

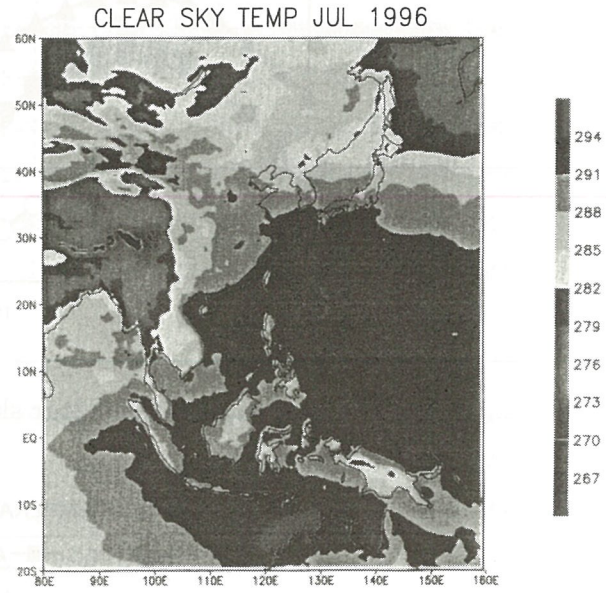

Fig.2. Clear sky radiation temperature (K).

2-2. Clear sky radiation temperature

Fig. 2 shows the monthly averaged clear sky radiation temperature. Water vapor absorption and decreased surface emissivity may make some effects to the radiation temperature. However it should be noted here that the figure can show climatologically reasonable distribution of temperature. It means this map can be used as a kind of index of surface temperature.

Fig. 3 shows diurnal variations in each season in Mongol (38N100E-43N110E) and Hua-Bei plane (32N114E-37N117E). The variation in Mongol as semi arid area has maximum in early afternoon (06Z) and minimum through the night in Fig. 3a. The variation in the Hua-Bei plane shows different variations between summer and other seasons in Fig. 3b. In July it looks stable like that in the ocean, and in other seasons it is like that in Mongol. It is derived that the algorithm picks up intermittent clear sky case in cloudy day in the month, because it is almost cloudy there in this season. Hence the surface appears to be wet and it is difficult to show large amplitude.

Fig. 4 shows seasonal change of clear sky radiation temperature and observational result at Mandalgovi in 1998. In night time (18Z), the observation is closer to the estimation from GMS-5. They will show more agreement after atmospheric correction.

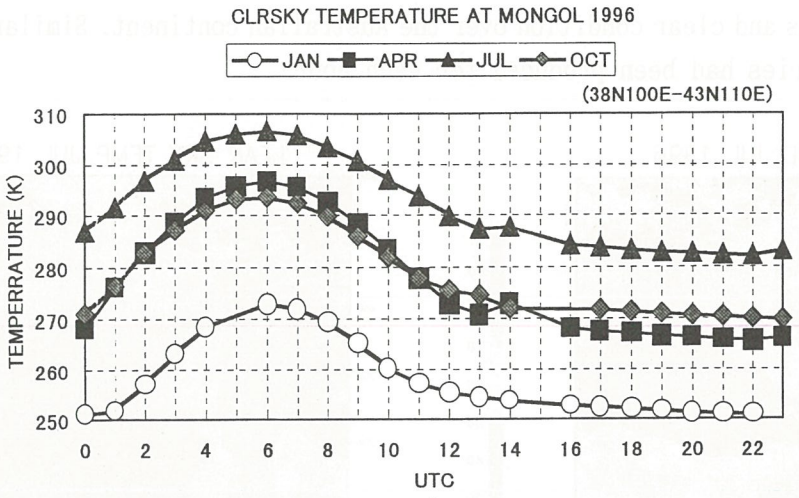

Fig.3a. Diurnal change of clear sky radiation temperature (Mongol).

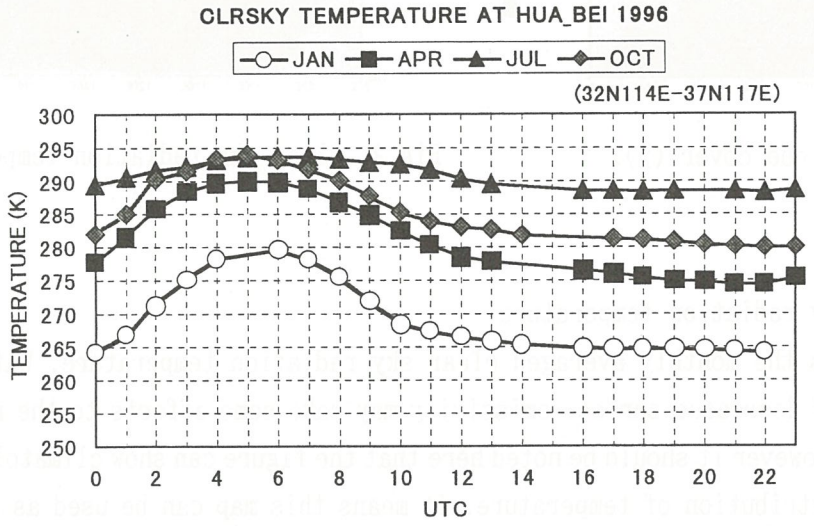

Fig.3b. Diurnal change of clear sky radiation temperature (Hua-Bei plane).

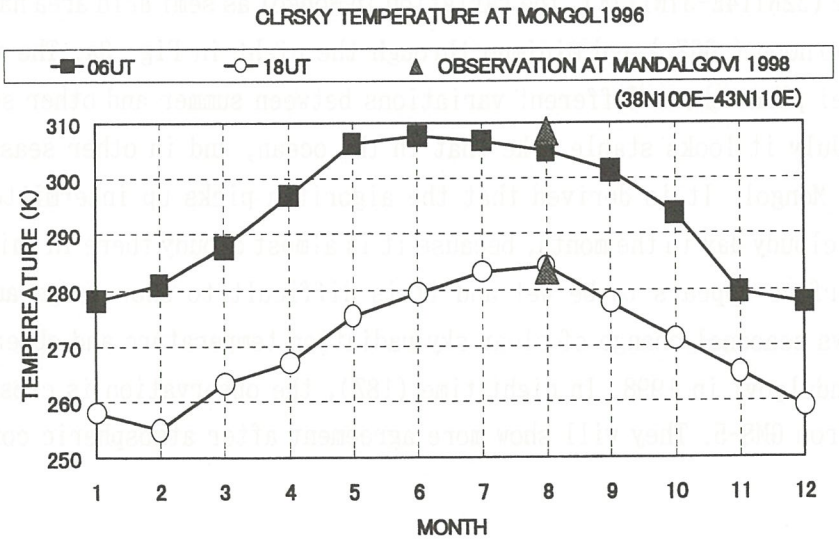

Fig.4. Seasonal change of clear sky radiaiton temperature (Mongol).

3. Surface solar radiation

Surface solar radiation is estimated from cloud information that are described at former chapter, ECMWF atmospheric data and GADS aerosol model. Radiation transfer model assumes plane parallel atmosphere and cloud. The RSTAR program package that was developed by Nakajima et al. is used for the two-stream calculation.

Optical thickness of cloud, ratio of ice cloud to water cloud, optical thickness of aerosol, effective water vapor amount, solar zenith angle and surface reflectance / ocean surface wind speed are adopted for parameters. Table of solar radiative flux is estimated from them, because too much time is needed to calculate the flux at each box.

Fig.5 shows an example of solar radiative flux at 03Z, July, 1996. This map is averaged at 03Z for all of days in the month. The fluxes in January, April, July and October in 1996 had been estimated. Fig.6 shows comparison of the estimations with observation in August 1998 at Mandalgovi, Mongol. Observation case appears to be consistent with seasonal change of the estimations from GMS-5.

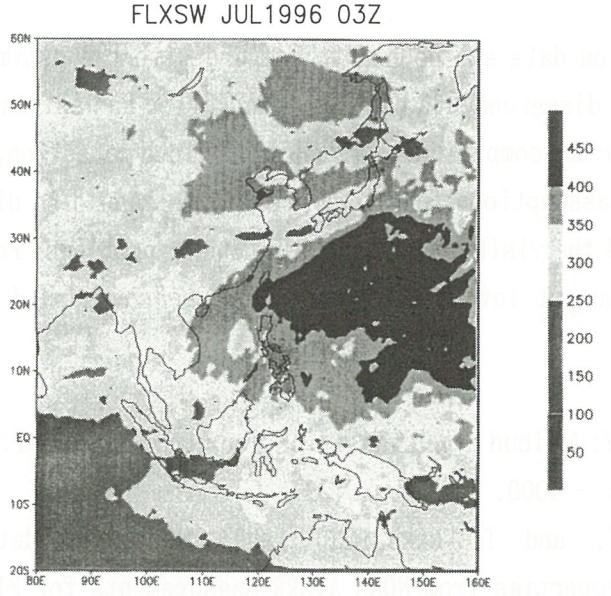

Fig.5. Surface solar radiative flux (W/m2).

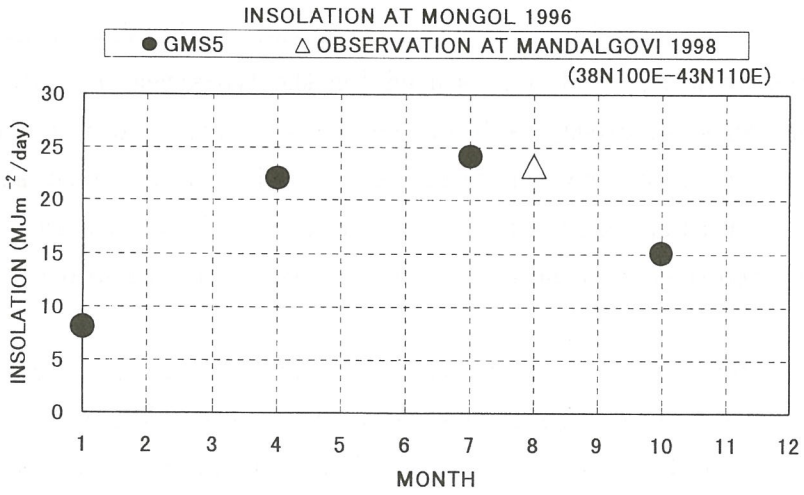

Fig.6. Seasonal change of daily accumulated surface solar radiation (Mongol).

More observation data are needed to compare with the estimation from GMS-5. The comparison makes disagreements between observation and estimation clear for various conditions. After the comparison, threshold of cloud detection, aerosol data, surface reflectance and assumptions for cloud properties should be discussed again. Change of sensitivity of the visible sensor is also one of problems. For this issue, longterm variability of output level from the visible sensor should be estimated exactly.

References

Inoue, T., 1987: A cloud type classification with NOAA-7 split window measurements, J.G.R., 92, 3991 - 4000.

Nakajima, T.Y. and T. Nakajima, 1995: Wide-area determination of cloud microphysical properties from NOAA AVHRR measurements for FIRE and ASTEX regions, J.A.S., 52, 4043-4059.

Rossow, W.B. and L.C. Garder, 1993: Cloud detection using satellite measurements of infrared and visible radiances for ISCCP, J.Climate, 6, 2341-2340.

MONITORING SURFACE MOISTURE AND VEGETATION STATUS BY NOAA AND GMS OVER NORTH CHINA PLAIN

A.Kondoh, S.Shindo, C.Tang * and Y.Sakura**

* Center for Environmental Remote Sensing, Chiba University

** Department of Earth Sciences, Chiba University

ABSTRACT

North China Plain(NCP) is the main granary in China, however, NCP is confronted with water shortage problem that may lead to the fall of the crop production. Thus monitoring NCP from space is very important to know how hydrologic environment affects the crop production. NCP has been monitoring by using NOAA/AVHRR for vegetation conditions. As a result, it is clarified that surface hydrological conditions clearly affect the crop production rate revealed by NDVI. Then the surface wetness is estimated by NOAA/AVHRR and GMS/S-VISSR. The slope parameter in the scattergram between vegetation index and surface temperature is examined for NOAA/AVHRR data. The difference in brightness temperatures between 8:00AM and 10:00AM(LT) is also investigated for GMS data. Both of which are considered to be the index of surface moisture condition. The distributions of surface wetness obtained from both methods well agree with each other. The results will be used for water management such as proper irrigation practice.

INTRODUCTION

North China Plain(NCP) is a granary of P.R.China, of which population is the largest in the world. The food situation in NCP is crucial for the future world food provision problem(Brown and Halweil,1998). The food problem in NCP is also water problem. Water for irrigation is supplied from surface water and groundwater. Recent news tell us that Yellow river does not flow to its mouse for most of the year. It is of course due to over extraction of surface water for irrigation in the upper streams. Groundwater is thus exploited for irrigation as another convenient water resource, however, water level has been declining for past several tens of years and it raises the cost of withdrawal. The price of grain may rise in near future because of the increase in irrigation cost or decrease in production by water shortage itself.

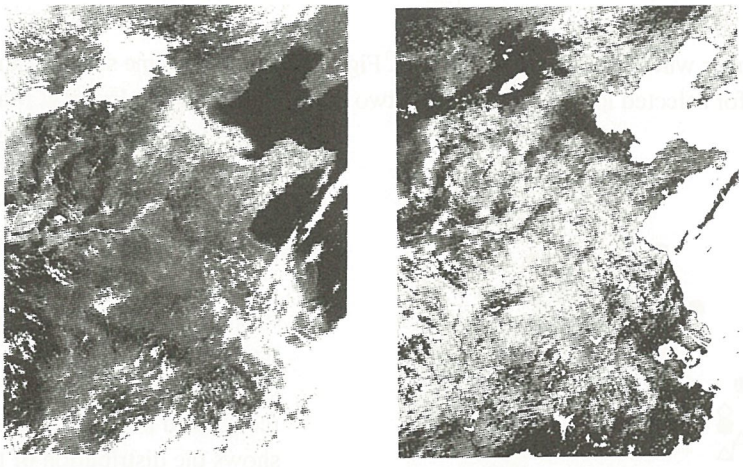

Fig.1 Visible (left) and NDVI (right) images of NOAA/AVHRR on 10 August, 1997.

Monitoring the NCP is thus very important for the various environmental and economical perspectives. The solution of water problem in NCP can only be attained by corporative research with various fields of scientists, however, the understandings of the real situation of hydrologic cycle and continuous monitoring of NCP are at least necessary. CEReS(Center for Environmental Remote Sensing, Chiba University) started to receive NOAA and GMS from 1997, and NCP is within the range. Continuos monitoring of NCP is attempted to monitor crop conditions and surface moisture status.

DATA

Since April 1997, NOAA/AVHRR and GMS/S-VISSR image data are available in CEReS. The images are geocoded to longitude and latitude coordinate and resampled to one km grid. The data are stored in the very large capacity archive system(100TB). The local dataset of North China Plain(N42,110E-N28,123E) has been creating from the archived data. Figure 1 shows a NOAA/AVHRR NCP image on10 August, 1997. The images cover the whole NCP, south of Great Wall, east of Taihan mountains and north of Huaihe river. In the middle of the image, Yellow river flows from west to north-east. Because of its worse hydrological condition, some hydrologist refer to NCP as the north of Yellow river.

METHODS TO MONITOR SURFACE MOISTURE STATUS

NOAA/AVHRR has two visible and near infrared bands and three thermal bands. GMS5 has one visible band, two thermal bands and one water vapor band. Considering the bands available, following two methods are selected to monitor surface moisture conditions in NCP.

1) Ts-VI method: Slope in surface temperature(Ts)-vegetation index(VI) relationship(Nemani and Running,1989)
2) dTs method: Increase rate of surface temperature(Ts) during morning(Wetzel et al. ,1984)

Kondoh *et al.*(1998) applied Ts-VI method to Huai-he plain, south of NCP, with NOAA/AVHRR/GAC data(4km resolution), and get very good correlation between the slope parameter and antecedent precipitation index(API). In this paper, NOAA/AVHRR/LAC(1km resolution) data are used to get the distributions of slope parameter. In the dTs method, the difference in digital count of thermal band of GMS between 8LST(Local Standard Time) and 10LST is regarded as a surface wetness index. This method is based on the concept that the difference in Ts is small when surface is in wet, and large when dry. These two methods are applied at the same time. The consistency of two independent methods will confirm the accuracy of the methods.

RESULTS

Crop Condition

The main crops in NCP are winter wheat and maize in summer. Figure 2 shows the time series of the NDVI (Normalized Difference Vegetation Index) for selected locations. There are two peaks in Vegetation Index at May and August which correspond to the growing of wheat and maize. It was a drought year in 1997, and crop growth was not satisfactory except for the area where much irrigation water was available.

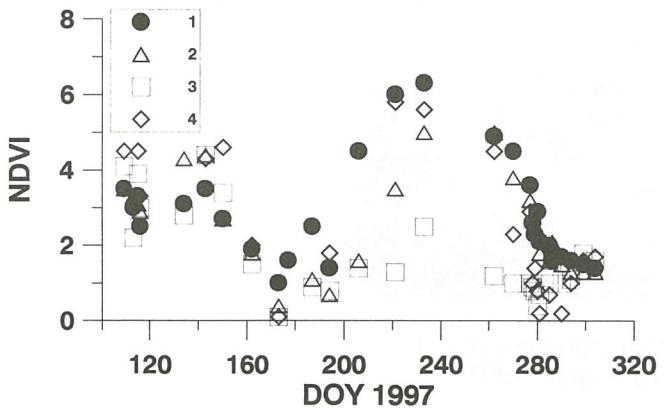

Fig.2 The seasonal trend in NDVI for selected locations. 1:116.6E,37.8N 2:116.0E,37.8N 3:115.1E,37.5N 4:114.5E,37.9N.

Fig.1b is a NDVI image on 10 August, 1997. There recognizes less vegetated area in Haihe catchment plain(northern half of NCP). Less vegetated area is recognized in Figure 1a as bright area. Figure 3 shows the distribution of total dissolved solid(TDS) in shallow groundwater in the north of NCP(Fei, 1997). There are regions with high TDS along Bohai Bay, and the high TDS zone extending northeast to southwest is recognized. It is considered that high TDS reduces the crop growing, and it is reflected on the NDVI image.

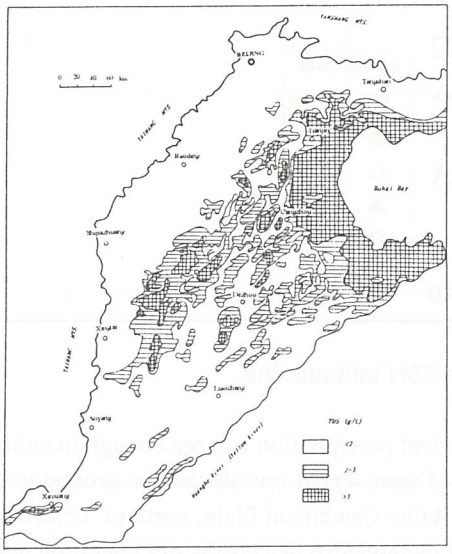

Fig.3 Distribution of Total Dissolved Solid(TDS) in shallow ground water(after Fei,1997).

Table 1. Precipitation of antecedent week

	Taiyuan	Shijiazhuang	Tianjin	Huimin
25 JUL.	60.2	33.0	21.1	22.1
18 SEP.	25.9	32.0	4.1	66.0

The coastal zone actually suffers the salinization, and it decreases the crop production. In the interior part, there exists topographic depressions, probably formed by fluvial process, where water table is shallow and easily suffers salinization. The low NDVI is the result of high salt density in the subsurface water. This means that surface and subsurface conditions reflects the crop production, and it can be seen from space. It shows the usefullness of satellite remote sensing for crop monitoring.

Monitoring Surface Moisture Status

Fig.4 shows the surface wetness estimated by Ts-VI and dTs methods. Wetness is expressed by grey scale. Black(intensity 0) in Ts-VI method denotes the area that could not calculate the slope parameter. Black(0) and white(255) in dTs method are the area where cloud prevent the application of the method.

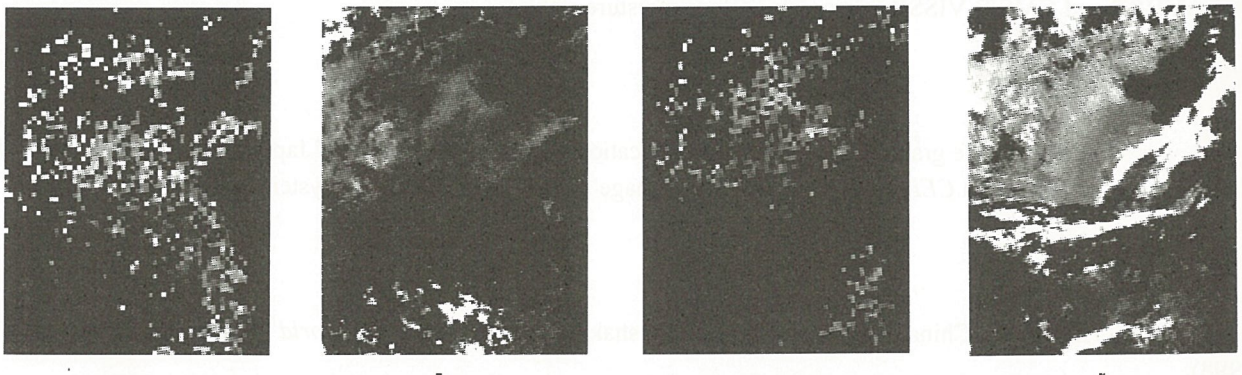

Fig.4 Surface wetness estimated by Ts-VI and dTs methods on 25 Jul. and on 18 Sep. Brightness denotes the dryness, and black(0) and white(255) are out of range. **a**:Ts-VI 25 Jul., **b**:dTs 25 Jul., **c**:Ts-VI 18 Sep., **d**:dTs 18 Sep.

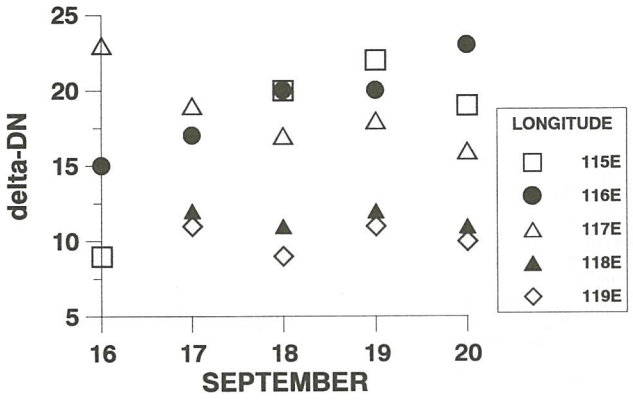

Fig.5 Time changes in dTs along the 38N latitude line.

Table 1 shows the amount of precipitation during last one week. Antecedent precipitation is large enough in entire region on 25 July. There seems little diference in surface wetness in both methods(Figure 4a). It reveals that the ground is relatively moist condition on 25 July. Clear wet and dry contrast is recognized in Haihe Catchment Plain, north of Yellow river, on 18 September case. The contrast is more distinct in dTs method, and Ts-VI method also detects the dry condition near Tianjing and its northwestern part of NCP. Huimin(near the mouth of Yellow river) had 66 mm of rain, however, Tianjing only received 4.1mm during last one week. The distribution of antecedent precipitation thus supports the estimated wetness.

Figure 5 shows the time series of dTs for selected sites along 38N latitudinal line after 16 Sep., 1997. The antecedent rain was received between 9th and 14th in NCP(Table.1). At 115E and 116E, dTs is increasing after precipitation. It is considered as a signal on surface drying. Eastern part where much rain had fallen, there is little change in dTs. Therefore, the two methods used in this study clearly catch the surface moisture condition.

These two wetness distributions are obtained from two independent methods. The sufficient consistency of both results reveals the accuracy of the methods. The important point is that both of NOAA and GMS are the most practical satellite to monitor the land surface. Practical methods are sometimes more useful than other sophisticated method.

CONCLUSION

Monitoring of surface vegetation(crop) condition and moisture status over NCP are attempted by using NOAA/AVHRR and GMS/S-VISSR. The NDVI image by AVHRR clearly explains that subsurface condition affects the crop production. Two methods to estimate surface wetness are applied independently and get consistent results. It reveals the usefulness of NOAA/AVHRR and GMS/S-VISSR to monitor surface moisture status.

ACKNOWLEDGMENTS

The work was supported by the grant of the Ministry of Education, Science and Culture of Japan. The authors appreciate Prof.Yasuda and colleagues in *CEReS* for their effort to manage receiving and archiving system of NOAA and GMS.

REFERENCES

Brown,L,R. And Halweil,B., China's water shortages could shake world food security, *World・Watch*, July/August, pp.10-18, (1998).

Fei., J., Groundwater of the North China plain, *Proc. Int'l. Symp. On hydro-Environment in Asia, CEReS, Chiba University*, pp.25-32(1997).

Kondoh,A., Higuchi,A., Kishi,S., Fukuzono,T., and Li,J., The Use of Multi-Temporal NOAA/AVHRR Data to Monitor Surface Moisture Status in the Huaihe River Basin, China. *Advances in Space Research*、(printing).

Nemani, R. And Running, S., Estimating regional surface resistence to evapotranspiration from NDVI and thermal-IR AVHRR data, *J. Appl. Meteorol.*, **28**, pp.276-284(1989).

Wetzel., P. J., Atlas, D. And Woodward, R.H., Determining soil moisture from geosynchronous satellite infrared data: A feasibility study, *J. Clim. and Applied Metorol.*, **23**, pp.375-391, 1984.

Global Image Network System for Ground Truth

Koji Kajiwara, Yoshiaki Honda
Center for Environment Remote Sensing Center (CEReS)、University of Chiba, Japan
1-33,Yayoi,Inage-ku Chiba 263, JAPAN
kaji@rsirc.cr.chiba-u.ac.jp

1.Introduction

GPS camera which can automatically record time and geographic information on the film has high utility value for collecting ground truth data. To build the database by using information which recorded on film will lead to development of GPS camera data for study. At the same time, utilization of GPS camera data leads to make standard data. In the other words, increase in these GPS camera image leads a standardization of save format of the GPS camera image and geographic data.

Recently, as the diffusion rate of personal computer increase, World Wide Web(using Internet) increase. At the same time we are can open and browse data(documents and images) by using Web server and Internet browser (ex. Netscape Navigator).Moreover development of WWW technology is growing, it has just started to distribute interactive pages in cooperation with Web server and database management system(DBMS) .

Therefore, in this study , for doing mutual use of resource(ex. images taken by GPS camera),it is method to develop network system that available to share GPS camera images by using Internet. and now we call that system "Global Image Network (GIN)".

2.Global Image Network (GIN)

At first we thought that it is necessary to gather meta data of GPS camera image in one place for sharing them globally and providing retrieval service . It was for that purpose that we are carrying study (develop system by using Internet)forward. we call that system "Global Image Network (GIN)" project. We are now on the development and when it completes, GIN will contribute to the research activity in the field of Remote sensing and others.

Figure.1 shows three constituent of GIN ,Meta data Center, Local data Center, GIN user.

Meta data Center is most important center in GIN project, it offers some convenient service. It manage catalogue information (meta data) which registered from Local data Center and provide retrieval service through the GIN home page on WWW.

Local data Center is organization which permitted to register GPS camera image to GIN through the Internet. Local data Center is necessary to be authorized by Meta data Center.

GIN users are users who access to GIN home page through the optional Web browser and get retrieval service.

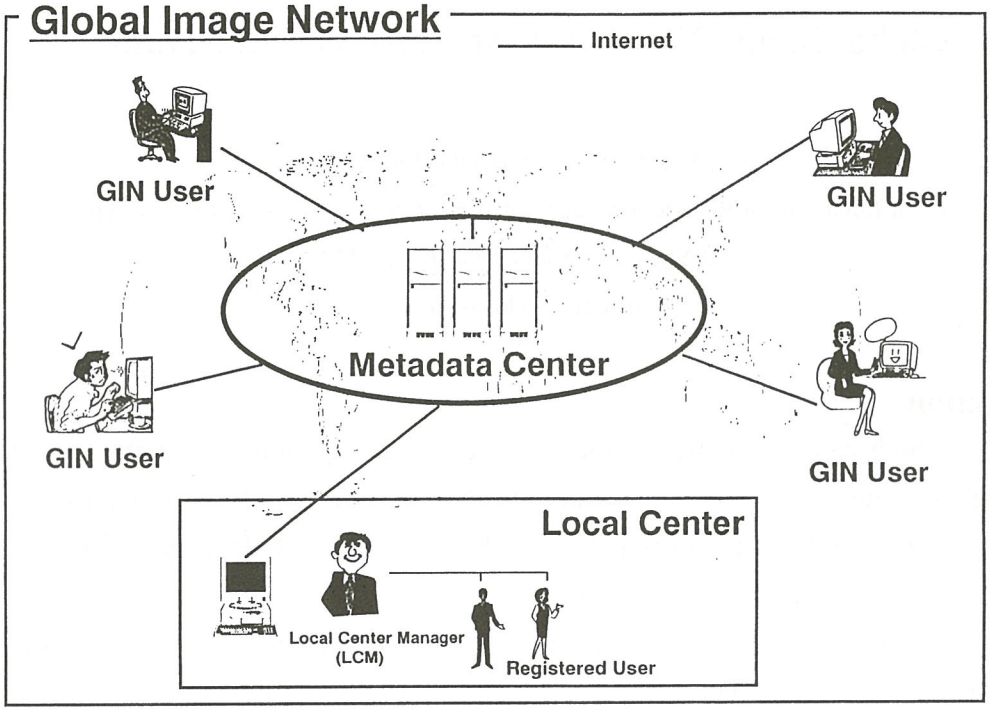

<Figure.1>

More detail definitions of each constituent are follows.

A).Meta data Center

Meta data Center which is center constutuent of GIN project is established on computer(named GIN) in Center for Environment Remote Sensing Center (CEReS) .It has main functions as follows.

1).Management of metadata

Meta data Center manage meta data concerning GPS camera image registered. It has URL of each GPS camera image, but it don't have any image. WWW technology has LINK function(use URL). Meta data Center is able to manage a lot of GPS camera images by using that function ,so it doesn't need a mount of hard disk drive volume. We use SQL Server(Microsoft) as database.

2).Authorization of Local data Center

Meta data Center authorize Local data Center. In the case of authorization request from organization , Meta data Center publish Local data Center account and password after examination.

3).Management of registered user

Meta data Center publish account to registered user (belong to Local data Center)on GIN home page.

4).data search service

Meta data Center open catalog data (registered image and data)on GIN home page, and it offers home page for search data. By means of that, GIN user can search and download GPS camera image.

B).Local data Center

Local data Center is organization and group that have registered image to GIN or can do. Local data Center is necessary to have the minimum system for being authorized from Meta data Center.

Local data Center needs the following lists.

Local data Center needs

1.WindowsNT Server (ver 3.51 later)

2.Web Server

There are two kinds of image on GIN.

1.Original image

Original image keeps on Local data Center server and registered user has its ownership. Image size isn't fixed.

2 .Thumbnail image.

Thumbnail keeps on Meta data Center server and is used on GIN home page as catalog image. Image size is fixed. If registered user want to register image, he has to prepare and send it to Meta data Center.

GPS camera original images are placed on Local data Center server machine, dividing into two kinds of permissions.

1.Full open data

open original image to everyone through GIN

2.Conditional open data

open only meta data to everyone through GIN. If someone wants this image ,owner opens original image to him conditionally. Meta data Center intermediates between the two sides.

C).registered user

Registered user must belong to Local data Center, they are permitted by Local data Center manager on his responsibility. Registered user registers GPS camera image by using Application for Image Registered(AIR),and he have to decide the permission for each image.

D).GIN user

If someone has the following system, he can access to GIN home page and download GPS camera image somewhere and every time.

GIN user needs

1. Internet connect system (personal computer, modem, etc)
2. Web browser (Netscape Navigator , Internet Explorer ,MOSAIC, etc)

3.development of GIN

At first ,we builded the database on the Meta data Center machine. When we build it, we utilize relational model. The second, we connected database to WWW server, so we can open the data through the Internet. The third, we developed AIR which creates Registration Information File(RIF). RIF is the key file to transport data between Meta data Center and Local data Center.

Registration Information File(RIF)

RIF is described information of Local data Center and registered user and registered image. It has kept on each registered user of personal directory on Local data Center server. When registered users want to register or update image, this file is used. Registered users have to tell to Meta data Center when he modify RIF. To be concrete, you have to pull trigger by using GIN home page to reflect modified contents of RIF to Meta data Center database. It has prescribed format, and must be written by ASCII code. Summary of prescribed format is following.

-RIF is divided into three block.

1. header section(Local data Center info, personal registered user info)
2. group info section (meta data of group info)
3. image info section (each registered image info)

-All of record of RIF must be written just one line.

-Each element is separated by TAB code(0x09).

Sample RIF written by prescribed format is published at the back of this paper.

If RIF is written by prescribed format, registered user don't need to use AIR. But they can make and modify RIF easier if they use AIR.

A).Building of GIN database

We built GIN database which is based on relational model. Built table is following.

1.Table for GPS camera image

Main function of this table is to manage information of GPS camera image. But this table isn't only designed for GPS camera data but also designed by using concept of grouping image. In the other words meta data is also included group information which made by registered user. So GIN user is able to find wanted image more easily by using group information(not only date and longitude ,latitude).

2.Table for managing registered user

This table is to manage information of Local data Center and registered user.

B). Linking between WWW Server and database

At present , it is popular that to use CGI(Common Gateway Interface) for linking between WWW Server and database. But we use ISAPI(Internet Server API).Because ISAPI is more faster than CGI.

C).Development of Application for Image Registered (AIR)

Registered user use AIR to register images to GIN. AIR is able to be downloaded from GIN home page. This application makes RIF by inputting , so Meta data Center get RIF (use FTP) after registered user pull trigger on GIN home page. (See Figure 2)

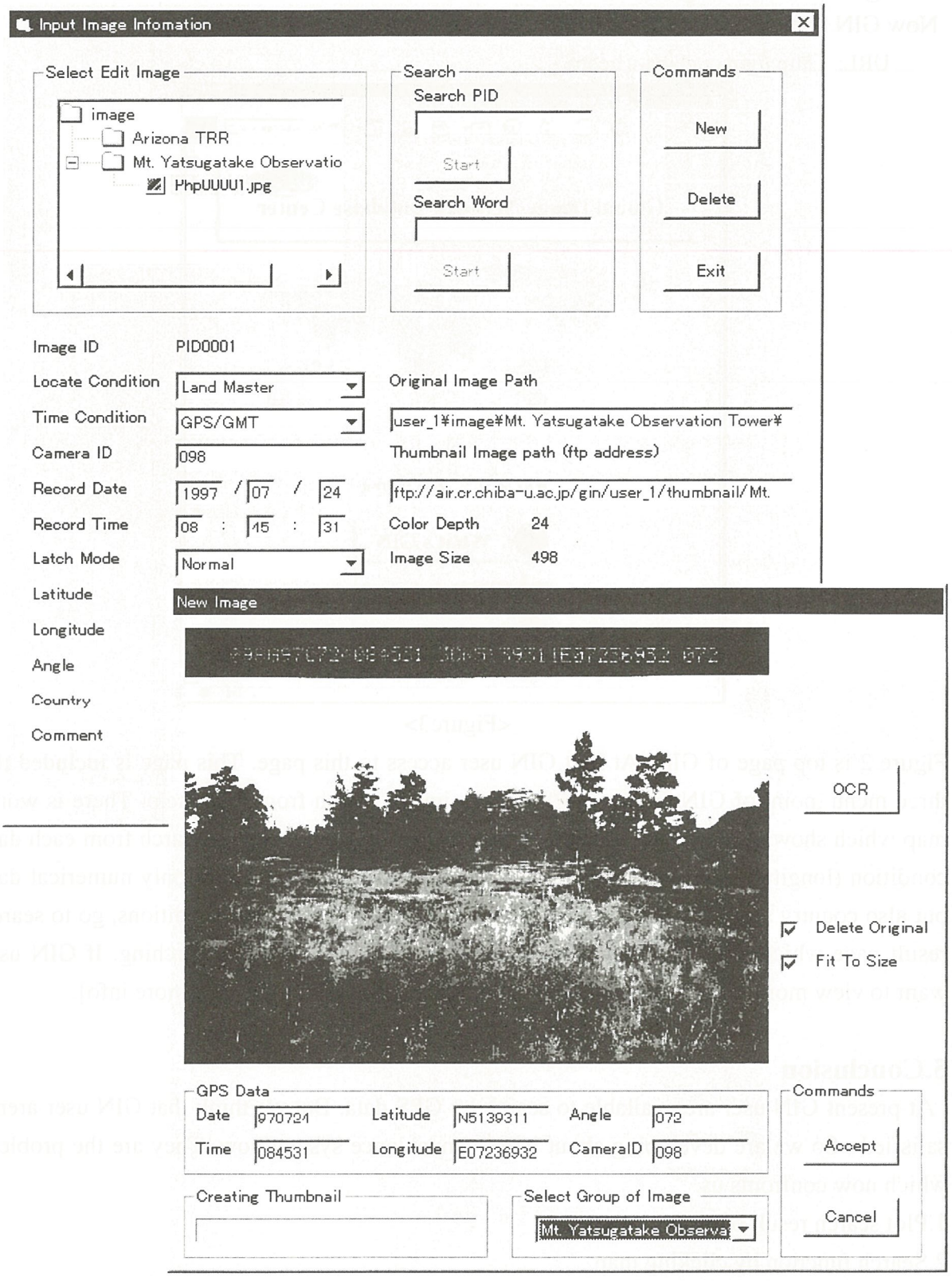
Input Image Infomation
Select Edit Image
image
Arizona TRR
Mt. Yatsugatake Observatio
PhpUUUU1.jpg
Search
Search PID
Start
Search Word
Start
Commands
New
Delete
Exit
Image ID
PID0001
Locate Condition
Land Master
Time Condition
GPS/GMT
Camera ID
098
Record Date
1997 / 07 / 24
Record Time
08 : 15 : 31
Latch Mode
Normal
Latitude
Longitude
Angle
Country
Comment
Original Image Path
user_1¥image¥Mt. Yatsugatake Observation Tower¥
Thumbnail Image path (ftp address)
ftp://air.cr.chiba-u.ac.jp/gin/user_1/thumbnail/Mt.
Color Depth
24
Image Size
498
New Image
OCR
Delete Original
Fit To Size
GPS Data
Date
970724
Time
084531
Latitude
N5139311
Longitude
E07236932
Angle
072
CameraID
098
Commands
Accept
Cancel
Creating Thumbnail
Select Group of Image
Mt. Yatsugatake Observa

< Figure 2>

4.Progress of development

Now GIN home page is trial open. URL is as follows.

URL: http://gin.cr.chiba-u.ac.jp/

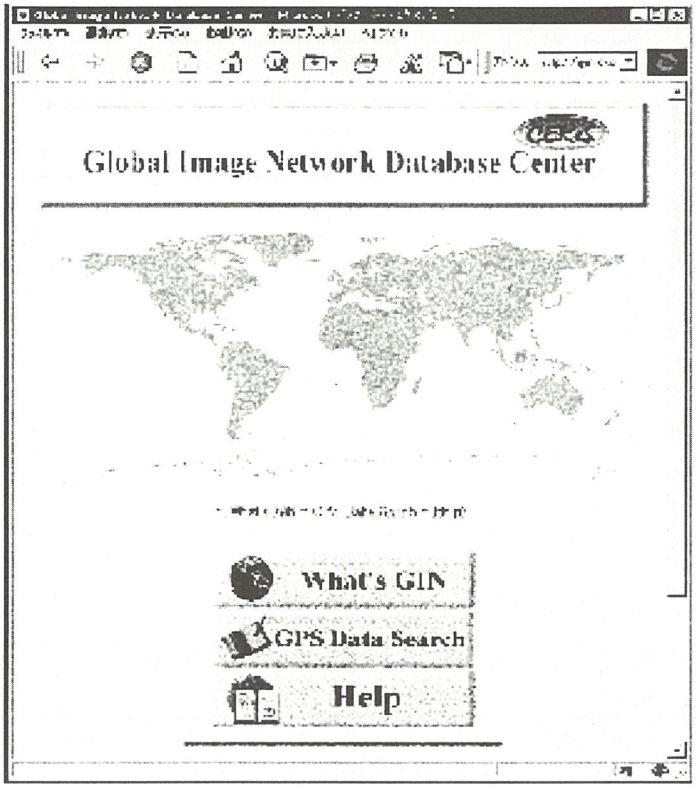

<Figure3>

Figure 2 is top page of GIN. At first GIN user access to this page. This page is included the three menu ,point of GIN project ,GPS camera image search from data, help. There is world map which shows existed data in GIN by red dot. Search page offers to search from each data condition (longitude ,latitude, date of taken picture etc).This page is not only numerical data but also country name. When you click search button after filling out conditions, go to search result page which page shows part of hitting GPS camera image by searching. If GIN user want to view more information of each image, they can view by clicking [more info].

5.Conclusion

At present GIN user are available to search by GPS data. But we think that GIN user aren't satisfied . So we are developing about more convenience system now. They are the problem which now confronts us.

1.Plot search result on map

2.Search function by clicking map

3.Narrow down search function

4.Package download function

At the same time we think that more addition and improvement are needed ,for all GIN user are satisfied.

Project for Establishment of Plant Production Estimation using Remote Sensing

Yoshiaki HONDA*, Koji KAJIWARA*, Hirokazu YAMAMOTO*, Toshiaki HASHIMOTO*, Masataka TAKAGI and Tamio TAKAMURA***

***Center for Environmental Remote Sensing (CEReS), Chiba University**
1-33. Yayoi-Cho, Inage-Ku Chiba 263-8522, Japan
Tel: +81-43-290-3845 Fax: +81-43-290-3857
E-mail: yhonda@rsirc.cr.chiba-u.ac.jp

****Dept. of Infrastracture Systems Engineering, Kochi University of Technology**
185, TosaYamada, Kochi 782-8502., Japan
Tel: +81-887-57-2409 Fax: +81-887-57-2420
E-mail: takagi@infra.kochi-tech.ac.jp

1. The Study Area

Our study area is around Mandalgobi in Mongolia. We conducted measurement in 3 types of grassland around Mandalgobi. First observation site, Site 1 is located in north side of Mandalgobi (N45deg 59' 41.5" E106 deg 19' 39.5") and this site is more dense vegetated area than other observation site. Measurement in this site is conducted during 3-9 Aug., 1998. Second site, Site 2 is located in western part of Mandalgobi (N45 deg 38' 51.9" E105 deg 39' 13.3") and this is sparse vegetated grassland area, and data is obtained in Aug. 10,1998. Third site, Site 3 is located in southern side of Mandalgobi (N45 deg 23' 23.6" E106 deg 14' 9.9") and measurement was conducted 11 Aug., 1998. Some observation (acquisition of weather condition data etc.) was done in Hydrometeorological and environmental Study Center, Dundgobi AIMAG, Mongolia.

Site 1 is almost 2.5km * 2.5km wide area, Site 2 and Site 3 are 1km * 1km. The area measured by Radio-controlled Helicopter Survey is about 100m * 100m. the area of biomass measurement is very close to the area measured by mobil measurement, BRDF measurement and RC-Heli survey.

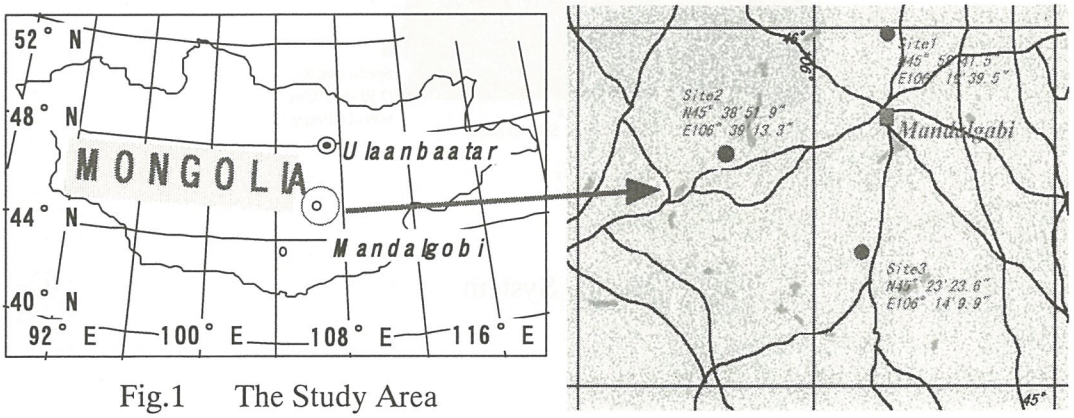

Fig.1 The Study Area

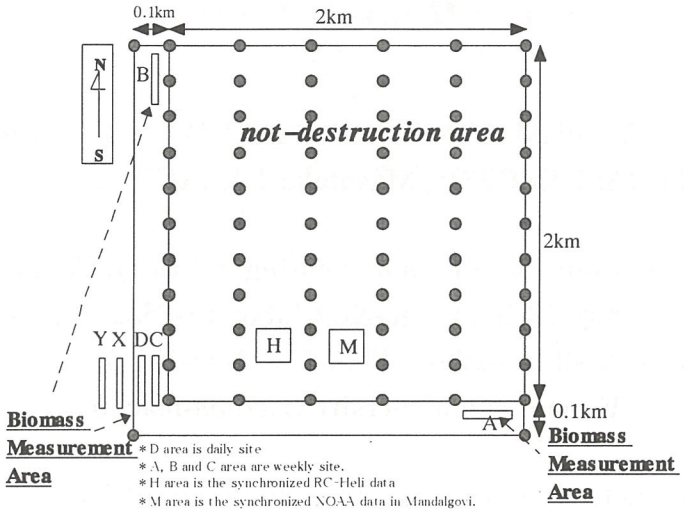

Fig.2 Whole Observation Area in Main Test Site (Site 1)

2. Mobile Measurement

We put the arm on the car-top, and the tip of the arm has multi sensor system. The height of the sensors from ground is approximately 2m. This multiple sensor system has Digital Still Camera (DSC,KONICA Corp.), CCD Camera (SONY CCD-MC-1) with Digital Video Recorder (SONY DCR-TRV9), GPS Camera (KONICA Corp.), 3D Scanner (PULSTEC INDUSTRIAL CO.,LTD TDS3100, 680nm laser scan), thermometer(HORIBA,Ltd., IT-540S) , GPS (NovAtel Inc., Single-GPS) and spectrometer (Soma Optics Inc.). All sensor's observation angle is nadir. By this system, we could obtain 100 each data in the short time (about 1.5 hour) in the wide area (Site1 : 2.5km*2.5km, Site2 & Site3 : 1km* 1km).

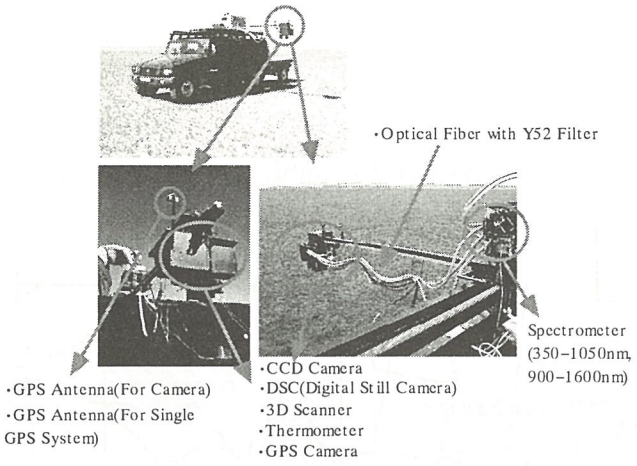

Fig.3 Mobile System

2.1 Spectral reflectance (350nm-1050nm) using spectrometer

Spectrometer has dual port, one is measurement for ground sample and the other is measurement for white reference board. This instrument can measure with 2048 channel in wavelegth from 350nm to 1050nm, but we measured with 512 channel mode because optical wavelength resolution of this spectrometer is approx. 1nm. FOV is approx. 19.5 deg. We also have obtainid soil reflectance at each observation site (Site 1, Site 2, Site 3).

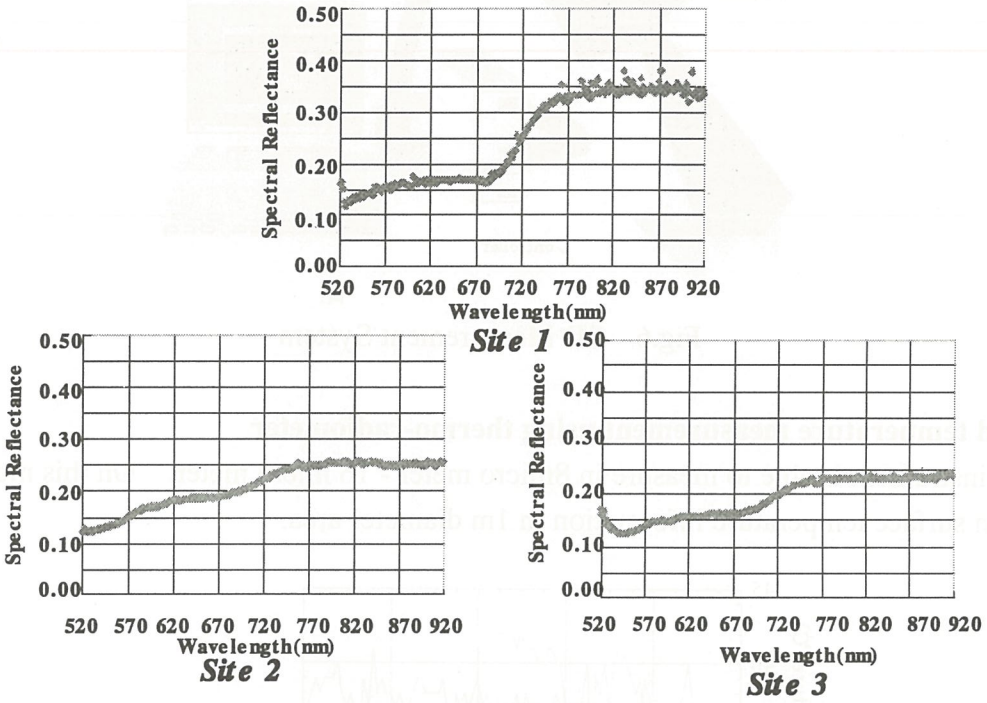

Fig.4 Averaged Spectral Reflectance for each site

2.2 Vegetation coverage ratio (VCR)

Calculation of vegetation coverage ratio is derived from Digital Still Camera (DSC) images and 3D scanner data (distance data and laser intensity data). FOV is 48.8 deg * 37.0 deg.

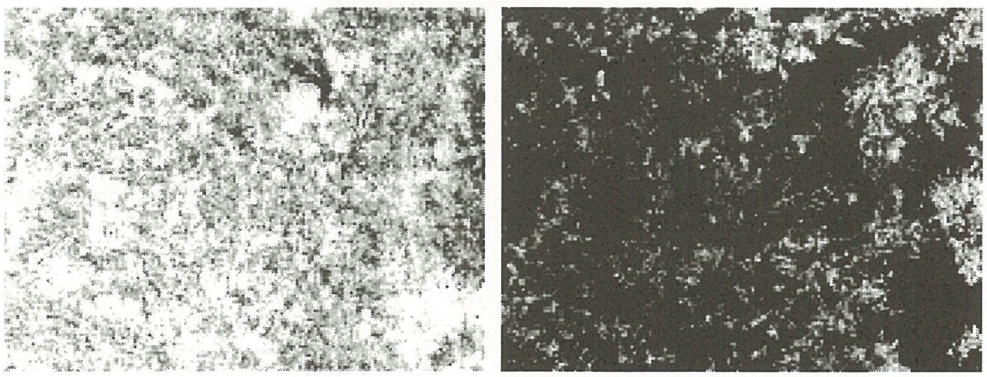

Fig.5 Digital Still Camera Original Image(Left) and Binarized Image(Right)

2.3 Geometric measurement of grass using 3D scanner

3D scanner can record distance data and laser intensity data. Laser wavelength is 680 nm, and disance data is able to exchanged into grass height data, therefore it can discriminate vegetation, soil and other components. FOV is 30 deg * 28 deg.

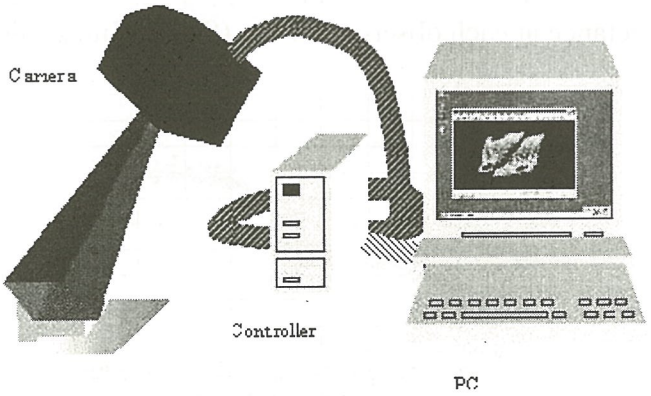

Fig.6 3D Measurement System

2.4 Ground temperature measurement using thermo-radiometer

This instrument is able to measure in 8micro meter - 16 micro meter. On this mobile system, it can obtain surface temperature information in 1m diameter area.

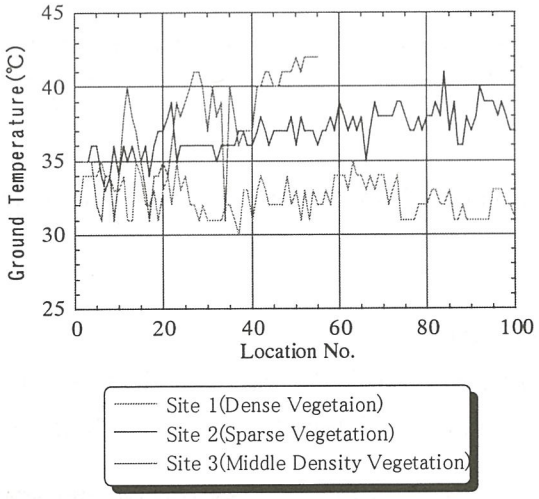

Fig.7 Ground Temperature obtained by Thermometer

2.5 Photograph of ground condition using GPS camera

These photograph will be able to put into GIN (Global Image Network database center).

2.6 Positioning data using single GPS

This system record not only GPS positioning data (x,y,z) but also UTC, standard deviation (x,y,z), GDOP (accuracy), direction and number of satellite in one ASCII file with every spectral information. We confirmed distribution of measurement point and accuracy each measurement points. The accuracy is about 15m -20m.

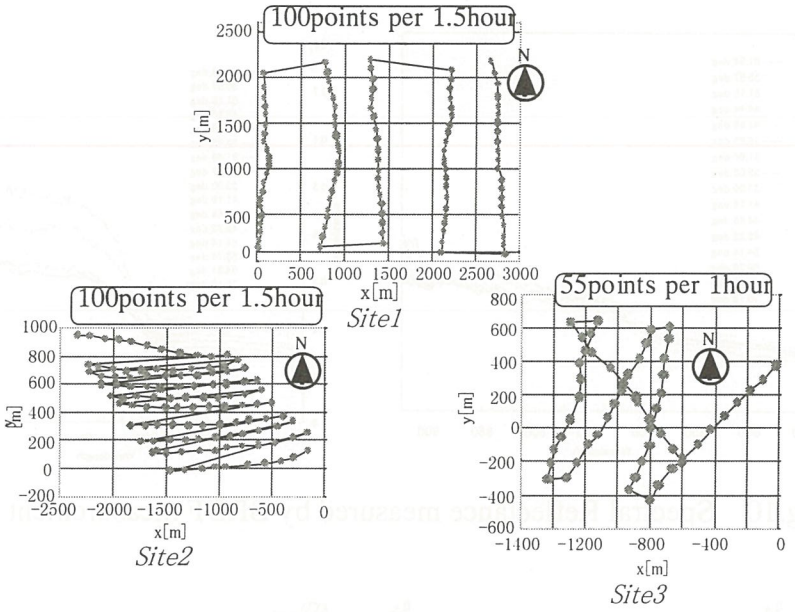

Fig.8 Distribution of Measurement Points

2.7 Real-time monitoring of ground and each instrument condition using CCD camera

CCD images were recorded by DVC. This system can real-time monitor spectral information and ground condition in the car. DSC and GPS camera is reconstructed to be able to release remote shutter. Therefore, mostly, we can operate these system inside of the car.

3. BRDF Measurement

This system has 2 axis stepping motor drive, therefore it can otain spectral information and images for 3 dimensionally. Measurement for one cycle required about 15 minutes. It is more short time than previous our developped system. This system is also put on the vehicle, therefore we can acquire BRDF data at each points in the wide area. Measurement height is about 5m.

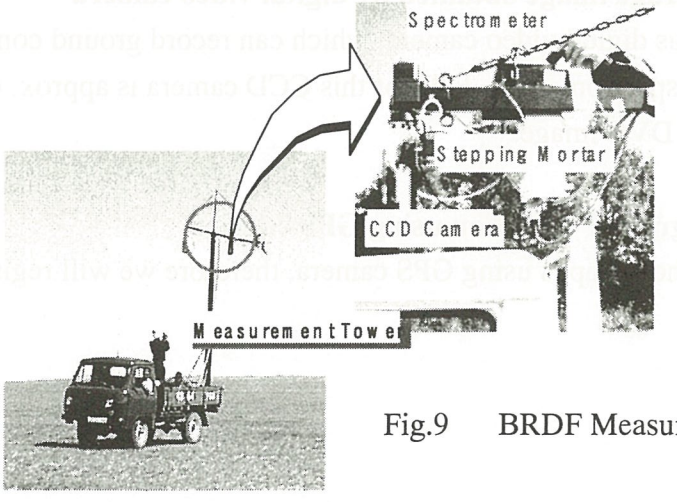

Fig.9 BRDF Measurement System

3.1 Spectral Reflectance(350nm-1050nm)

This instrument is the same as the spectrometer of mobile measurement system. We measured each spectral reflectance with azimuth angle 0deg to 360deg, zenith 0deg to 60deg (all data is 512 channel).

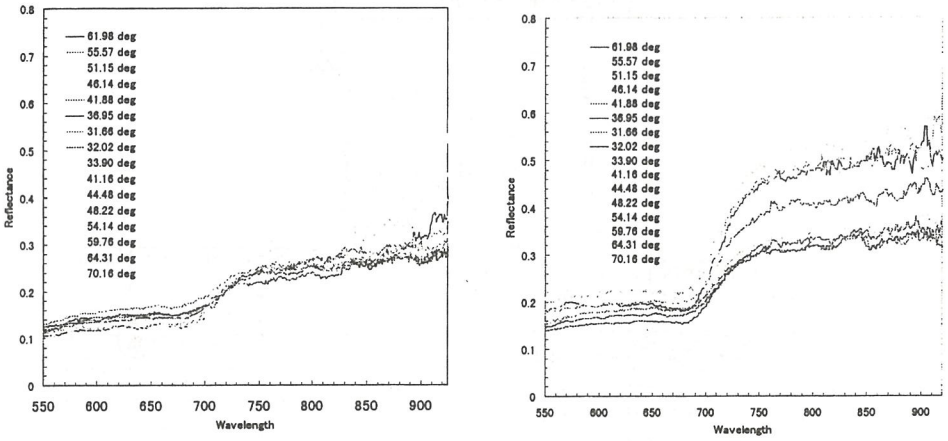

Fig.10 Spectral Reflectance measured by BRDF measurement system

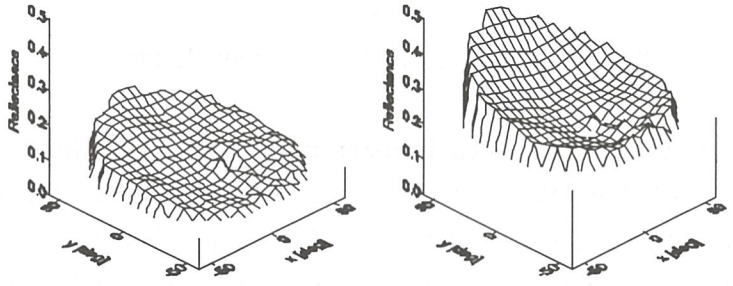

VIS 580nm – 680nm NIR 725nm – 920nm

1998/ 8Ø9 17:00

Fig.11 Directional Reflectance Profile in the RED (580-680nm) and NIR(725-920nm)

3.2 Vegetation coverage image obtained by digital video camera

This system has digital video camera, which can record ground condition in the same direction as view of spectrometer. FOV of this CCD camera is approx. 65 deg. Also we can calculate VCR from DVC image.

3.3 Photograph of ground condition using GPS camera

We also took photographs using GPS camera, therefore we will register these images to GIN.

4. Radio-controlled helicopter (RC Heli) survey

This instrument is able to obtain ground condition image and spectral reflectance from higher position than the ground measurement (approx. 1-150m). It is easy to understand representative spectral information in the wide area.

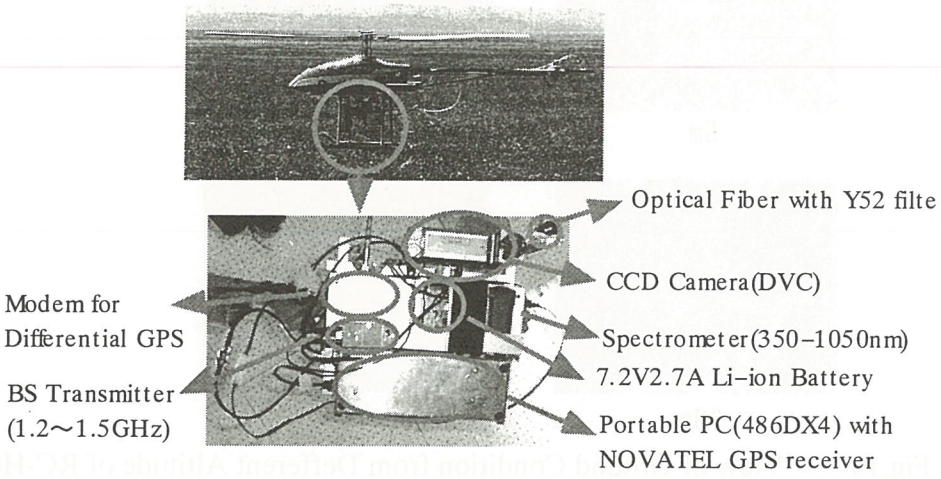

Fig.12 Radio-controlled Helicoper Survey System

4.1 Spectral Reflectance(350nm-1050nm) using spectrometer

This instrument is the same as mobile measurement system and BRDF measurement system.

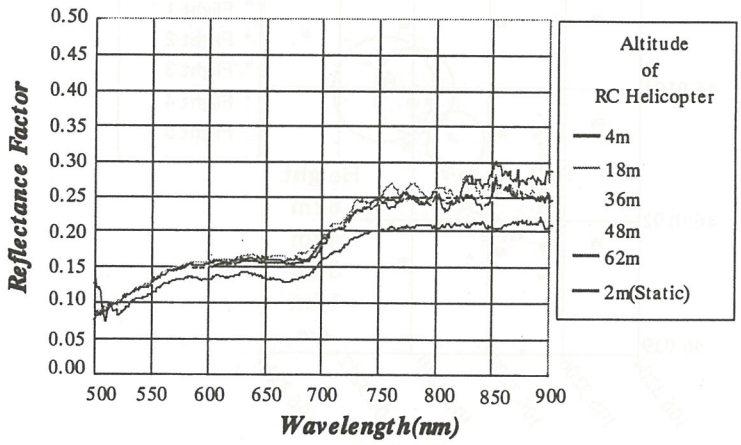

Fig.13 Spectral Reflectance obtaied by Spectrometer mounted on RC Heli system

4.2 Vegetation coverage image obtained by digital video camera(DVC)

This system also has DVC for confirmation of ground cover condition in the view from sensors. It is easy to check the data quality obtained by this system.

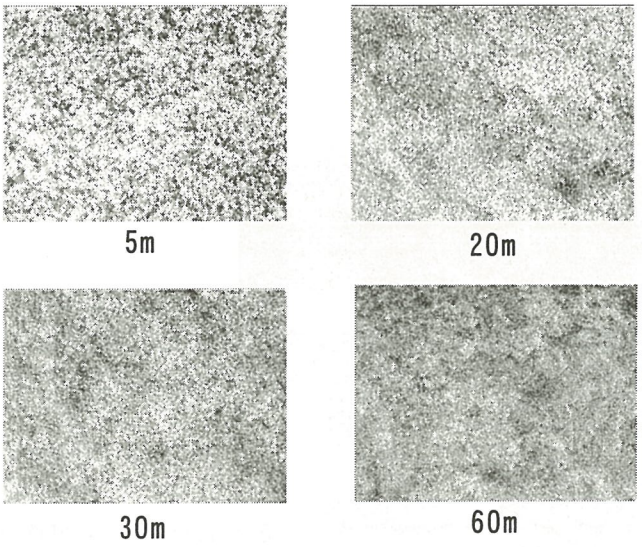

Fig.14 View of Ground Condition from Defferent Altitude of RC-Heli

4.3 Positioning data with differential GPS

This system use differential GPS, therefore it can obtain precise latitude, longitude and altitude data. The accuracy of this GPS system is 0.75m - 1m.

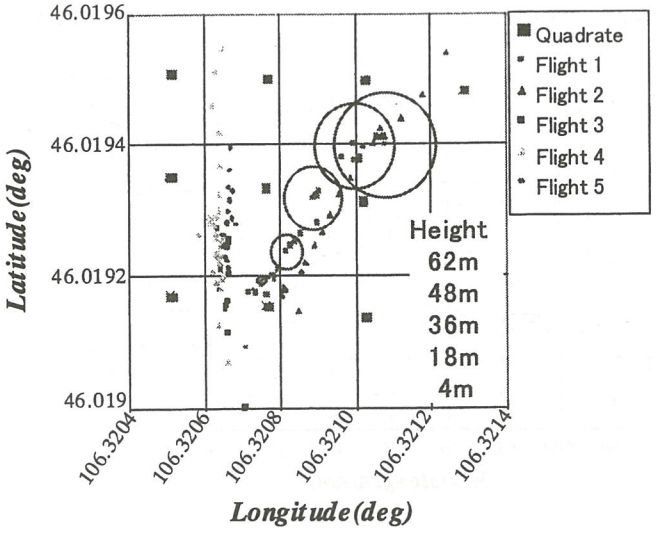

Fig.15 Measurement points of RC Heli Survey system

5. Biomass measurement

The purpose of this measurement is to grasp the amount of living plant and the change of that amount as possible as precisely. The measurement height of this system is about 2m.

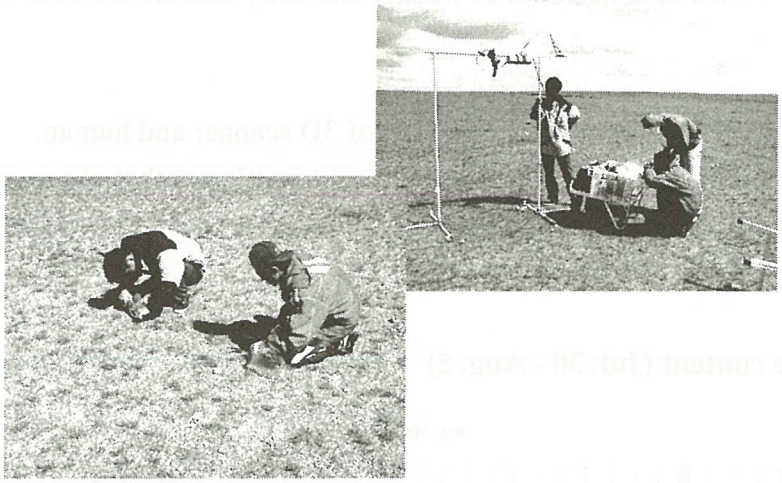

Fig.16 Biomass measurement

5.1 Component of plant

This measurement was conducted by Mongolian botanist, Dr. Ganbold.

5.2 Vegetation coverage ratio using digital still camera

Calculation method is the same as mobile measurement. This measurement is also used DSC image data and 3D scanner data.

5.3 Spectral reflectance (350nm - 1050nm)

Measurement instrument is the same as the spectrometer of mobile measurement system and BRDF measurement system. We measured spectral reflectance before and after grass cutting, therefore we also obtained soil reflectance.

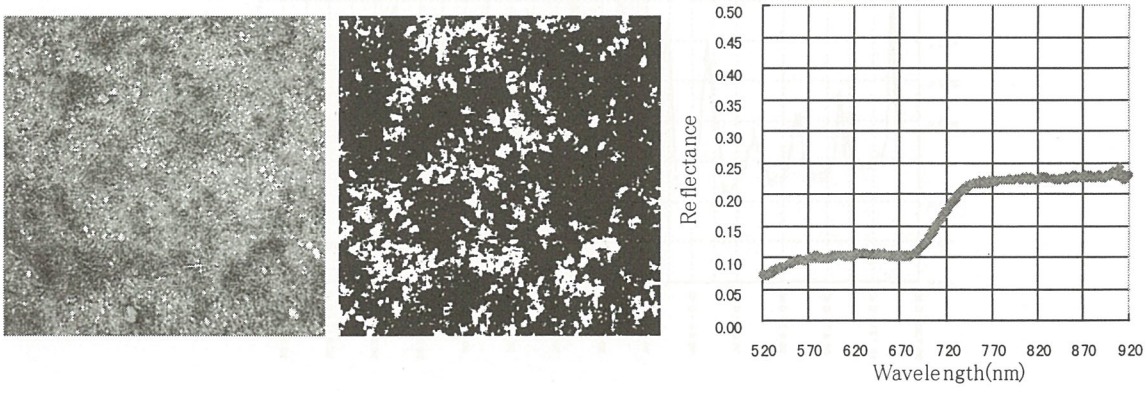

Fig.17 Original Image and Binarized Image Obtained by DSC and Spectral Reflectance

5.4 Wet grass weight and dry grass weight

Grass cutting area is 1m*1m. We measured the weight of wet grass and well dryed grass by drying machine. We set about 100 quadrats in whole survey area, but very close to other observation area. We obtained both of weekly and daily data from 30 Jul to 12 Aug.

5.5 Grass height

This measurement was conducted by both of 3D scanner and human.
And we also measured other information using by automatic weather observation equipments in Hydrometeorological and environmental Study Center, Dundgobi AIMAG in Mandalgobi (Fixed observation).

5.6 Soil moisture content (Jul. 30 - Aug. 5)

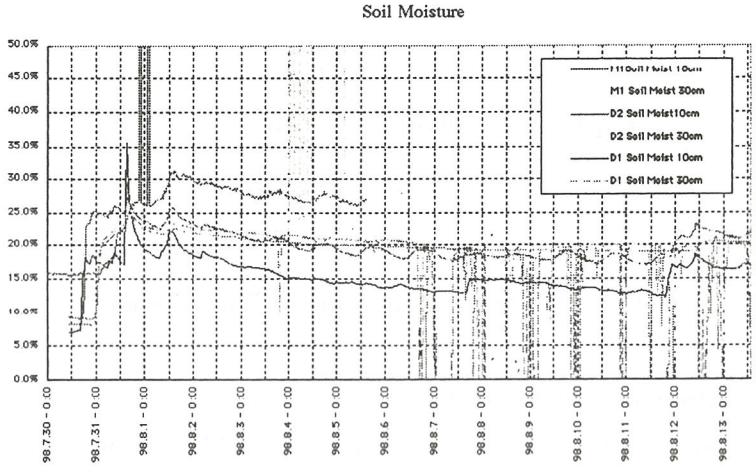

5.7 Surface and ground tempareture (Jul. 30 - Aug. 13)

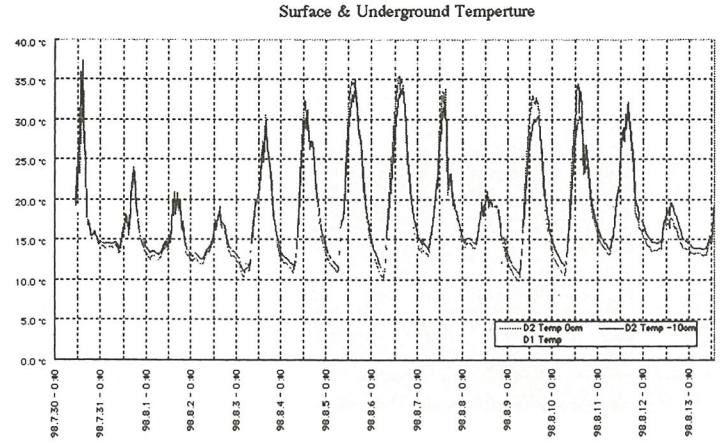

5.8 Solar radiation (Jul. 30 - Aug. 5)

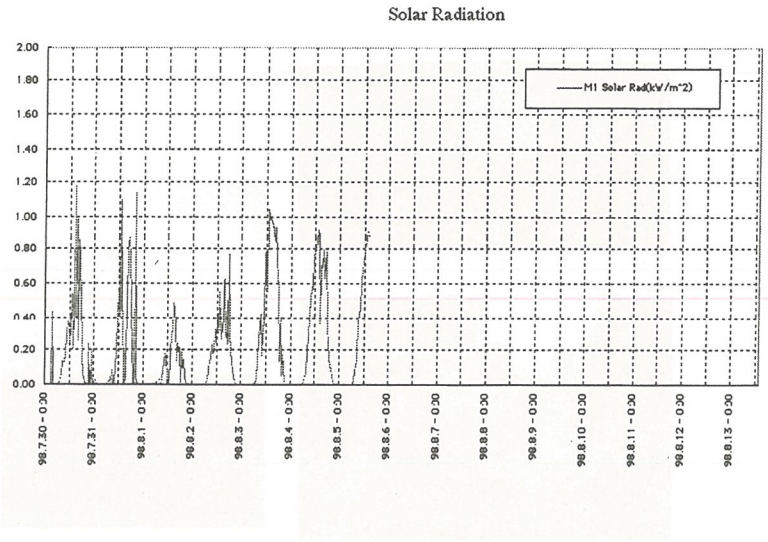

5.9 Rainfall (Jul. 30 - Aug. 5)

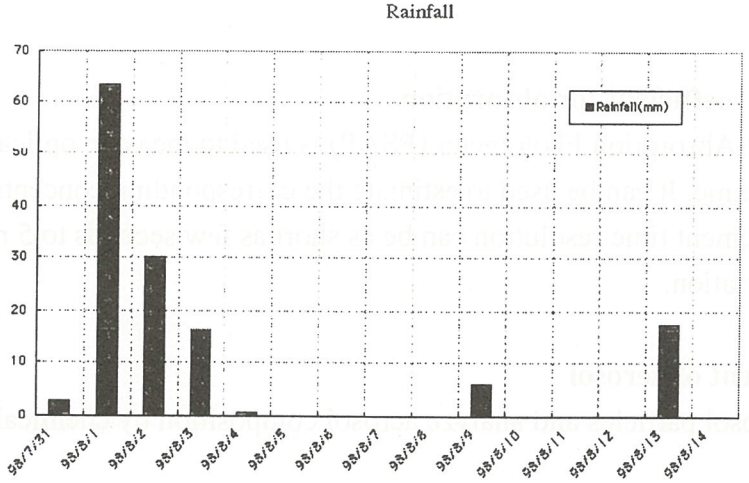

6. Atomospheric Measurement - 1

The objective of this measurement is to derive the following items.

*Aerosol optical thickness

*Aerosol size distribution

*Aerosol complex refractive index

*Chemical constituent of aerosol

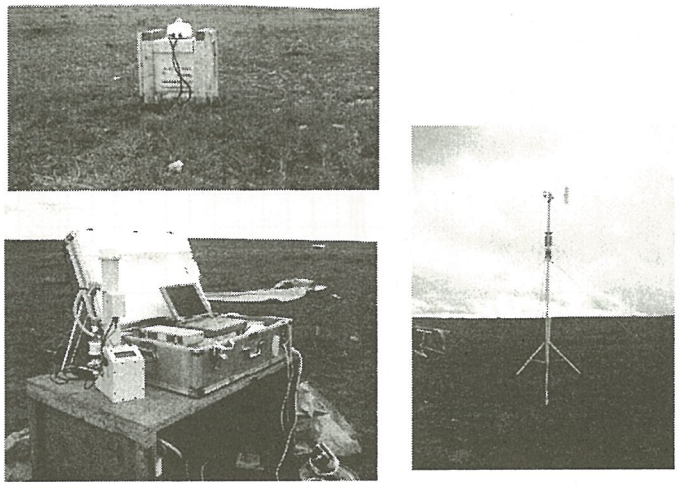

Fig.18 Atmospheric Measurement

6.1 Optical extinction coefficient for absorption

The Particle Soot/Absorption Photometer (PSAP) is used to measure optical extinction coefficient in near real time. It can be used to estimate the corresponding concentration of fine particle soot. Measurement time resolution can be as short as few seconds to 5 minutes depending on aerosol soot concentration.

6.2 Chemical constituent of aerosol

It was filtered aerosol particles and analyze aerosol composition by chemically.

6.3 Sky radiance distribution

It was mesured by the Sky Radiometer at each wavelength (315, 400, 500, 675, 870, 940, 1020nm). And it will be retrieves aerosoloptical thickness and particle size distribution.

6.4 Direct solar radiation

This was measured by Field Spec and handy type Sun Photometer. And we will calculate aerosol optical thickness at each wavelength. Field Spec has large number of channels (340-1070nm, 512channels) and which has been calibrated at Mauna Loa observatory, Hawaii. It can perform precise observation of direct solar radiation.

6.5 Irradiance on a plane surface

These are measured by the Pyranometer. Irradiance is derived from the direct solar radiation and from the diffuse radiation incident from the hemisphere above, therefore the Pygeometer is designed for the measurement of (unidirectional) global incoming or outgoing longwave terrestrial radiation.

6.6 Rayleigh scattering extinction coefficient

It was measured by the Integrated Nepherometer. Pressure and temperature sensors automatically correct for changes in air Rayleig scattering. Rh also is monitored and recorded. The light source is a variable rate flashlamp with a wavelength defining optical filter (530nm).

6.7 Brightness temperature of the sky (bottom of the cloud) and the ground surface

It was measured by thermo-radiometer.

6.8 Weather condition data

Atmospheric measurement was also obtained weather condition data at the same time. These ware measured by Anemometer, Thermometer, Hygrometer and Barometer These equipments. Observation item is such as the following.

- Wind speed
- Wind direction
- Temperature
- Relative humidity
- Atmosphere pressure

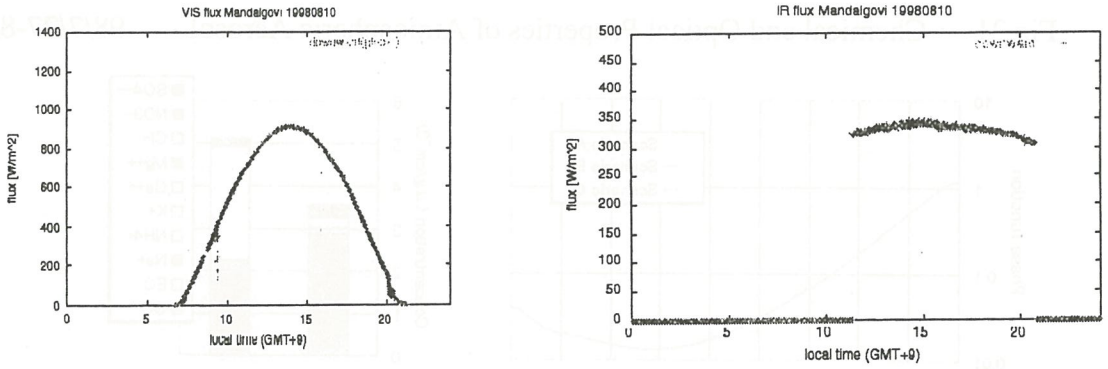

Fig19. VIS Downward Flux (Left) and IR Downward Flux(Right) in Mandalgobi

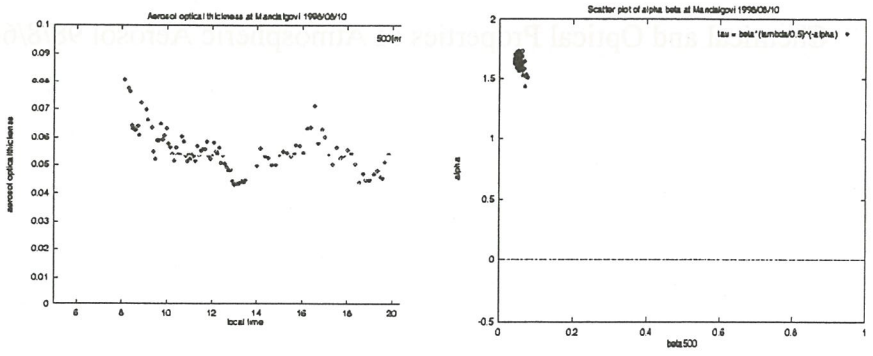

Fig.20 Aerosol Optical Thickness(Left) and Scatter plot of Alpha Beta(Right)

7. Atomospheric Measurement - 2

7.1 Chemical composition of atmospheric aerosol

Chemical component was measured by using Andersen sampler. It will be analyzed by Ion chromatography and chemical mass balance method will derived the origins of atmospheric aerosol.

7.2 Aerosol's refractive index and phase function

These data will be calculated by using the above data obtained by Andersen sampler.

7.3 Measurement of the Mie scattering

A Mie sampler was used for monitoring temporal behavior of aerosol.

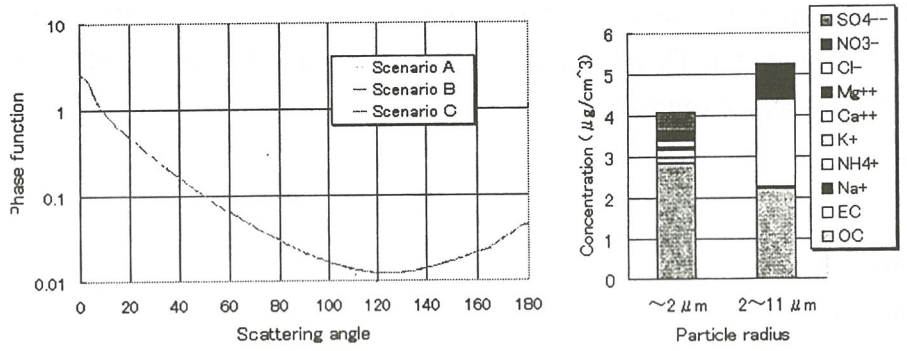

Fig.21 Chemical and Optical Properties of Atmospheric Aerosol 98/7/27-8/2

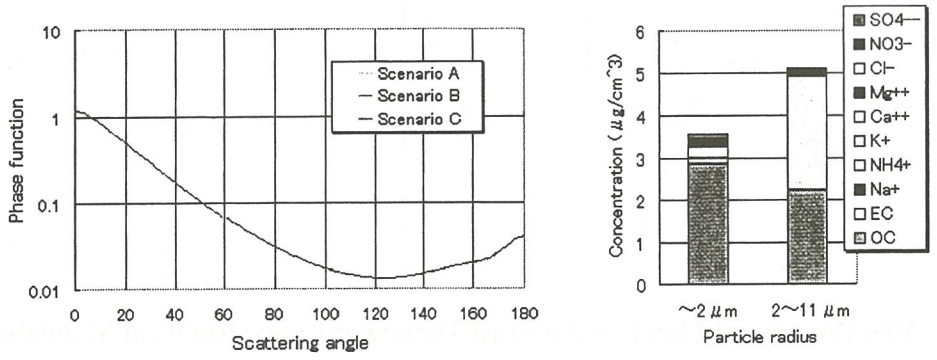

Fig.22 Chemical and Optical Properties of Atmospheric Aerosol 98/8/6-8/10

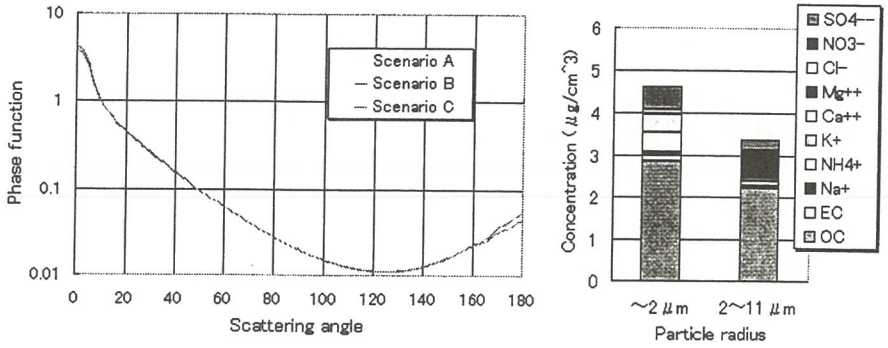

Fig.23 Chemical and Optical Properties of Atmospheric Aerosol 98/8/11-8/13